

A study of Seismic Evaluation of Existing Building in Indonesia
(インドネシアの既存建物の耐震評価に関する研究)

July, 2020

Doctor of Philosophy (Engineering)

Alex Kurniawandy
アレックス・クルニアワンディ

Toyohashi University of Technology

Date of Submission: July 06th, 2020

Department Architecture and Civil Engineering	Student ID Number 179502	Supervisors Shoji Nakazawa Taiki Saito Yukihiro Matsumoto
Applicant's name Alex Kurniawandy		

Abstract (Doctor)

Title of Thesis	A study of Seismic Evaluation of Existing Building in Indonesia
-----------------	--

Indonesia has often suffered major damaging earthquakes. It is difficult to precisely estimate the magnitude and location of earthquakes that will occur during the life of a building. There are still thousands of buildings in earthquake-prone regions that require seismic evaluation and rehabilitation. In recent years, the structure design code has experienced changes significantly because of the increased demand for structural capacity. The revision of the Indonesia hazard map is proposed by referring to the International Building Code where spectral acceleration values at peak ground acceleration, at 0.2 second and 1.0 second were applied for general buildings. Generally, the analysis shows the values of PGA relatively higher than in the previous Indonesian code. As a result, the existing buildings are no longer meets the standard requirement of applicable earthquake standard.

The introduction part in Chapter 1 clarifies the background problems and the motives for performing this study. The main objective is to develop a systematic evaluation of existing buildings in Indonesia. In order to achieve the objective, this research is conducted the study of the possibility of screening evaluation in the preliminary stage. There are fifteenth buildings evaluated in Chapter 2. These buildings are evaluated by Rapid Visual Screening (RVS), and then the static nonlinear analysis is used to confirm the result of the RVS. This RVS method can be used for the preliminary evaluation for the large numbers of buildings in a city against the earthquake risk.

The next stage of evaluations is a rapid evaluation method. The reliability of this method is described in Chapter 3 of this study. The rapid evaluation has been demonstrated by selecting cases of the 6th story steel moment-resisting frame system, and the 10th story braced frame system. Nonlinear static and dynamic analysis is performed to confirm the result of this method. The result of the evaluation, there are deficiencies founded in the basic configuration of the moment frame building because of non-compliant in the weak and soft story. The strong column weak beam criteria are not fulfilled in this building. It is confirmed by non-linear static and dynamic analysis, where the story failure likely to occur in the same stories with the screening result. The same evaluation method is also applied in the brace frame building.

There is no soft-story effect in this building, but the requirement of the strength capacity among the adjacent story is insufficient. This chapter shows that rapid evaluation can be implemented to evaluate the existing structure against the risk of an earthquake.

An index for evaluating the existing building performance is also proposed in this study. Two existing buildings were evaluated in Chapter 4. The first building consisted of five stories, and the second has four stories. Both buildings were moment-resisting frame system. An index is represented as the seismic performance of the existing building by following the Japanese standard. The building A has a seismic index in transversal direction larger than in the longitudinal direction. Meanwhile, building B has the same seismic index in both directions. The application of a seismic index based on the Japanese standard needs some adjustments for other countries. In this study, a set procedure was proposed to determine a seismic index based on the result of the pushover analysis. The result of the seismic index is higher than it obtained by the Japanese standard, due to the calculation of structural capacity was carried out until post elastic conditions. While the calculation based on the Japanese standard was based on the average shear stress on the resisting elements of lateral force. Furthermore, the seismic demand index is also developed with the same method with following to target response spectrum.

The dynamic seismic index dI_s and the dynamic ductility index dF of buildings, where located in Indonesia are introduced in this study. Both of these indexes show good accuracy in evaluating the seismic performance of a structure. A collection of simulated ground motions was used in linear and nonlinear dynamic analysis, which had Indonesia's response spectrum code as the target. The ductility index could be estimated by the estimation method without conducting the dynamic analysis in this study. Two estimation methods were also introduced that the first was the characteristic displacement response method which formulated from the relationship of the critical ductility factor μ_{cr} and the ductility index, and the second was the equivalent linearization method.

Finally, this study concludes that several stages can be carried out to overcome the problem in evaluating the performance of existing buildings. Seismic index methods such as those conducted in Japan, with some adjustments, can be used as guidelines to be applied in Indonesia to assess the performance of the building. The dynamic seismic index and ductility index can be predicted without conducting the nonlinear dynamic analysis by using the proposed methods, as confirmed in this study.

Acknowledgements

First of all, I would like to express my thanks to ALLAH Subhanallohu Wa Ta'ala, the Almighty, the Lord of the universe, for giving me the strength and ability to carry on this study and uncountable blessings throughout my life.

I would like to express my sincere thanks to Prof. Shoji Nakazawa for his guidance, supervision and patience throughout my PhD study and research. This thesis would not have been possible without his expertise. Great thanks to all my fellow labmates at Nakazawa's laboratory for your support during my study. Thank you very much for your friendship and for every kindness and hospitality.

I would also like to acknowledge support from the Indonesian Endowment Fund for Education (LPDP), Ministry of Finance; and the Directorate General of Higher Education (DIKTI), Ministry of Research, Technology and Higher Education, Republic of Indonesia; and also University of Riau Indonesia, particularly Civil Engineering department which gave chance and support to study at Toyohashi University of Technology.

Finally, my deepest gratitude to my beloved wife, June Endayani, and my lovely daughter, Alya Kinanti, for their endless support, sacrifice and patience during the completion of my study. I would like to extend my gratefulness to my parents for their prayer on my best wishes. The author would like to dedicate this thesis to them. I hope this work makes them proud.

Table of Contents

Abstract	i
Acknowledgements	iii
Table of Contents	iv
List of Figures	vi
List of Tables.....	viii
Abbreviations	ix
 Chapter 1 Introduction	 1
1.1. Background	1
1.2. Research Objective.....	4
1.3. Thesis Outline	5
 Chapter 2 Structural Building Screening with Rapid Visual Screening (RVS)	 6
2.1. Introduction	6
2.2. Methodology	7
2.3. Rapid Visual Screening	8
2.3.1. Number of Stories.....	12
2.3.2. Vertical Irregularity	13
2.3.3. Plan Irregularity.....	14
2.3.4. Post-Benchmark	15
2.3.5. Soil Type	15
2.4. Indonesian Code for Earthquake Resistance Building Design.....	16
2.4.1. Seismic Ground Motion Maps.....	17
2.4.2. Adjustments to Spectral Response for Site Class Effects.....	18
2.4.3. General Design Response Spectrum.....	19
2.4.4. Seismic Response Coefficient	20
2.5. Static Nonlinear.....	22
2.6. Cases Study	23
2.7. Result.....	26
2.8. Conclusion.....	32
 Chapter 3 Structural Seismic Evaluation of Indonesia Buildings	 33
3.1. Introduction	33
3.2. Methodology	34
3.2.1. Screening Evaluations	34
3.2.2. Static Nonlinear Analysis	36
3.2.3. Dynamic Nonlinear Analysis.....	37
3.2.4. Simulated Ground Motion	39
3.3. Case Study.....	40

3.4. Result and Analysis.....	42
3.4.1. Screening Evaluations Result	42
3.4.2. Result of Nonlinear Static Analysis.....	47
3.4.3. Result of Nonlinear Dynamic Analysis	51
3.5. Conclusion.....	62
 Chapter 4 A Proposal of Seismic Index for Existing Buildings in Indonesia using Pushover Analysis.....	63
4.1. Introduction	63
4.2. Methodology	64
4.2.1. Seismic Index	64
4.2.2. Pushover Analysis	65
4.3. Case Study.....	68
4.4. Results of the Seismic Evaluation.....	71
4.4.1. Seismic Index	71
4.4.2. Seismic Index Base on Pushover Analysis.....	73
4.4.3. Evaluation of Structure Performance.....	76
4.5. Conclusion.....	77
 Chapter 5 The Dynamic Seismic Performance Index of Building in Indonesia	78
5.1. Introduction	78
5.2. Numerical Model	79
5.3. Methodology	80
5.3.1. Input Earthquake Motions	81
5.3.2. Simulated Ground Motions	83
5.3.3. Dynamic Seismic Index and Ductility Index.....	84
5.3.4. Estimation Method of Ductility Index.....	85
5.4. Analysis Result.....	88
5.4.1. Dynamic Seismic Index.....	88
5.4.2. Dynamic Ductility Index	90
5.4.3. Estimation of Ductility Index	91
5.5. Conclusion.....	95
 Chapter 6 Conclusion.....	97
6.1. Summary	97
6.2. Future works.....	99
 References.....	101
Appendix	105

List of Figures

Figure 1.1. The historical of earthquake epicenter in Indonesia [5].....	2
Figure 1.2. The history of the seismic hazard map of Indonesia [6]	3
Figure 2.1. Seismic map of Pekanbaru city of Indonesia.....	7
Figure 2.2. The complete form of the RVS	9
Figure 2.3. Section description in the RVS form	10
Figure 2.4. The irregularities potential in a vertical direction [16]	13
Figure 2.5. Plan views of various building configurations showing plan irregularities; arrows indicate possible areas of damage.....	14
Figure 2.6. S_s , Risk-adjusted maximum considered earthquake (MCE_R) ground motion parameter for Indonesia for 0.2s spectral response acceleration (5% of critical damping) [10]	17
Figure 2.7. S_I , Risk-adjusted maximum considered earthquake (MCE_R) ground motion parameter for Indonesia for 1.0s spectral response acceleration (5% of critical damping) [10]	18
Figure 2.8. General design response spectrum with 5% damping [10].....	20
Figure 2.9. Moment-rotation relationship of typical plastic hinge	22
Figure 2.10. Plastic hinge properties of column and beam	23
Figure 2.11. Roof drift and roof drift ratio [26]	23
Figure 2.12. Design spectral response of Pekanbaru city.....	24
Figure 2.13. Pictures of the various building to be evaluated	25
Figure 2.14. Picture of the Faperika building.....	27
Figure 2.15. Scoring result of rapid visual screening.....	28
Figure 2.16. Roof deformation.....	29
Figure 2.17. Roof deformation (continued)	30
Figure 2.18. Roof drift ratio	31
Figure 3.1. Tall Story and soft story.....	34
Figure 3.2. Moment-rotation relationship of typical plastic hinge	37
Figure 3.3. Bilinear model.....	38
Figure 3.4. Perspective and floor plan.....	41
Figure 3.5. Spectral response acceleration of Padang city (5% of critical damping) [10].	42
Figure 3.6. Total shear capacity per layer of MF and BF building	42
Figure 3.7. The total stiffness of MF and BF building in any stories.....	44
Figure 3.8. The capacity curve of MF structure in X-direction and Y-direction	47
Figure 3.9. The capacity curve of MF building for any stories in X-direction	48
Figure 3.10. The capacity curve of MF building for any stories in Y-direction	48
Figure 3.11. The capacity curve of BF structure in X-direction and Y-direction	49
Figure 3.12. The capacity curve of BF building for any stories in X-direction	50
Figure 3.13. The capacity curve of BF building for any stories in Y-direction	50
Figure 3.14. The mode shape displacement of MF building in both direction	51

Figure 3.15. The mode shape displacement of BF building in both direction	52
Figure 3.16. Simulated spectrum acceleration	53
Figure 3.17. Maximum response of MF building	54
Figure 3.18. Nonlinear dynamic response due to El Centro earthquake of MF building in X- direction	55
Figure 3.19. Nonlinear dynamic response due to Kobe earthquake of MF building in X-direction.....	55
Figure 3.20. Nonlinear dynamic response due to Taft earthquake of MF building in X-direction.....	56
Figure 3.21. Nonlinear dynamic response due to El Centro earthquake of MF building in Y- direction	56
Figure 3.22. Nonlinear dynamic response due to Kobe earthquake of MF building in Y-direction.....	57
Figure 3.23. Nonlinear dynamic response due to Taft earthquake of MF building in Y-direction.....	57
Figure 3.24. Maximum response of BF building	58
Figure 3.25. Nonlinear dynamic response due to El Centro earthquake of BF building in X- direction	59
Figure 3.26. Nonlinear dynamic response due to Kobe earthquake of BF building in X-direction.....	59
Figure 3.27. Nonlinear dynamic response due to Taft earthquake of BF building in X-direction.....	60
Figure 3.28. Nonlinear dynamic response due to El Centro earthquake of BF building in Y- direction	60
Figure 3.29. Nonlinear dynamic response due to Kobe earthquake of BF building in Y-direction.....	61
Figure 3.30. Nonlinear dynamic response due to Taft earthquake of BF building in Y-direction.....	61
Figure 4.1. Moment-rotation relationship of typical plastic hinge	66
Figure 4.2. Converting the capacity curve to be an elastoplastic curve by the constant energy principle	67
Figure 4.3. Perspective and plan view of building A.	68
Figure 4.4. Perspective and plan view of building B.	70
Figure 4.5. Seismic index of building A and B	73
Figure 4.6. Seismic index (I_s) of building A and B	75
Figure 4.7. Performance point of Building A and B	76
Figure 5.1. SDOF system with bilinear hysteretic model	79
Figure 5.2. The design response spectrum of Indonesian code.....	82
Figure 5.3. Simulation of the acceleration response spectrum.....	84
Figure 5.4. Relationship between shear force coefficient C and ductility factor μ	85
Figure 5.5. Characteristics of maximum displacement	86
Figure 5.6. The spectrum of the dynamic seismic index (dI_s).....	89
Figure 5.7. Relationship dynamic ductility index (dF) and critical ductility (μ_{cr}).....	90
Figure 5.8. Spectrum of dynamic ductility index (dF).....	91
Figure 5.9. Relationship dynamic ductility index and estimation ductility index	92
Figure 5.10. Relationship ductility factor and dynamic ductility index on several estimation methods.....	94

List of Tables

Table 2.1. Hazard intensity based on spectral acceleration.....	11
Table 2.2. The basic score of all buildings type.....	11
Table 2.3. Score modifier for concrete moment-resisting frame buildings.....	12
Table 2.4. Values of site coefficient F_a as a function of site class and mapped spectral response acceleration at short periods, S_S	19
Table 2.5. Values of site coefficient F_v as a function of site class and mapped spectral response acceleration at 1.0 period, S_1	19
Table 2.6. Importance factors by risk category of buildings.....	21
Table 2.7. Coefficient for the upper limit on the calculated period	21
Table 2.8. The building list as cases study	26
Table 2.9. The screening checklist	27
Table 2.10. The rapid visual screening result.....	28
Table 2.11. Roof drift ratio.....	31
Table 3.1. Summarize section property in the 6 th story structure.....	40
Table 3.2. Summarize section property in the 10 th story structure.....	40
Table 3.3. Basic configuration evaluation of building A (MF) and building B (BF).....	43
Table 3.4. Structural evaluation of the moment frame (MF) structure	45
Table 3.5. Structural evaluation of the brace frame (BF) structure.....	46
Table 3.6. Ductility factor in any stories of MF building.....	47
Table 3.7. Ductility factor in any stories of BF building	49
Table 3.8. Dynamic properties of MF building.....	51
Table 3.9. Dynamic properties of BF building.....	52
Table 3.10. Simulated earthquake ground motions.....	53
Table 4.1. Material properties of building A and B	69
Table 4.2. Beam and column dimension of the building A.....	69
Table 4.3. Beam and column dimension of the building B	70
Table 4.4. Seismic index of building A.....	72
Table 4.5. Seismic index of building B	72
Table 4.6. The lateral force in building A and B.....	73
Table 4.7. The capacity curve of building A and building B	74
Table 4.8. Seismic index using pushover analysis	75
Table 4.9. Seismic index comparison.....	76
Table 4.10. Evaluation of the structure performance	77
Table 5.1. Selected ductility factor when varying T_0 and C_y	81
Table 5.2. Simulated earthquake ground motions.....	83
Table 5.3. The shear coefficient of C_0	88
Table 5.4. The percentage of error estimation for each dF estimation	93
Table 5.5. The percentage of error comparison for both estimation method	95

Abbreviations

AIJ	Architectural Institute of Japan
AISC	American Institute of Steel Construction
ASCE	American Society of Civil Engineering
ATC	Applied Technology Council.
BF	Brace Frame
BSL	Building Standard Law
CM	Center of Mass of the story
CR	Center of Rigidity of the story
CSM	Capacity Spectrum Method
DBE	Design Basis Earthquake
ELM	Equivalent Linearization Method
FEMA	The Federal Emergency Management Agency
IBC	International Building Code
JBDPA	The Japan Building Disaster Prevention Association
MCE	Maximum Considered Earthquake Ground Motion
MDOF	Multi Degree of Freedom
MF	Moment Frame
MRF	Moment Resisting Frame
NEHRP	National Earthquake Hazard Reduction
PGA	Peak Ground Acceleration
RVS	Rapid Visual Screening
REM	Rapid Evaluation Method
SCWB	Strong Column Weak Beam
SDOF	Single Degree of Freedom
SMF	Special Moment Frame
SIMEQ	Simulated of Earthquake ground motion

Chapter 1

Introduction

1.1. Background

Over the past 50 years, Indonesia has often suffered major damaging earthquakes. It is difficult to precisely estimate the magnitude and number of earthquakes that will occur during the life of a building. There are still thousands of buildings in earthquake-prone regions that require seismic evaluation and rehabilitation [1]. A series of earthquake events have occurred in Indonesia in the past. The most recent earthquakes located along the Sumatran-Andaman plate was in 1797 with the magnitude in between 8.7 - 8.9. In 2004, The great earthquake of magnitude 9.1 and immediately following by devastating tsunami occurred in Simeulue Island of Banda Aceh. There was an earthquake in September 2007 of magnitude 8.5 in Mentawai island. A magnitude of 7.6 due to the subducting plate caused considerable damage in Padang in 2009 and a magnitude of 7.8 in 2010 again occurred in the Mentawai island caused a tsunami on the west coast of those islands [2, 3]. The historical earthquake epicenter can be seen in Figure 1.1.

In recent years, the earthquake resistance structure design has experienced changes significantly because of the increased demand for enhancement of structural capacity in order to minimize the level of damage, economic loss, and structure repair costs. Several researchers have been studied the seismic hazard of Indonesia and the earthquake-resistant standard design for the building. Asrurifak et al., 2010, studied in updating the spectral hazard map of Indonesia with a return period of 2500 years earthquake. The spectral hazard map was analyzed using the total probability method and three-dimensional source models with recent seismotectonic parameters. Four source models were used in

this analysis: shallow background, deep background, fault, and subduction source models. This study proposed the revision of the Indonesia hazard map by referring to International Building Code (IBC) where spectral acceleration values at peak ground acceleration, at 0.2 seconds and at 1.0 seconds were applied for general buildings with a return period of 2500 year. Generally, the results of the analysis show the values of PGA with a return period of 2500 years relatively higher 1.2-3.0 times than in Indonesia seismic code at that time [4].

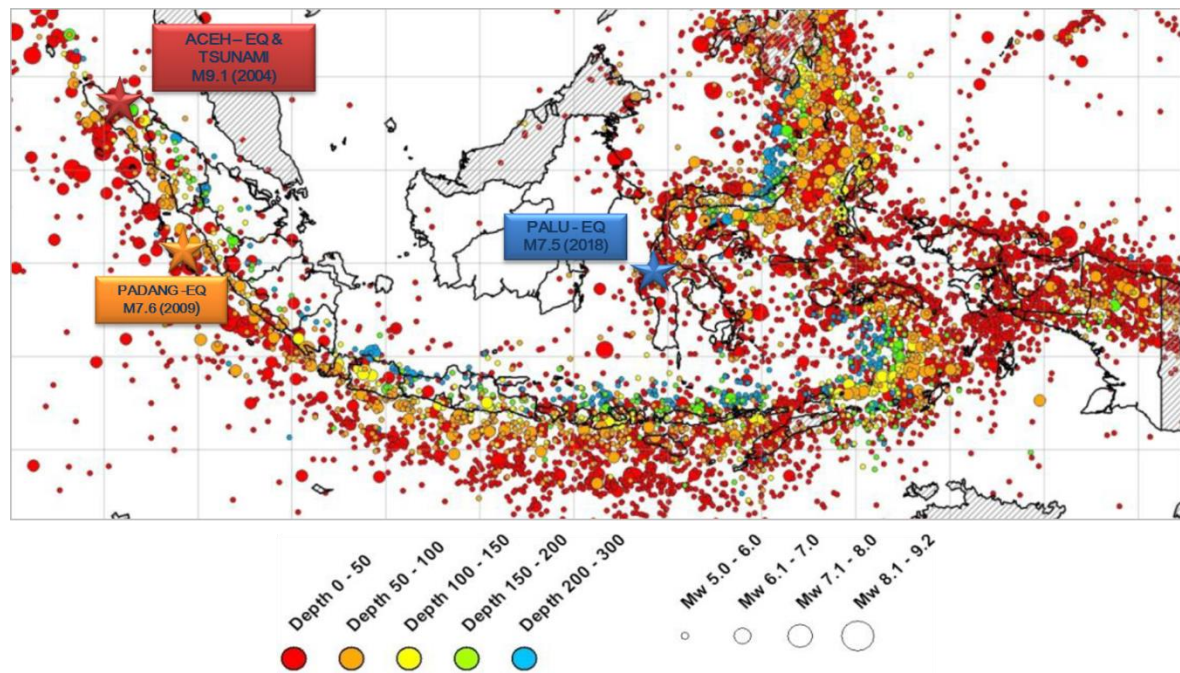


Figure 1.1. The historical of earthquake epicenter in Indonesia [5]

Irsyam et al., 2017, presents the progress in developing Indonesia seismic hazard maps. The revision of seismic hazard maps has been developed based upon updated: seismotectonic data, fault models, and attenuation function. Important information is considered for updating seismic hazard maps such as significant results of recent active-fault studies utilizing trenching, carbon dating, epicenter relocation, strain analysis as well as the availability of the recently available data. The new information was gathered in order to obtain a more accurate tectonic model and their seismic parameters, such as maximum magnitudes and slip-rates. Finally, probabilistic and deterministic analyses were then performed in order to develop new seismic hazard maps [3].

The earthquake resistance design code for building in Indonesia has been updated from time to time to minimize risk and human life fatalities. Figure 1.2 shows the historical of the seismic hazard map of Indonesia, and consequently the seismic load demand also increases. The existing buildings

may not comply with the requirements of the current code anymore. It needed evaluation to show the performance against the current code. Several evaluation methods can be used to evaluate existing buildings. The nonlinear analysis is a reliable method to confirm existing structural performance. However, a large number of buildings in Indonesia makes it difficult to carry out detailed structural evaluations. The tons of buildings in a city need a rapid method to conduct an evaluation.

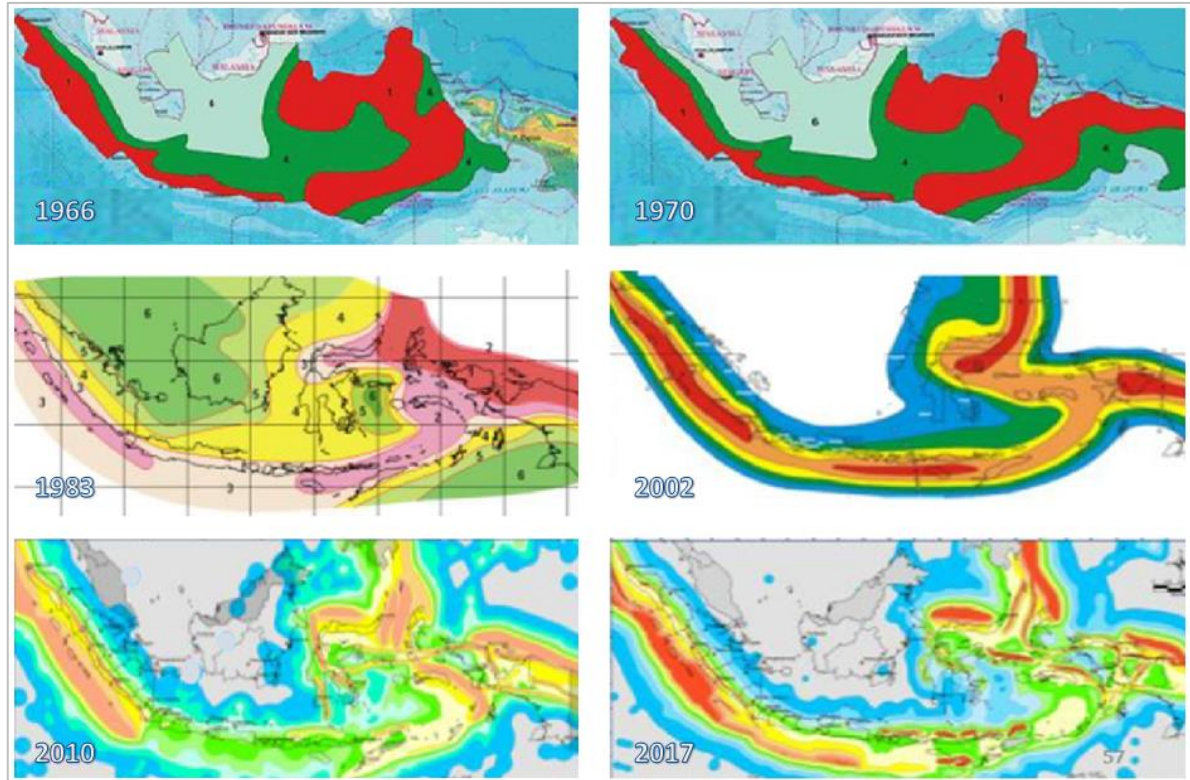


Figure 1.2. The history of the seismic hazard map of Indonesia [6]

Nakazawa et al. have been conducted several researches to evaluate the existing structure performance in Japan. In 2011, Nakazawa has been studied evaluation of dynamic ductility index of a school gymnasium [7]. The paper discussed the seismic resistance capacity of the school gymnasium subjected to earthquake motions in the span direction. Based on the result of the elasto-plastic dynamic analysis depending on various input levels, the values of dI_s and dF for the gable frame structure were calculated. As numerical parameters, critical plastic rotation, θ_p^{cr} , of the gable frame structure was adopted, and the effects on dI_s and dF were investigated. Two kinds of fundamental gable frames, Frames A and B, were studied. The results show that the skeleton curves of Frame A and B became tri-linear and bi-linear types, respectively. Plastic rotation θ_p of Frame A was greatly large compared with θ_p of Frame B. Therefore, the energy absorption performance of Frame B was superior to that of

Frame A. Criteria of plastic angle θ_p^{cr} were assumed to be 0.005, 0.01, 0.02, 0.03, 0.04 and 0.05. The dI_s and dF became large with the increase in θ_p^{cr} . The dF of Frame A was distributed from 0.71 to 1.82 and dI_s was distributed from 0.28 to 0.72. The dF of Frame B was distributed from 1.40 to 4.89 and dI_s was distributed from 0.76 to 2.66. In 2013, Nakazawa has been studied a method of evaluation for Japan's steel gymnasium with the dynamic structural seismic index and dynamic ductility index based on pushover analysis [8]. The resistance capacity subjected to horizontal seismic motions in the span direction was investigated. The correspondence of the time history analysis and pushover analysis based on a capacity spectrum method was studied in detail with respect to some adjustment factors to increase accuracy. The proposed pushover analysis using some adjustment factors proved as a design tool for evaluating the important seismic index. In 2017, Nakazawa proposed an estimation method of the dynamic ductility index using the equivalent linearization method (ELM) [9]. The ELM expresses a system with nonlinear restoring force as a linear system with equivalent stiffness and equivalent damping factor. The equivalent stiffness, k_{eq} , is defined as the maximum shear force divided by the maximum point stiffness. Further, the equivalent natural period, T_{eq} , corresponding to the equivalent stiffness, can also be obtained. The equivalent linearization method is a simple method for estimating the ductility index without conducted a nonlinear dynamic analysis. The dynamic structural seismic index was determined with corresponding to the critical deformation of a member. A steel gymnasium supported by a substructure was use as a case study and it modeled as a single degree of freedom (SDOF) system when the rigidity of the upper roof structure assumed quite high. The validity of the proposed estimation method show good accuracy in estimating the index.

1.2. Research Objective

The purpose of this study is to develop a systematic evaluation of the performance of existing buildings in resilience to face major earthquakes that may occur in the future and can also measure how much the lack of performance of existing buildings against the update code that currently apply. This study takes several cases of the existing building in Pekanbaru and Padang city of Indonesia in collecting building information. Various structural types and building occupancies in these two cities are the objects of this study. Therefore, this study aims as follow:

1. To learn the possibility of a rapid evaluation method as the initial screening procedure that can be carried out in a short time, taking into consideration the large number of buildings to be assessed.

2. To investigate a further rapid evaluation by examining the general aspects of building and the characteristic of the structural system and geological information.
3. To formulate an index to measure the level of the existing building performance and estimate the level of safety by comparing to the demand hazard in a certain location.
4. To investigate the actual of the existing building performance with reliable methods such as static and dynamic nonlinear analysis guide in considering the accuracy of the proposed evaluation method.

1.3. Thesis Outline

This thesis will be outlined as follow. Chapter 1 is an introduction that describes the background of this study and the research objective. Then, chapter 2 will describe the application of the Rapid Visual Screening (RVS) method in the Pekanbaru city of Indonesia. The selected 15 buildings as case studies were investigated. The result is then confirmed with a static pushover analysis method and describing reliability that this method can be used as a preliminary evaluation. The next chapter, chapter 3, will represent the Rapid Evaluation Method (REM) which is a further screening evaluation to investigate the structure configuration and the element component for resisting an earthquake load. The REM is developed in the two of the checklists procedure: the configuration structure checklist and the element for resisting the earthquake load checklist. In this chapter, the case study is selected for the steel structure in differing structural systems. Afterward, chapter 4 will be a chapter about a method of calculation of a seismic index with the pushover analysis method. The seismic index is an index to describe the performance of the existing building which is popular in Japan. The safety limit of the seismic index called a seismic demand index is proposed by considering Indonesia's seismic hazard which is defined in the current seismic code in Indonesia. The last chapter, chapter 5, describes the conclusion of this thesis.

Chapter 2

Structural Building Screening with Rapid Visual Screening (RVS)

2.1. Introduction

An earthquake is a sudden shift from soil layers due to the movement of the earth's surface. The shift creates a vibration called seismic waves. An earthquake will shake building in horizontally and vertically. The vertical forces rarely make structural collapse, but the horizontal force potentially makes it as long as this force exceeds the capacity of the structure. An earthquake is a disaster that can be harmful to the community, such as financial loss and loss of human life. Pekanbaru is a city which is located in the middle of Sumatera Island. Even though Pekanbaru is a rarely occurring earthquake, but Pekanbaru has ever felt the impact of a big earthquake that occurred in West Sumatera in September 2009. As we know, Indonesia located between the Eurasian plate, Pacific plate and Indo-Australian plate. Particularly the Sumatera Island, which has the Semangko fault or the great Sumatra fault along the island from north to south due to shift of Eurasian and Indo-Australian Plates. An earthquake is not killing people but the collapse of building around the people could be killing them.

Generally, before building constructed there was the structural design which established with certain earthquake loads comply to a standard, but for the existing of the buildings which have a lack of the standard design and inadequate structure capacity to resist earthquake load has become a serious problem. Since 2012, there was a new code for the design of earthquake resistance in Indonesia, namely “The design procedures of the earthquake resistance for building and non-building structures” [10]. This was a revision and updated of the previous code that has been released since 2002. Figure

2.1 shows the comparison of seismic maps of Pekanbaru city based on before and after updated code [10, 11]. The preventive action to avoid the damage of the building will become severe damage should be taken into consideration. There are various evaluation methods to anticipate the building in severe damage when hit by an earthquake. One of the methods is a performance base evaluation. The performance base evaluation can provide sufficient information to what extent the earthquake will affect the structure of the building [12].

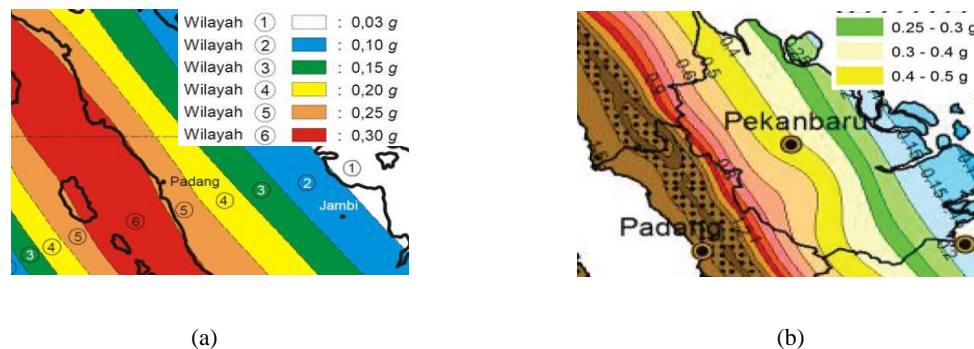


Figure 2.1. Seismic map of Pekanbaru city of Indonesia
(a). Indonesia code SNI 03-1726-2002 [13] (b). Indonesia code SNI 1726:2012 [10]

The objective of this research is to make an assessment of the existing building and to conduct evaluation using rapid visual screening method in order to get further consideration against the earthquake load. Non linear static analysis is used as a comparison. Therefore the result provide recommendations for the facility owner about their building condition and taking preventive action against inadequate resistance due to an earthquake load.

2.2. Methodology

A methodology for assessing building vulnerability is needed. A screening procedure in the initial stage of evaluation useful for a large number of building population. The screening procedure issued by the Federal Emergency Management Agency (FEMA) will be studied in this research. The FEMA 154 introduces screening evaluation of the existing structure. Several buildings were selected in Pekanbaru city and it will be evaluated by using these methods.

Ramly et al. conducted a seismic assessment of existing buildings in Bukit Tinggi in Pahang of Malaysia [14]. Six general building occupancies that are easy to recognize have been defined. These are listed on the data collection form as residential, commercial, industrial, educational, government, assembly, history and emergency services. A total of 1166 were identified in Bukit Tinggi. The highest occupancy class is residential as much as 84 percent. The results of preliminary visual

inspection were completed for these buildings. A total of 26 percent of the buildings indicated that the buildings need to be further evaluated by the professionals based on engineering practice because the buildings have a probability of damage due to ground motion activity. Whereas, another 74 percent of buildings are safe from the ground motion. The results revealed that the score determined for the factor of primary structural lateral load resisting system (building types), has the highest contribution to the final score of the buildings. Other than that, most of the multi-story buildings have a soft story which is a large opening at the ground level commonly for parking areas. The buildings in Bukit Tinggi are on a steep hill so that over the up-slope dimension of the building the hill raises at least one story height. A problem may exist because along the lower side of the story, the horizontal stiffness may be different from the uphill side. Additionally, the stiff short columns attract the seismic shear forces and may fail. These contribute to the reduction of the final score due to the vertical irregularity.

M. Syah et al. used the RVS method to determine the vulnerability of buildings in two districts of Jeddah Saudi Arabia [15]. The screening evaluation was performed on over 1000 residential buildings structures in two different time periods with an aim to evaluate the differences between older and recent buildings in a rapidly-expanding city of Saudi Arabia. Results of the visual screening were consistent and reasonable considering the age of buildings based on the data obtained previously. Results of the visual screening were consistent and reasonable considering the age of buildings based on the data obtained previously. Upon the results of the investigation, the used typical structure and state of the buildings can be determined. A clear distinction can be made concerning the different age of the building resulting in different structures. Residential buildings in Al-Balad district are old and buildings in As-Salamah district were built recently based on new seismic codes. This information allows the furthermore detailed seismic analysis of existing buildings.

2.3. Rapid Visual Screening

Rapid Visual Screening (RVS) is a fast method to identify a risk of building and it can be conducted without performing any structural analysis. Buildings are rapidly evaluated via a “sidewalk survey” to identify features that affect the seismic performance of the building. Many of the RVS methods have been developed in the worldwide [16–18]. According to the difference in building codes and construction practices, the scoring system and parameters are taken for assessing the vulnerability of buildings that differ from place to place. One of the methods and scoring systems for rapid screening was developed by FEMA [4]. The results can be used as guidance to make consideration for the next action. If the results indicate that the building does not meet the requirements, then the

next action will be evaluated by the detailed evaluation before making a final decision for retrofitting or demolishing. The RVS method is carried out by filling the form as shown in Figure 2.2. Various features were considered during this procedure. These features may include building type, seismicity, soil conditions and irregularities. The inspection, data collection and decision-making process typically occurs at the building site, and is expected to take around 20 min for each building [19].

HIGH Seismicity

Sketch :

Address : Kampus Bina Widya
Universitas Riau

Other Identifiers xx

No. Stories 5 Year +/- 2014

Screener tbm Date 2016

Total Floor Area (sq. ft.) _____

Building Name Gedung Surya Dumai

Use Hospital

OCCUPANCY				SOIL		TYPE								FALLING HAZARDS			
Assembly	Govt	Office	Number of Persons	A	B	C	D	E	F								
Commercial	Historic	Residential	0 - 10	Hard	Avg.	Dense	Stiff	Soft	Poor								
Emer. Services	Industrial	School	101 - 1000	Rock	Rock	Soil	Soil	Soil	Soil								
			1000+														

BASIC SCORE, MODIFIERS, AND FINAL SCORE, S

BUILDING TYPE	W1	W2	S1 (MRF)	S2 (BR)	S3 (LM)	S4 (RC SW)	S5 (URM INF)	C1 (MRF)	C2 (SW)	C3 (URM INF)	PC1 (TU)	PC2	RM1 (FD)	RM2 (RD)	URM
Basic Score	4.4	3.8	2.8	3	3.2	2.8	2	2.5	2.8	1.6	2.6	2.4	2.8	2.8	1.8
Mid Rise (4 to 7 stories)	N/A	N/A	0.2	0.4	N/A	0.4	0.4	0.4	0.4	0.2	N/A	0.2	0.4	0.4	0
High Rise (>7 stories)	N/A	N/A	0.6	0.8	N/A	0.8	0.8	0.6	0.8	0.3	N/A	0.4	N/A	0.6	N/A
Vertical Irregularity	-2.5	-0.2	-1	-1.5	N/A	-1	-1	-1.5	-1	-1	N/A	-1	-1	-1	-1
Plan Irregularity	-0.5	-0.5	-0.5	-0.5	-0.5	-0.5	-0.5	-0.5	-0.5	-0.5	-0.5	-0.5	-0.5	-0.5	0.5
Pre - Code	0	-1	-1	-0.8	-0.6	-0.8	-0.2	-1.2	-1.0	-2.0	-0.8	-0.8	-1	-0.8	-0.2
Post- Benchmark	2.4	2.4	1.4	1.4	N/A	1.6	N/A	1.4	2.4	N/A	2.4	N/A	2.8	2.6	N/A
Soil Type C	0	-0.4	-0.4	-0.4	-0.4	-0.4	-0.4	-0.4	-0.4	-0.4	-0.4	-0.4	-0.4	-0.4	-0.4
Soil Type D	0	-0.8	-0.6	-0.6	-0.6	-0.6	-0.4	-0.6	-0.6	-0.4	-0.6	-0.6	-0.6	-0.6	-0.6
Soil Type E	0	-0.8	-1.2	-1.2	-1	-1.2	-0.8	-1.2	-0.8	-0.8	-0.4	-1.2	-0.4	-0.6	0.8
FINAL SCORE, S								2.6	4.3						

COMMENTS

> *There are two system of structure, i.e: MRF and SW*

> *Irregularity in horizontal (plan) direction*

> *Final score >= 2, No detail evaluation needed*

Detail Evaluation Required

YES
NO

Figure 2.2. The complete form of the RVS

The RVS form as shown in Figure 2.2 consist of several sections. On the top left of this sheet, it is for illustrating a sketch of a building structure. And following in the top right is for the detail of identification of the building location. The building image can also be attached in the middle of this sheet. The occupancy criteria, soil type and the potential falling hazard can be described in the middle of this sheet as zoom in Figure 2.3 (a),(b) and (c) respectively. The main part of this sheet is in the determination of basic score and score modifier in next to the middle of this sheet. FEMA 154 assigns a basic structural score based on seismic hazard intensity of the region, building type and lateral load resisting system of the building. Performance modifiers are specified to take into account the effect of a number of stories, plan and vertical irregularities, pre-code or post-benchmark code detailing, poor condition of the building and type of soil.

There are several types of structure base on composing material including wood, steel, concrete, prestressed concrete and unreinforced masonry. Each type of structure has a different basic score as shown in Figure 2.3 (d) and it describes in Table 2.2.

OCCUPANCY SOIL				
Assembly	Govt	Office	Number of Persons	
Commercial	Historic	Residential	0 - 10	11 - 100
Emer. Services	Industrial	School	101 - 1000	1000+

(a) Building categories and Occupancy

SOIL TYPE					
A	B	C	D	E	F
Hard	Avg.	Dense	Stiff	Soft	Poor
Rock	Rock	Soil	Soil	Soil	Soil

(b) Soil Type

FALLING HAZARDS			
<input type="checkbox"/>	<input type="checkbox"/>	<input type="checkbox"/>	<input type="checkbox"/>
Unreinf.	Parapets	Cladding	Other
Chimneys			

(c) Potential Falling hazard.

BASIC SCORE, MODIFIERS, AND FINAL SCORE, S															
BUILDING TYPE	W1	W2	S1 (MRF)	S2 (BR)	S3 (LM)	S4 (RC SW)	S5 (URM INF)	C1 (MRF)	C2 (SW)	C3 (URM INF)	PC1 (TU)	PC2	RM1 (FD)	RM2 (RD)	URM
Basic Score	4.4	3.8	2.8	3	3.2	2.8	2	2.5	2.8	1.6	2.6	2.4	2.8	2.8	1.8
Mid Rise (4 to 7 stories)	N/A	N/A	0.2	0.4	N/A	0.4	0.4	0.4	0.4	0.2	N/A	0.2	0.4	0.4	0
High Rise (>7 stories)	N/A	N/A	0.6	0.8	N/A	0.8	0.8	0.6	0.8	0.3	N/A	0.4	N/A	0.6	N/A
Vertical Irregularity	-2.5	-0.2	-1	-1.5	N/A	-1	-1	-1.5	-1	-1	N/A	-1	-1	-1	-1
Plan Irregularity	-0.5	-0.5	-0.5	-0.5	-0.5	-0.5	-0.5	-0.5	-0.5	-0.5	-0.5	-0.5	-0.5	-0.5	0.5
Pre - Code	0	-1	-1	-0.8	-0.6	-0.8	-0.2	-1.2	-1	-2	-0.8	-0.8	-1	-0.8	-0.2
Post- Benchmark	2.4	2.4	1.4	1.4	N/A	1.6	N/A	1.4	2.4	N/A	2.4	N/A	2.8	2.6	N/A
Soil Type C	0	-0.4	-0.4	-0.4	-0.4	-0.4	-0.4	-0.4	-0.4	-0.4	-0.4	-0.4	-0.4	-0.4	-0.4
Soil Type D	0	-0.8	-0.6	-0.6	-0.6	-0.6	-0.4	-0.6	-0.6	-0.4	-0.6	-0.6	-0.6	-0.6	-0.6
Soil Type E	0	-0.8	-1.2	-1.2	-1	-1.2	-0.8	-1.2	-0.8	-0.8	-0.4	-1.2	-0.4	-0.6	0.8

(d) Basic score and score modifiers

Figure 2.3. Section description in the RVS form

Table 2.1. Hazard intensity based on spectral acceleration

Level of seismic hazard intensity	Calculated 2/3 SA for a period of 0.2 second (or S_{Ds})	Calculated 2/3 SA for a period of 1.0 second (or S_{D1})
Low	Less than 0.167 g	Less than 0.067 g
Moderate	Greater than or equal to 0.167 g but less than 0.5 g	Greater than or equal to 0.067 g but less than 0.2 g
High	Greater than or equal to 0.5 g	Greater than or equal to 0.2 g

The basic score as shown in Table 2.2 classified in three-level seismic intensities consists of high hazard intensity; moderate hazard intensity ; low hazard intensity. The higher the seismicity level will be the lower of the basic score.

Table 2.2. The basic score of all buildings type

Building Type		Seismicity		
		Low	Moderate	High
Lightwood frame single or multiple family dwelling of one or more stories in height	(W1)	7.4	5.2	4.4
Wood frame commercial and industrial buildings with a floor area larger than 5,000 square feet	(W2)	6.0	4.8	3.8
Steel moment-resisting frame buildings	(S1)	4.6	3.6	2.8
Braced steel frame buildings	(S2)	4.8	3.8	3.0
Light metal buildings	(S3)	4.6	3.8	3.2
Steel frame buildings with concrete shear walls	(S4)	4.8	3.6	2.8
Steel frame buildings with unreinforced masonry infill walls	(S5)	5.0	3.6	2.0
Concrete moment-resisting frame buildings	(C1)	4.4	3.0	2.5
Concrete shear wall buildings	(C2)	4.8	3.6	2.8
Concrete frame buildings with unreinforced masonry infill walls	(C3)	4.4	3.2	1.6
Tilt-up buildings	(PC1)	4.4	3.2	2.6
Precast concrete frame buildings	(PC2)	4.6	3.2	2.4
Reinforced masonry buildings with flexible floor and roof diaphragms	(RM1)	4.8	3.6	2.8
Reinforced masonry buildings with rigid floor and roof diaphragms	(RM2)	4.6	3.4	2.8
Unreinforced masonry bearing-wall buildings	(URM)	4.6	3.4	1.8

The hazard Intensity is part of the Rapid Visual Screening forms since the vulnerability of existing buildings is related to the intensity of the earthquake hazard, greater the intensity higher the damage the building will sustain and higher will be its vulnerability. Hence each level of seismic intensity forms the basis of one Rapid Visual Screening Form and the number of such forms will be equal to the number of seismic intensity zones. According to FEMA 154 (2002), the level of hazard intensity will be determined in the following manner. From the seismic hazard map of the country, find the spectral accelerations design (SA) for a natural period of 0.2 seconds and 1.0 seconds, then multiply the value by a factor of 2/3 and check the calculated values as in Table 2.1.

The basic score of the selected building type will be modified with several score modifiers as shown in Table 2.3. The score modifier can be a positive value that will be added to the basic score otherwise it can be a negative value that will be deducted the basic score.

Table 2.3. Score modifier for concrete moment-resisting frame buildings

	Seismicity		
	Low	Moderate	High
Mid Rise (4 to 7 stories)	0.4	0.2	0.4
High Rise (> 7 stories)	1.0	0.5	0.6
Vertical Irregularity	-1.5	-2.0	-1.5
Plan Irregularity	-0.8	-0.5	-0.5
Pre - Code	N/A	-1.0	-1.2
Post- Benchmark	0.6	1.2	1.4
Stiff Soil (Type D)	-0.6	-0.6	-0.4
Soft Soil (Type E)	-1.4	-1.0	-0.6
Poor Soil (Type F)	-2.0	-1.6	-1.2

The use of the RVS which is expected to have acceptable seismic performance should establish an appropriate score call as a “cut-off” score. A score of 2 is suggested as a “cut-off “ base on seismic design criteria. A building having a score of 2 or less should be investigated by further detail evaluation.

2.3.1. Number of Stories

From Table 2.3, the top two modifiers are related to a number of stories. The basic score will be modified with a positive value of a modifier score. If the building has 4 to 7 stories, it is considered a mid-rise building, and the positive score modifier associated with this attribute should be circled. If the building has 8 or more stories, it is considered a high-rise building, and the score modifier associated

with this attribute should be circled. The high-rise building has a score modifier higher than the mid-rise building.

2.3.2. Vertical Irregularity

If a structure has vertical irregularity, the score modifier will be deducted from the basic score. The amount of a modifier varies in range -1.5 until -4.0 for all types of buildings. Examples of vertical irregularity include buildings with setbacks, hillside buildings, and buildings with soft stories (see illustrations of potential vertical irregularities in Figure 2.4). If the building is irregularly shaped in elevation, or if some walls are not vertical, then apply the modifier. If the building is on a steep hill so that over the up-slope dimension of the building the hill rises at least one story height, a problem may exist because the horizontal stiffness along the lower side may be different from the uphill side. In addition, in the up-slope direction, the stiff short columns attract the seismic shear forces and may fail. In this case the performance modifier is applicable.

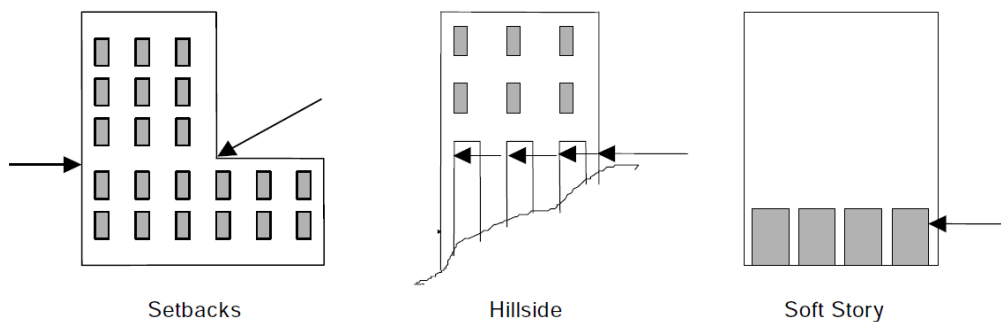


Figure 2.4. The irregularities potential in a vertical direction [16]

A soft-story exists if the stiffness of one story is dramatically less than that of most of the others such as shear walls or infill walls not continuous to the foundation. Soft stories are difficult to verify without knowledge of how the building was designed and how the lateral forces are to be transferred from story to story. There may be shear walls in the building that are not visible from the street. However, if there is a doubt, it is best to be conservative and indicate the existence of a soft story by circling the vertical irregularity score modifier. Use an asterisk and the comment section to explain the source of uncertainty. In many commercial buildings, the first story is soft due to large window openings for display purposes. If one story is particularly tall or has windows on all sides, and if the stories above have a few windows, then it is probably a soft story. A building may be adequate in one direction but be “soft” in the perpendicular direction. For example, the front and back walls may be open but the sidewalls may be solid. Another common example of a soft story is pilotis building.

Several past earthquakes have shown the vulnerability of this type of construction. Vertical irregularity is a difficult characteristic to define, and considerable judgment and experience are required for identification purposes.

2.3.3. Plan Irregularity

Plan irregularity is one of the criteria for modifying score and it can affect all building types. If a structure has this kind of irregularity, the score modifier will be deducted from the basic score. The amount of a modifier is -0.8 for low seismicity and -0.5 for moderate and high seismicity. Examples of plan irregularity include buildings with re-entrant corners, where damage is likely to occur; buildings with good lateral-load resistance in one direction but not in the other; and buildings with major stiffness eccentricities in the lateral force-resisting system, which may cause twisting (torsion) around a vertical axis.

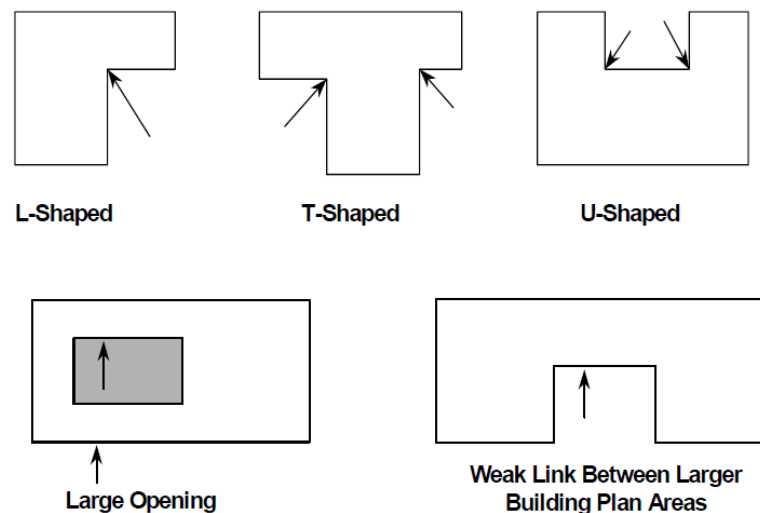


Figure 2.5. Plan views of various building configurations showing plan irregularities; arrows indicate possible areas of damage.

Buildings with re-entrant corners include those with long wings that are E, L, T, U, or + shaped (see Figures 2.5). Plan irregularities causing torsion are especially prevalent among corner buildings, in which the two adjacent street sides of the building are largely windowed and open, whereas the other two sides are generally solid. Although plan irregularity can occur in all building types, the primary concern lies with wood, tilt-up, pre-cast frame, reinforced masonry and unreinforced masonry construction. Damage at connections may significantly reduce the capacity of a vertical-load-carrying element, leading to partial or total collapse.

2.3.4. Post-Benchmark

The post-benchmark score modifier is applicable if the building being screened was designed and constructed after significantly improved seismic codes applicable were adopted and enforced by the local jurisdiction. In high and moderate seismicity regions, the basic structural hazard scores for the various building types are calculated for buildings built after the initial adoption of seismic codes, but before substantially improved codes were adopted. For these regions, score modifiers designated as “Pre Code” and “Post Benchmark” are provided, respectively, for buildings built before the adoption of codes and for buildings built after the adoption of substantially improved codes. In low seismicity regions, the basic structural hazard scores are calculated for buildings built before the initial adoption of seismic codes. for buildings in these regions, the score modifier designated as “Pre Code” is not applicable (N/A), and the Score Modifier designated as “Post Benchmark” is applicable for buildings built after the adoption of seismic codes.

In the case of the post-benchmark in this study, a justification was proposed and used to apply RVS for Indonesian conditions. Indonesia seismic code was first introduced in 1966 and then updated several times in 1983, 2002 and recently in 2012. The 1983 seismic code has significant changes compared with previous code, therefore this year is used as a post benchmark in studies this. Buildings built in 1983 and above are considered adding a score modifier so that the post-benchmark is chosen. Otherwise the building constructed under 1983 is simulated by reducing the score modifier by selecting the pre-code.

2.3.5. Soil Type

Soil type has a major influence on amplitude and duration of shaking, and thus structural damage. The six soil types considered in the RVS procedure: hard rock (type A); average rock (type B); dense soil (type C), stiff soil (type D); soft soil (type E), and poor soil (type F). A shear wave velocity (V_s) is a parameter to determine the classification of soil type. Score Modifiers are provided for soil type C, Type D, and Type E. The appropriate modifier should be circled if one of these soil types exists at the site. If sufficient guidance or data are not available during the planning stage to classify the soil type as A through E, a soil type E should be assumed. However, if the actual site conditions are not known for one- or two-story buildings with a roof height equal to or less than 25 feet (or 7.5 m), a class D soil type may be assumed. There is no score modifier for Type F soil because buildings on soil type F

cannot be screened effectively by the RVS procedure. A geotechnical engineer is required to confirm the soil type F and an experienced professional engineer is required for building evaluation.

2.4. Indonesian Code for Earthquake Resistance Building Design

As mentioned in the introduction, the design of Indonesian building codes has undergone several changes since it was first developed in 1966. The most current code still in effect today is SNI 1726-2012. The objective of the building code philosophy for seismic design is to prevent collapse in the extreme earthquake likely to occur at a building site. Seismic criteria adopted by current model codes involve a two-level approach to seismic hazard, which are the design bases earthquake (DBE) and maximum considered earthquake (MCE). DBE's ground motion has a 10% probability of being exceeded in 50 years (475 year-return period earthquake). The DBE is the design-basis earthquake for conventional building design, with margins provided by the inherent conservatism built into the NEHRP (National Earthquake Hazard Reduction) 1997 Provisions. The ground motion at the DBE level is defined as being two-thirds of the MCE as follow,

$$DBE = \frac{2}{3} \times MCE \dots\dots\dots (2.1)$$

The MCE ground motions are defined as the maximum level of earthquake shaking that is considered reasonable to design a normal structure to resist or the worst-case scenario of an earthquake to be expected. The MCE ground motion is taken as 2% probability of being exceeded in 50 years (2500-year return period earthquake). It is implied that the design in the MCE shaking level has a target performance of near to collapse.

Procedure to determine response spectral design at MCE's condition consider the following parameters,

- 1) Site coefficient corresponding to a short period (F_a)
- 2) Site coefficient corresponding to the 1.0 second period (F_v)
- 3) Mapped spectral response acceleration of MCE ground motion at a short period (S_s)
- 4) Mapped spectral response acceleration of MCE ground motion at the 1.0 second period (S_l)
- 5) Spectral coefficient at a short period (S_{MS})
- 6) Spectral coefficient at the 1.0 second period (S_{MI})
- 7) Spectral coefficient of DBE ground motion at a short period (S_{DS})
- 8) Spectral coefficient of DBE ground motion at the 1.0 second period (S_{DI})
- 9) Fundamental of period (T)

2.4.1. Seismic Ground Motion Maps

In Indonesian Code, SNI 1726-2012, the 5% damped response spectra are constructed from the mapped maximum considered earthquake spectral response at two points. The 1st point denoted as S_S , corresponds to short periods, and the second point denoted as S_I corresponds to the 1.0 second period. Maps for Indonesia seismic intensity have been developed and are shown in Figure 2.6 and 2.7. From the first map, the mapped risk target maximum considered earthquake (MCE_R) spectral response acceleration for a short period, S_S , is found based on the location of the site. The second map is used to determine the mapped MCE_R spectral response acceleration for a 1.0 second period, S_I .

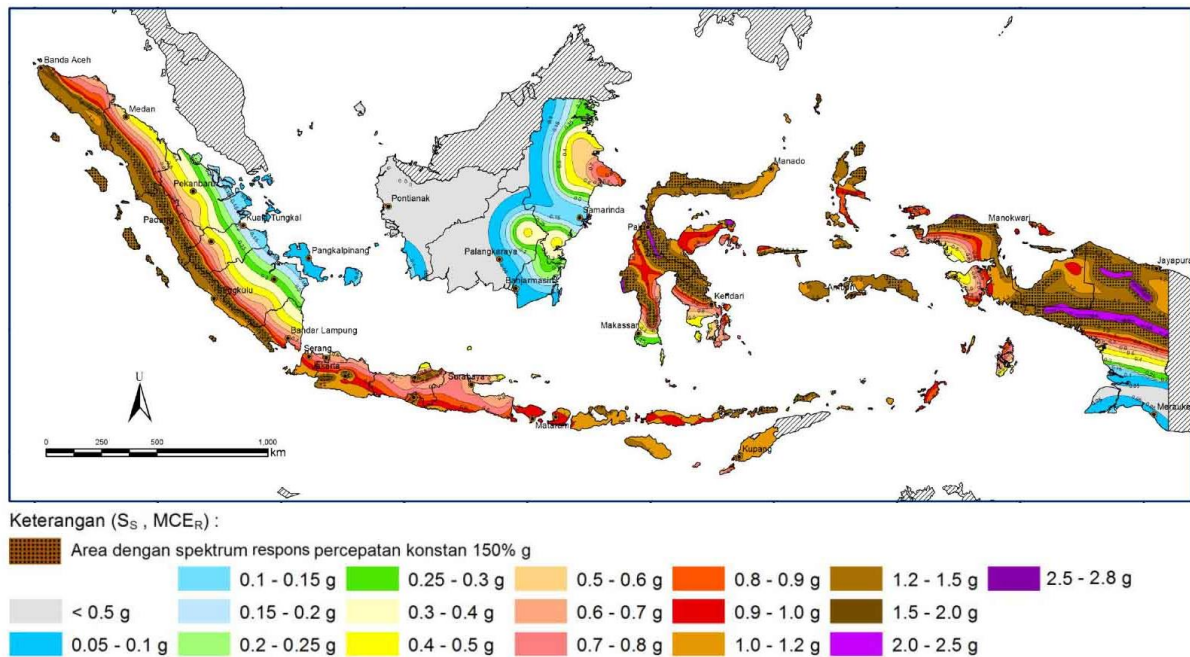


Figure 2.6. S_S , Risk-adjusted maximum considered earthquake (MCE_R) ground motion parameter for Indonesia for 0.2s spectral response acceleration (5% of critical damping) [10]

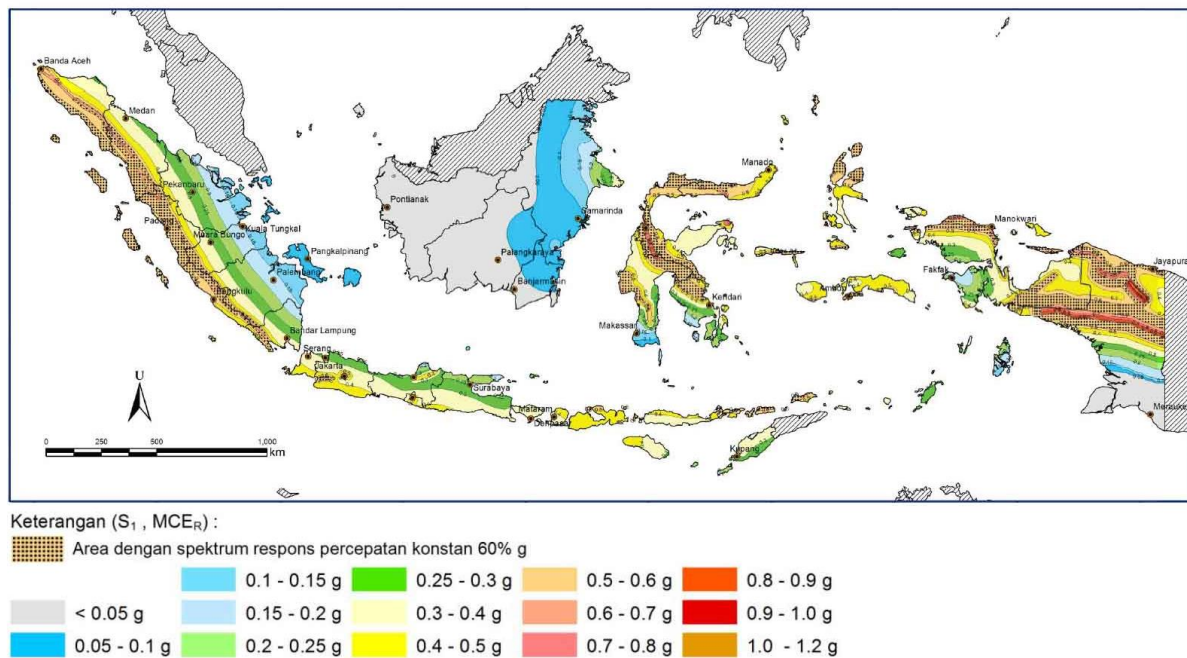


Figure 2.7. S_1 , Risk-adjusted maximum considered earthquake (MCE_R) ground motion parameter for Indonesia for 1.0s spectral response acceleration (5% of critical damping) [10]

2.4.2. Adjustments to Spectral Response for Site Class Effects

The S_S and S_1 values correspond to a site class B, and adjustments must be made if the site in question is other than a site class of B profile. The S_S and S_1 values are adjusted for the site effects by the following formulas:

$$S_{MS} = F_a \times S_S \quad \text{..... (2.2)}$$

$$S_{M1} = F_v \times S_1 \quad \text{..... (2.3)}$$

where F_a is a site coefficient for a short period response, and F_v is a site coefficient for 1 second period response. S_{MS} and S_{M1} are the 5% damped spectral response acceleration of MCE at short and 1.0 second periods, respectively. The values of F_a and F_v are defined by both the local soil condition and the values of S_S and S_1 by using Table 2.4 and Table 2.5.

In Table 2.4 and Table 2.5, Site Class represents a soil condition that consists of 5 classes. Site Class A, B, C, D, and E, which classify as Hard rock, Rock, Dense Soil, Stiff soil and Soft Soil, respectively. The site coefficient seems to increases with the softening of the soil and decrease with decreasing the response acceleration.

Table 2.4. Values of site coefficient F_a as a function of site class and mapped spectral response acceleration at short periods, S_S

Site Class	Mapped Spectral Response Acceleration at Short Periods				
	$S_S \leq 0.25$	$S_S = 0.5$	$S_S = 0.75$	$S_S = 1.0$	$S_S \geq 1.25$
A	0.8	0.8	0.8	0.8	0.8
B	1.0	1.0	1.0	1.0	1.0
C	1.2	1.2	1.1	1.0	1.0
D	1.6	1.4	1.2	1.1	1.0
E	2.5	1.7	1.2	0.9	0.9

A = Hard rock, B = Rock, C = Dense soil, D = Stiff soil, E = Soft soil

Note: Use straight-line interpolation for intermediate values of mapped spectral acceleration at short periods, S_S .

Table 2.5. Values of site coefficient F_v as a function of site class and mapped spectral response acceleration at 1.0 period, S_1

Site Class	Mapped Spectral Response Acceleration at 1 second Period				
	$S_1 \leq 0.1$	$S_1 = 0.2$	$S_1 = 0.3$	$S_1 = 0.4$	$S_1 \geq 0.5$
A	0.8	0.8	0.8	0.8	0.8
B	1.0	1.0	1.0	1.0	1.0
C	1.7	1.6	1.5	1.4	1.3
D	2.4	2.0	1.8	1.6	1.5
E	3.5	3.2	2.8	2.4	2.4

A = Hard rock, B = Rock, C = Dense soil, D = Stiff soil, E = Soft soil

Note: Use straight-line interpolation for intermediate values of mapped spectral acceleration at 1.0 periods, S_1 .

2.4.3. General Design Response Spectrum

To determine the general design response spectrum with 5% damping, two quantities, the 5% damped design spectral response acceleration at short periods, S_{DS} , and at 1-second periods, S_{D1} , are determined by the following equations:

$$S_{DS} = \frac{2}{3} \times S_{MS}$$

$$S_{D1} = \frac{2}{3} \times S_{M1} \dots\dots\dots (2.4)$$

General design response spectrum $S_{A0}(T)$ as a demand acceleration response spectrum with 5% damping of Indonesian code is obtained by the following equation,

$$S_{A0}(T) = \begin{cases} S_{DS} \left(0.4 + 0.6 \frac{T}{T_0} \right) & \dots T \leq T_0 \\ S_{DS} & \dots T_0 < T \leq T_s \\ \frac{S_{D1}}{T} & \dots T > T_s \end{cases} \dots \dots \dots (2.5)$$

where, $T_0 = 0.2 \frac{S_{D1}}{S_{DS}}$, $T_s = \frac{S_{D1}}{S_{DS}}$

The T_0 and T_s is a range of period where the acceleration response has a constant value equal to S_{DS} . Figure 2.8 shows the design response spectrum, Design Bases Earthquake (DBE) ground motions, as it conforms to Indonesian code SNI 1726-2012 [10].

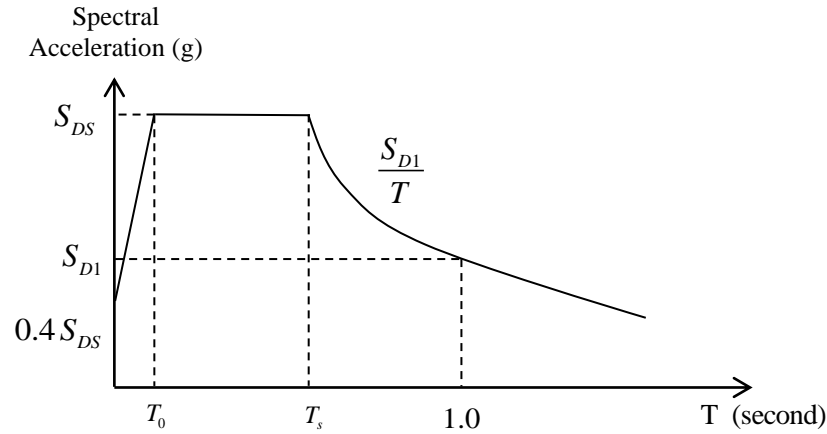


Figure 2.8. General design response spectrum with 5% damping [10]

2.4.4. Seismic Response Coefficient

Seismic base shear, V , in a given direction is obtained by a seismic response coefficient (C_s) and the weight of a structure (W) with the following equation:

$$V = C_s \cdot W \dots \dots \dots (2.6)$$

The seismic response coefficient, C_s , can be determined with considering S_{DS} , a response modification factor (R) and an Importance factor (I_e) as follow:

$$C_s = \frac{S_{DS}}{\left(\frac{R}{I_e} \right)} \dots \dots \dots (2.7)$$

The value of C_S computed with Eq. 2.7 should not be less than 0.01 or $\frac{0.5 \cdot S_1}{(R/I_e)}$ when $S_1 \geq 0.6$ (g).

The response modification response, R , depends on structural material and the structural system. In general, R is in the range of 2.0 to 8.0. The structure that has high ductility will have a high R value.

The importance factor focus on earthquake cause, I_e , depends on a risk factor categorizing from level I until IV and building occupancy. The high risk will have a high important factor, as shown in Table 2.6. The building occupancy generally is in risk category II or III.

Table 2.6. Importance factors by risk category of buildings

Risk Category	Seismic Importance Factor (I_e)	Building Occupancy
I	1.00	Low risk to human life in the event of failure
II	1.00	Except those listed in Risk Categories I, III, and IV
III	1.25	Substantial risk to human life in the event of failure, not included in Risk Category IV
IV	1.50	Essential facilities such as: Fire station, Hospital, Power station (including, but not limited to, facilities that manufacture, process, handle, store, use, or dispose of such substances as hazardous fuels, hazardous chemicals, or hazardous waste)

A fundamental period of the structure, T , is established using the structural properties and deformational characteristics in a proper analysis. In the preliminary analysis, it begins with approximating the fundamental period (T_a). The approximate fundamental period, for structure not exceeding 12 stories could be obtained by the following equation,

$$T_a = 0.1 \cdot N \dots\dots\dots (2.8)$$

in which N is the number of stories above the base.

The fundamental period shall not exceed the upper limit of period $C_u \cdot T_a$, where C_u is an upper limit coefficient. The upper limit coefficient depends on the design spectral acceleration of S_{DI} . Table 2.7 shows the list of the upper limit coefficient.

Table 2.7. Coefficient for the upper limit on the calculated period

Design spectral acceleration of S_{DI}	Coefficient C_u
≥ 0.4	1.4
0.3	1.4
0.2	1.5
0.15	1.6
≤ 0.1	1.7

2.5. Static Nonlinear

The static nonlinear analysis method is used to confirm the existing building condition in this study. The method is also known as pushover analysis, which is to analyze the capacity of a structure until a collapsed state of the structure is reached [20–25]. When a structure is subjected to gravity loading, a monotonic lateral load is applied and continuously increased with an incremental load through elastic and inelastic behavior until an ultimate condition. The lateral load represents a range of base shear induced by earthquake loading, and its configuration is proportional to the distribution of mass along with building height or mode shapes. The output will generate a capacity curve that plots a strength-based parameter against deflection. In general, the load magnification factor in a step is given for a certain value, and then it is calculated to obtain an incremental displacement of a certain node.

When analyzing frame objects, material nonlinearity is assigned to discrete hinge locations where plastic rotation occurs [26–28]. Beam and column components are modeled as nonlinear frame elements by defining plastic hinges at both ends of the elements. As shown in Figure 2.9, The plastic hinges properties have five points labeled A, B, C, D, and E, which defined the force-deformation behavior. The same type of curve is also used for moment and rotation relationship. The value assigned to each of these points varies depending on the type element, material properties, and section size.

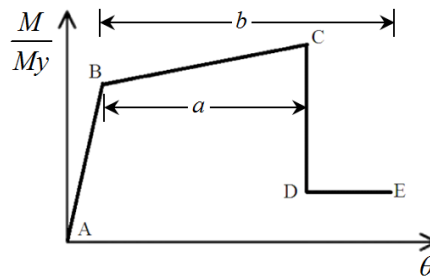
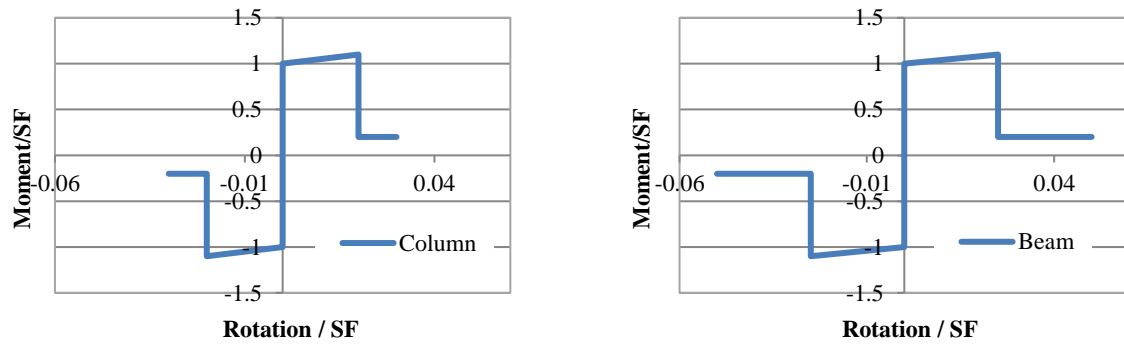


Figure 2.9. Moment-rotation relationship of typical plastic hinge

A linear response is related to a line between point A and an effective yield point B. The slope from point B to point C is typically a small percentage (0% to 10%) of the elastic slope and is included to represent phenomena such as strain hardening. Point C has an ordinate that represents the strength of the element and an abscissa value equal to the deformation at which significant strength degradation begins (line CD). Beyond point D, the element responds with substantially reduced strength until point E. At deformations greater than point E, the seismic element strength is essentially zero [28]. The properties of the plastic hinges for each column and beam are shown in Figure 2.10.



(a) Column plastic hinges

(b) Beam plastic hinges

Figure 2.10. Plastic hinge properties of column and beam

The result of roof drift at maximum shear force is calculated, and the roof drift ratio is determined based on the roof drift divided by the height of the roof structure (see below equation), as shown in Figure 2.11.

$$\text{roof drift ratio} = \frac{\text{roof drift}}{H} \dots\dots\dots (2.9)$$

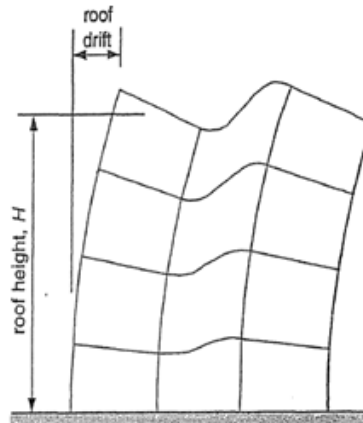


Figure 2.11. Roof drift and roof drift ratio [26]

2.6. Cases Study

In this study, the whole buildings located in Pekanbaru city, Riau province of Indonesia, is selected as a case study. Pekanbaru city has a latitude of 0.507 and a longitude of 101.447 of the Indonesia seismic map [10]. The value of S_S and S_I are determined based on this location from Figures 2.6 and 2.7. For Pekanbaru city, it got S_S of 0.435 (g) and S_I of 0.273 (g). The site classification is soft soil clay, or its classified as D class. The soil amplification as for site coefficient got from Table 2.4,

and 2.5 are F_A of 1.9 and F_V of 2.9. Therefore, the design spectral response can be calculated as follow:

$$S_{DS} = \frac{2}{3} \cdot S_s \cdot F_A = \frac{2}{3} \cdot 0.435 \cdot 1.89 = 0.548$$

$$S_{D1} = \frac{2}{3} \cdot S_1 \cdot F_v = \frac{2}{3} \cdot 0.273 \cdot 2.89 = 0.527 \dots\dots\dots (2.10)$$

The level of the seismic hazard is got high intensity for the S_{DS} greater than 0.5 (g), and S_{D1} is greater than 0.2 (g) refer to Table 2.1.

The range of period where the constant acceleration response occurred is obtained using equation (2.4) as follow:

$$T_0 = 0.2 \cdot (S_{D1} / S_{DS}) = 0.2 \cdot (0.527 / 0.548) = 0.192$$

$$T_s = S_{D1} / S_{DS} = 0.527 / 0.548 = 0.961 \dots\dots\dots (2.11)$$

Therefore, the response spectrum design for the Pekanbaru city in DBE level is plotted in Figure 2.12 as follow:

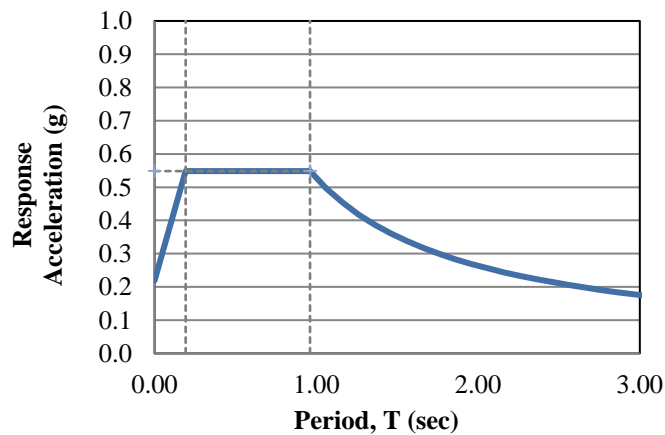


Figure 2.12. Design spectral response of Pekanbaru city (5% damping, soft soil: site class E)

There are fifteen buildings selected to be screened in this study. The entire building is made of reinforced concrete frames classified in categories C1 and C2 according to FEMA 154. The occupancy categories varies including school, residential, office and hospital. All of these buildings have similarity in soil characteristics as the soft soil type. The picture of the building can be seen in the Figure 2.13.



Figure 2.13. Pictures of the various building to be evaluated

The list of the building can be seen in Table 2.8. The highest buildings are the Surya Dumai and the Awal Bros which are 10 stories. Both buildings have a shear wall structure system to resist lateral load.

Table 2.8. The building list as cases study

No	Building	Stories	Occupancy	Structure Type
1	Fmipa	2	School	C1
2	Rusunawa	5	Residential	C1
3	Fisipol	2	School & Office	C1
4	Fkip	2	School & Office	C1
5	FT	3	School & Office	C1
6	RS-UR	5	Hospital & Office	C1
7	Surya Dumai	10	Office	C2
8	Rektorat	4	Office	C1
9	Fekon-1	2	School & Office	C1
10	Fekon-2	2	School & Office	C1
11	Faperika	2	School & Office	C1
12	SPI-UR	2	Office	C1
13	Library	2	School & Office	C1
14	Lemlit	2	Office	C1
15	Awal Bros	10	Hospital & Office	C2

2.7. Result

The rapid visual screening, as mentioned in FEMA P-154, has been done over the 15 buildings as listed in the previous table. The results can be seen in Table 2.9. As can be seen in this table, buildings were built in different years from 1995 to 2014.

The type of structure is typical for the whole building except the Surya Dumai building and Awal Bros as shown in Table 2.8. The main structural type is the concrete moment-resisting frame and the basic score is taken of 2.5. The soil type where the whole building located in the soft soil and it coded by D soil type. The irregularity in the vertical direction only occurred in the Faperika building. It has an irregularity in a vertical direction due to the piloti structure in front of the building as shown in Figure 2.14.

Table 2.9. The screening checklist

No	Building Name	Built (Year)	Structural Type	Soil Type	Vertical Irregularity	Plan Irregularity	Final Score
1	Fmipa	1995	C1	D	-	-	2.7
2	Rusunawa	2014	C1	D	-	-	3.1
3	Fisipol	2010	C1	D	-	X	2.2
4	Fkip	2010	C1	D	-	X	2.2
5	FT	2004	C1	D	-	X	2.2
6	RS-UR	2014	C1	D	-	X	2.6
7	Surya Dumai	1995	C2	D	-	X	2.8
8	Rektorat	1995	C1	D	-	-	3.1
9	Fekon-1	2010	C1	D	-	-	2.7
10	Fekon-2	2014	C1	D	-	-	2.7
11	Faperika	2000	C1	D	X	-	1.2
12	SPI-UR	2014	C1	D	-	X	2.2
13	Library	2010	C1	D	-	X	2.2
14	Lemlit	2000	C1	D	-	-	2.7
15	Awal Bros	2015	C2	D	-	X	2.8



Figure 2.14. Picture of the Faperika building.

The scoring modifier of the whole buildings is described in Table 2.10. The building, below 4 stories, has no scoring modifier, but for buildings that have 4 floors to 7 floors are classified as the mid-rise building and have a scoring modifier of 0.4.

In this study, the building of Rusunawa, RS-UR and Rektorat are classified as mid-rise buildings. The building, which is more than 7 stories, will be modified with the scoring of 0.6. The Surya Dumai building and the Awal Bros building have a modifier value of 0.6.

Table 2.10. The rapid visual screening result

	Reference score	FMIPA	Rusunawa	FISIPOL	FKIP	FT	RS-UR	Surya Dumai	Rektorat	Fekon-1	Fekon-2	FAPERIKA	SPI-UR	Library	Lemlit	Awal Bros
		1	2	3	4	5	6	7	8	9	10	11	12	13	14	15
Basic Score	2.5	2.5	2.5	2.5	2.5	2.5	2.5	2.5	2.5	2.5	2.5	2.5	2.5	2.5	2.5	2.5
Mid Rise (4 to 7 stories)	0.4		0.4				0.4		0.4							
High Rise (>7 stories)	0.6							0.6								0.6
Vertical Irregularity	-1.5											-1.5				
Plan Irregularity	-0.5			-0.5	-0.5	-0.5	-0.5	0.5					-0.5	0.5		0.5
Pre - Code	-1.2															
Post-Benchmark	1.4	1.4	1.4	1.4	1.4	1.4	1.4	1.4	1.4	1.4	1.4	1.4	1.4	1.4	1.4	1.4
Soil Type C	-0.4															
Soil Type D	-0.6															
Soil Type E	-1.2	-1.2	-1.2	-1.2	-1.2	-1.2	-1.2	-1.2	-1.2	-1.2	-1.2	-1.2	-1.2	-1.2	-1.2	-1.2
Final Score (S)		2.7	3.1	2.2	2.2	2.2	2.6	2.8	3.1	2.7	2.7	1.2	2.2	2.2	2.7	2.8
Detail Evaluation required		No	No	No	No	No	No	No	No	No	No	Yes	No	No	No	No

As shown in Table 2.10, The irregularity of the building will be deducted the basic score with a certain modifier value. The modifier value for vertical irregularity is larger than vertical irregularity. The final score is plotted in the columns chart as shown in Figure 2.15. Form this chart, it is easily detected that the whole building no detail evaluation required except for the Faperika building.

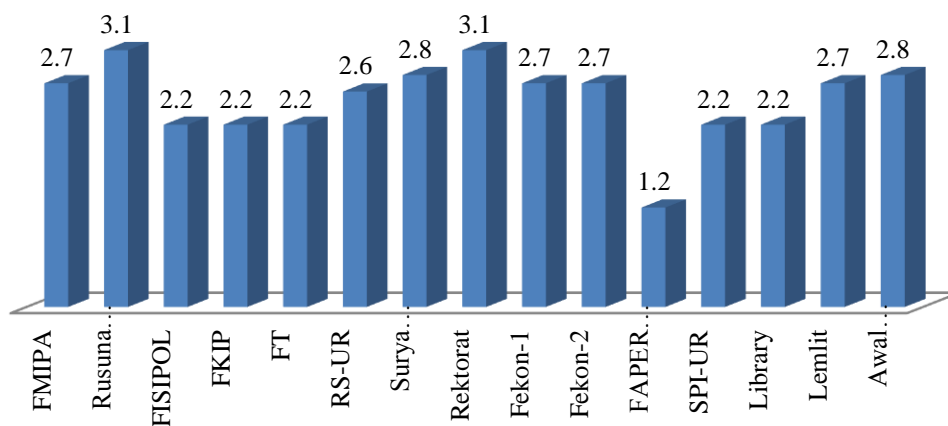


Figure 2.15. Scoring result of rapid visual screening

Nonlinear static analysis was performed over all the above buildings. The deformation of the roof story in the x-axis versus the lateral shear force in the y-axis is plotted on a line chart which namely the capacity curve. Figures 2.16 and 2.17 show the capacity curve of each building, respectively. The tall buildings and also buildings that have a larger floor area will produce a greater shear force.

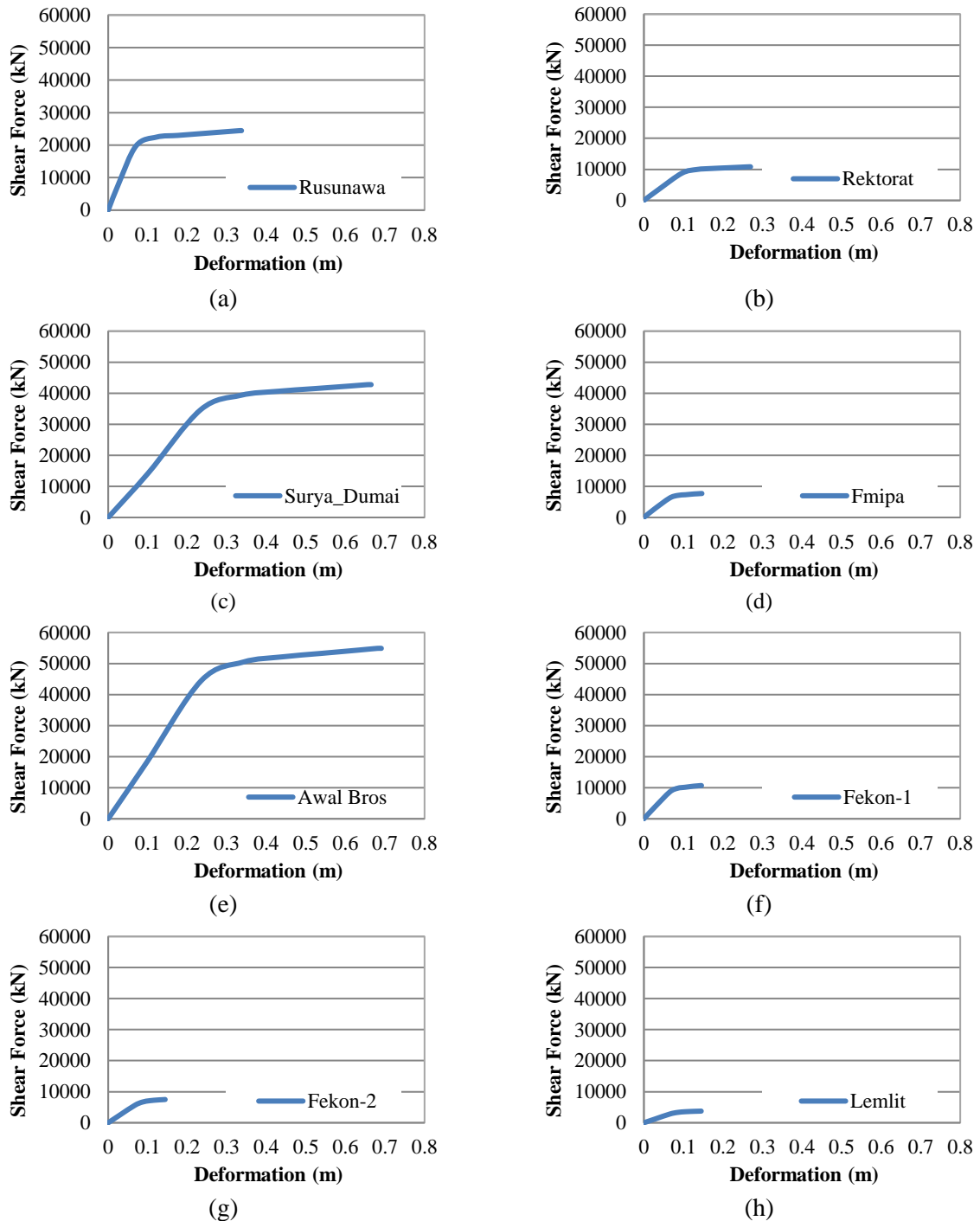


Figure 2.16. Roof deformation

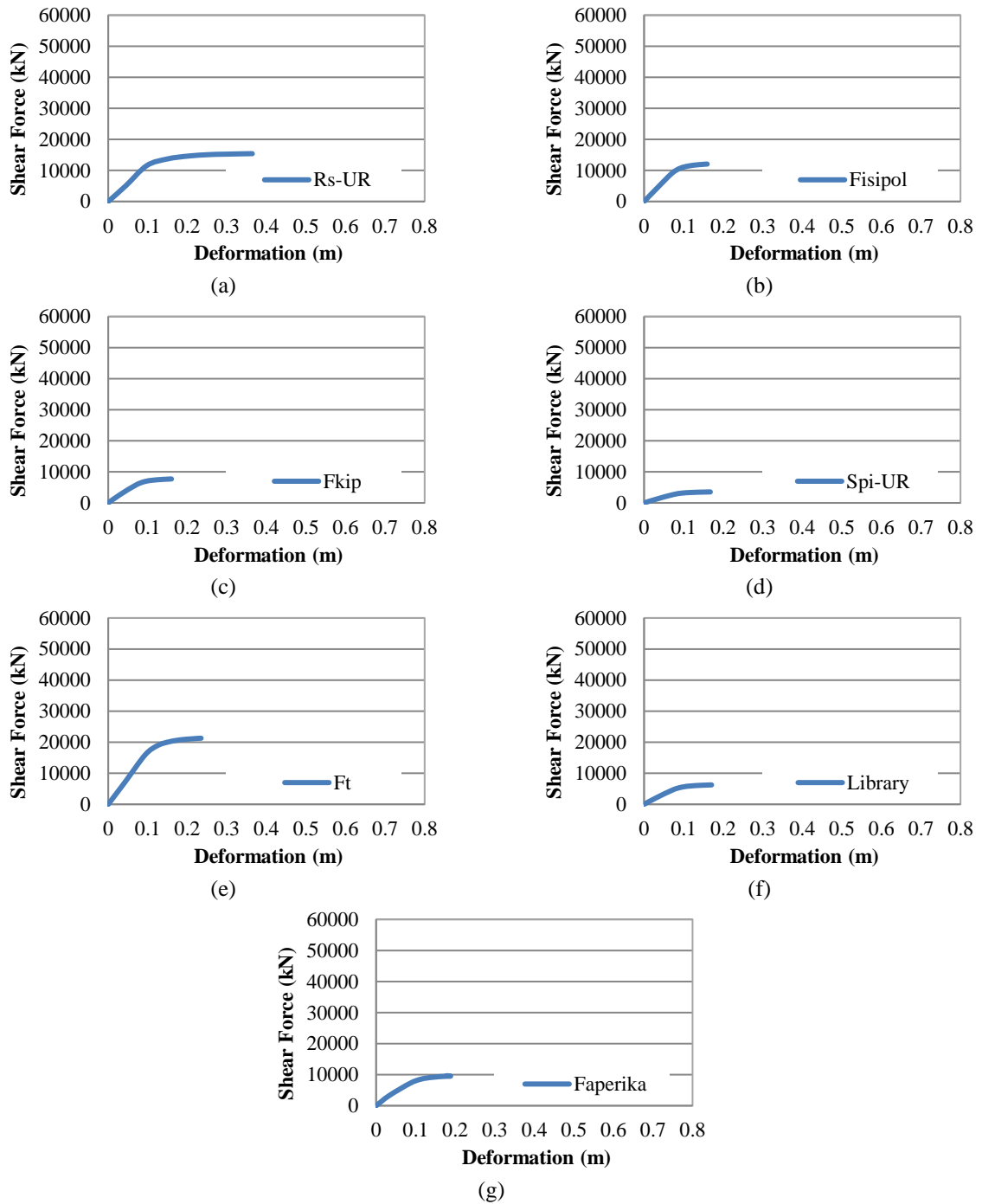


Figure 2.17. Roof deformation (continued)

The comparison between the scoring of RVS, roof deformation and roof drift ratio are described in Table 2.11. At point 11 of Table 2.11 shows that the Faperika building has the roof drift ratio of 0.021 which is beyond the drift limit of 0.02. It confirmed that further detailed evaluation is needed for the

lowest evaluation scoring in the Faperika building. Figure 2.18 is to illustrate the comparison of the roof drift ratio and shear force for each building. The roof drift ratio of the Faperika building has the longest line.

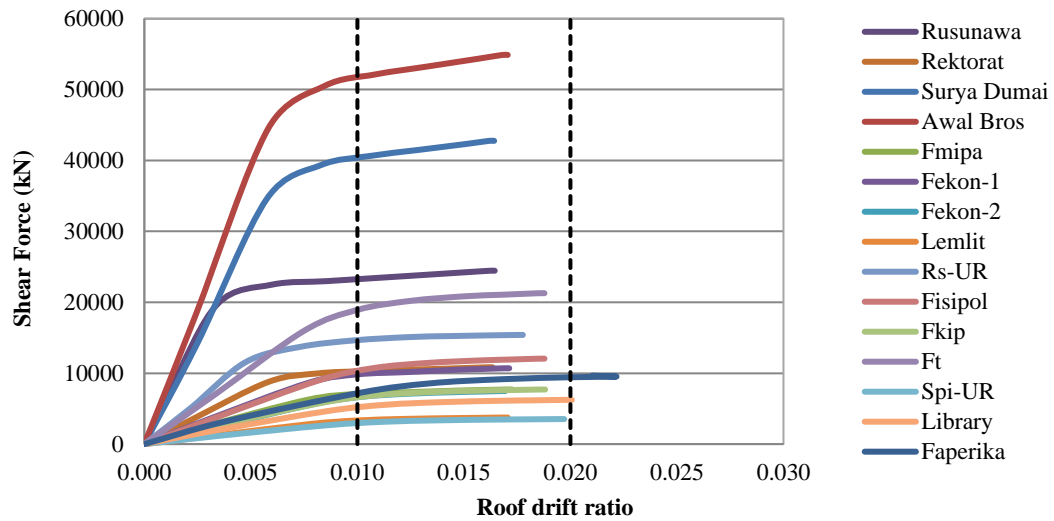


Figure 2.18. Roof drift ratio

Table 2.11. Roof drift ratio

No	Building	Score	Detail Evaluation required	Roof deformation (m)	Roof drift ratio
1	Fmipa	2.7	No	0.145	0.017
2	Rusunawa	3.1	No	0.332	0.016
3	Fisipol	2.2	No	0.157	0.019
4	Fkip	2.2	No	0.158	0.019
5	FT	2.2	No	0.231	0.019
6	RS-UR	2.6	No	0.359	0.018
7	Surya Dumai	2.8	No	0.655	0.016
8	Rektorat	3.1	No	0.266	0.016
9	Fekon-1	2.7	No	0.143	0.017
10	Fekon-2	2.7	No	0.143	0.017
11	Faperika	1.2	Yes	0.179	0.021
12	SPI-UR	2.2	No	0.165	0.019
13	Library	2.2	No	0.168	0.020
14	Lemlit	2.7	No	0.143	0.017
15	Awal Bros	2.8	No	0.680	0.017

2.8. Conclusion

There are fifteen buildings in evaluating in this study. The whole building is located in Pekanbaru city of Indonesia and these were designed by using Indonesian code. These buildings are evaluated by Rapid Visual Screening (RVS) and then the static non-linear analysis is used to confirm the result of the RVS. Only one building is recommended for further evaluation while the rest does not need further evaluation because there is no risk of facing earthquake hazards base on the RVS method. This is confirmed by comparing with the non-linear static analysis method where the results of the roof drift ratio show that buildings that require further evaluation have a roof drift ratio that is greater than the drift limit. Therefore this RVS method can be used for the preliminary evaluation for the large numbers of buildings in a city against the earthquake risk.

Chapter 3

Structural Seismic Evaluation of Indonesia Buildings

3.1. Introduction

Indonesia is an earthquake-prone country that has often experienced an earthquake in the past. The main cause is due to the territory of Indonesia located in the interface of three tectonic plates: Eurasian, Pacific, and Indo-Australian. These plates will continue to move and collide with each other [1, 29].

It is difficult to estimate how big an earthquake during the life of the building will occur. In the experience, many existing buildings collapsed and took many casualties. Currently, SNI 1726: 2012 as a standard building code in Indonesia use to estimate the earthquake demand load [10]. The building, which has been built following the previous standard of SNI 1726-2002 [13] will not meet the regulation of the current standard, and it needs to evaluate.

A large number of buildings in Indonesia makes it difficult to carry out detailed structural evaluations. Therefore, a rapid evaluation is needed to evaluate the number of buildings by screening building characteristics. ASCE 41-13 [28] provides a guideline to evaluate the existing building. The implementation of this procedure will be confirmed in this study, particularly for a screening method. The steel structure with two different systems is selected as case studies. Therefore, the purpose of this study is to evaluate the steel structure with the moment frame and brace frame system, which have been designed following the previous Indonesian code by using a screening evaluation and confirmed with nonlinear static and dynamic analysis.

3.2. Methodology

In this study, a methodology for evaluation begins with screening evaluation by referring to seismic evaluation and retrofit of existing building standards in ASCE 41-13 [28]. The screening procedure is modified in some parts to speed up an evaluation with considering that it will be used for a large number of the existing building in reality. Nonlinear static analysis is performed to analyze the existing capacity of a structure. This method is useful to evaluate the performance of structure until in-elastic conditions under gravity loads of the self-weight of the structure and lateral load as an equivalent of the seismic load. Moreover, nonlinear dynamic analysis is carried out to confirm the existing structure performance.

3.2.1. Screening Evaluations

In general, the evaluation can divide into two parts. The first part considers the general aspects of building and configuration. The existence of tall stories and soft stories, as shown in Figure 3.1, will be observed. The second part focusses on the seismic force-resisting system structure. The general aspect evaluation is carried out by examining the shape of the building, whether it stands upright or not, and the layout of each floor. Then, the existence of mezzanine floors and the surrounding condition is also observed.

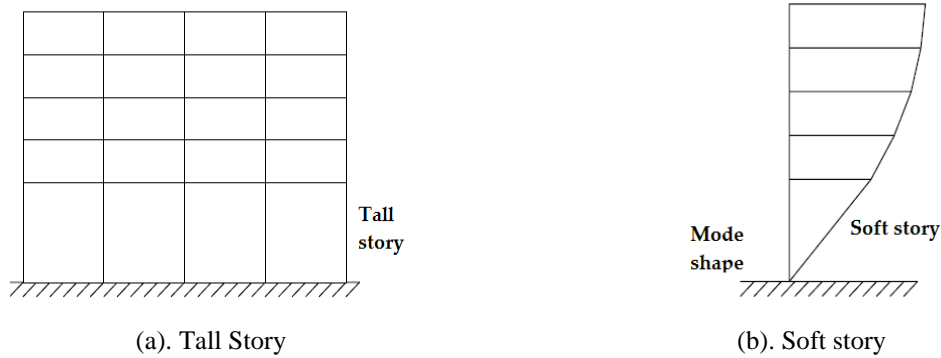


Figure 3.1. Tall Story and soft story

Analysis of the building configuration of the entire structure is required to obtain the seismic demands of strength and stiffness. The weak story will occur if the total of the shear strengths in any story is less than 80% of the strength in the adjacent story. The weak story occurs if vertical discontinuities exist or if a member size is reduced significantly.

The nominal shear strength, V_n , of unstiffened or stiffened webs, according to the limit states of shear yielding and shear buckling for singly or doubly symmetric members, is obtained as follow:

$$V_n = 0.6 \cdot F_y \cdot A_w \cdot C_v \dots\dots\dots (3.1)$$

where F_y is the yield stress, A_w is the area of the shear section, and C_v is a ratio of critical web stress to shear yield stress. The value of C_v depends on whether the limit state is web yielding, web inelastic buckling, or web elastic buckling. For the double symmetric section in the major axis direction, the shear area is calculated with considering the web area (A_w), where is the total height of section (h) multiplied by the web thickness (t_w). But in the minor axis direction, the shear area is determined by considering the area of both flange (A_f), where the flange width (b_f) is multiplied by the flange thickness (t_f). Due to this, for the wide-flange section (W-section), the shear strength in the minor axis is larger than the major axis.

In order to maintain a soft story, the stiffness of the lateral force-resisting system in any story should not be less than 70% of the above story stiffness or should not be less than 80% of the average stiffness of the above three stories. This condition commonly occurs in commercial buildings with open fronts on the ground floor with particularly tall first stories, as shown in Figure 3.1a. A tall story or a change in the type of seismic force-resisting system is an obvious indication that a soft story might exist. A gradual reduction of seismic-force-resisting elements as the building increases in height is typical and is not considered a soft story condition. Another simple first step might be to plot and compare the story drifts, as indicated in Figure 3.1b if analysis results happen to be available. The difference between “soft” and “weak” stories is the difference between stiffness and strength. A change in column size can affect strength and stiffness, and both need to be considered.

Evaluation of the seismic force-resisting system consists of three groups. Group 1 is for the seismic force-resisting component, group 2 is for connecting component, and group 3 is for diaphragms component. The axial stress subjected to overturning forces, denoted by P_{ot} , caused by gravity loads at the column base shall be calculated by:

$$P_{ot} = \frac{1}{M_s} \cdot \left(\frac{2}{3}\right) \cdot \left(\frac{V \cdot h_n}{L \cdot nf}\right) \cdot \left(\frac{1}{A_{col}}\right) \dots\dots\dots (3.2)$$

Where nf is the total number of frames, V is a pseudo seismic force, h_n is the height above the base to the roof level, M_s is system modification factor and A_{col} is an area of the column. The axial stress is compliant if P_{ot} less than $0.10 F_y$.

In a brace frame system, the axial stress in a diagonal bracing component can be obtained by the following equation:

$$f_j^{avg} = \frac{1}{M_s} \cdot \left(\frac{V_j}{s \cdot N_{br}} \right) \cdot \left(\frac{L_{br}}{A_{br}} \right) \dots\dots\dots (3.3)$$

Where L_{br} is the average length of the braces, N_{br} is the number of braces in tension and compression, s is the average span length of braced spans, A_{br} is the average area of a diagonal brace, V_j is the maximum story shear at each level and M_s is the system modification factor. The axial stress in the diagonals is maintained be less than $0.50 F_y$.

The redundancy of moment frame numbers in each principal direction shall be considered to be equal or greater than 2. The compact or non-compact section shall be calculated based on the ratio width over the thickness of the section. The ratio limit for moderate ductile members is taken as $0.38\sqrt{E/F_y}$ for flange and $3.76\sqrt{E/F_y}$ web.

Steel columns that are part of the seismic force-resisting system must be connected to the transfer of uplift and shear forces at the foundation. The floor and roof diaphragms must be adequately connected to the steel frames to provide a complete load path for shear transfer between the diaphragms and the frames. This connection may consist of shear studs or welds between the metal deck and steel framing. Evaluation of diaphragms observes opening in the frame, plan irregularities, and reinforcement at the opening. Large openings at moment frames or braced frames significantly limit the ability of the diaphragm to transfer seismic forces to the frame.

3.2.2. Static Nonlinear Analysis

Static nonlinear analysis is also known as pushover analysis is a method to analyze the capacity of a structure until an ultimate condition or a collapsed state of the structure is reached [26]. When a structure is subjected to gravity loading, a monotonic lateral load is applied and continuously increased with an incremental load through elastic and inelastic behavior until an ultimate condition. The lateral load represents a range of base shear induced by earthquake loading, and its configuration is proportional to the distribution of mass along with building height or mode shapes. The output will generate a capacity curve that plots a strength-based parameter against deflection. There are two kinds of the incremental method can be used in this analysis, there are a load increment method and a displacement increment method. This study uses a displacement increment method. In general, the load magnification factor in a step is given for a certain value and then it is calculated to obtain an incremental displacement of a certain node.

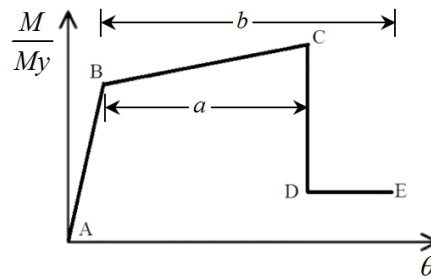


Figure 3.2. Moment-rotation relationship of typical plastic hinge

In order to obtain force-deformation behavior, a couple of hinges are assigned in each frame of a component in a structure. A flexural hinge may represent a moment-rotation relation of a beam or a column with certain properties that can be seen in Figure 2. As shown in this figure, a hinge curve has five points of A, B, C, D, and E which defined a force-deformation or a moment-rotation relationship.

The value assigned to each point varies depending on the element type, material properties, and section size. A linear response is related to a line between point A and an effective yield point B. The slope from point B to point C is typically a small percentage (0% to 10%) of the elastic slope and is included to represent phenomena such as strain hardening. Point C has an ordinate that represents the strength of the element and an abscissa value equal to the deformation at which significant strength degradation begins (line CD). Beyond point D, the element responds with substantially reduced strength until point E. At deformations higher than point E, the seismic element strength is essentially zero [28].

3.2.3. Dynamic Nonlinear Analysis

Nonlinear response analysis is the relationship between the deformation of the structure and the restoring force is in a nonlinear relationship. In actual structures, when the structures are subjected to excessive earthquake motions, large deformations occur, and phenomena such as yielding and cracking of members, buckling of members, and slipping of joints will appear. In these cases, the relationship between the deformation and the restoring force does not only show a linear relationship but also show inelastic loop properties. This type of force-displacement relationship is called the hysteretic restoring force characteristics. As buildings undergo strong earthquakes, the structural frames may inevitably undergo plastic deformation due to cyclic yields. Hence, the ability of inelastic deformation and the capacity of hysteretic energy absorption of structures are essential in considering structural safety. In order to evaluate the seismic resistance capacity of building structures, it is

indispensable to perform a nonlinear (inelastic) seismic response analysis considering the material nonlinearity [25].

Numerical integration methods by using Newmark β method is used to solve the nonlinear seismic response of the structure. In general, the equations of the Newmark β method are expressed as,

$$\dot{u}_{i+1} = \dot{u}_i + \frac{\ddot{u}_i + \ddot{u}_{i+1}}{2} \Delta t \quad (3.4)$$

$$u_{i+1} = u_i + \dot{u}_i \Delta t + \left(\frac{1}{2} - \beta \right) \Delta t^2 \ddot{u}_i + \beta \Delta t^2 \ddot{u}_{i+1} \quad (3.5)$$

$$m \cdot \ddot{u}_{i+1} + c \cdot \dot{u}_{i+1} + k \cdot u_{i+1} = -m \cdot \ddot{u}_{g \ i+1} + g \cdot (u_{i+1}) \quad (3.6)$$

$$g(u_{i+1}) = k_L u_{i+1} - Q(u_{i+1}) \quad (3.7)$$

Setting β to various values between 0.0 and 1.0 can give a wide range of results. Typically $\beta = 1/4, 1/6$ which yield the constant average acceleration method and the linear acceleration method, are used.

An important part of the nonlinear response analysis is the modeling of the restoring force of the structure. In general, the restoring force is not uniquely determined by the displacement, but it varies depending on the incremental displacement (loading or unloading) and the previous loading history. A simplified analytical model is needed to carry out nonlinear seismic response analysis by referring to the characteristics of actual restoring force which obtain from experimental results.

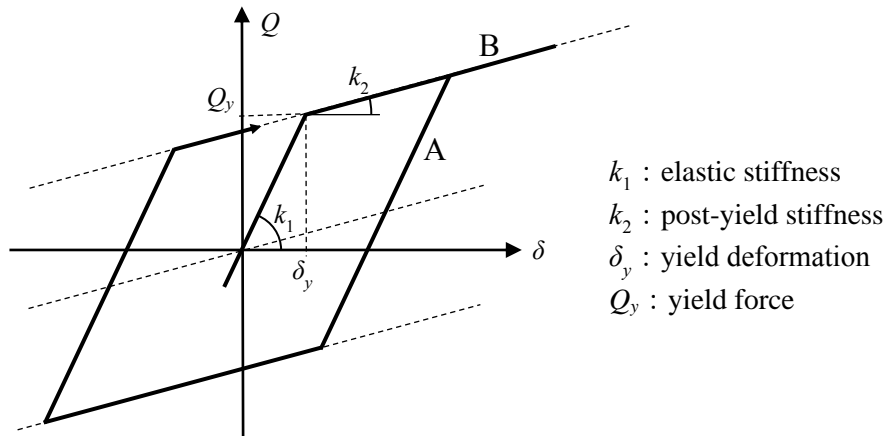


Figure 3.3. Bilinear model

Figure 3.3 illustrates a bilinear model in which the post yielding stiffness $k_2 = \kappa.k$ takes on the positive or negative values (where κ = stiffness ratio; k = linear elastic stiffness). In general, the bilinear models are widely adopted as a numerical model of a steel frame structure and a buckling restrained brace frame. The numerical algorithm of the bilinear model is used in this study.

3.2.4. Simulated Ground Motion

A nonlinear dynamic analysis is performed with subjected to earthquake ground motions to obtain forces and displacements. The calculation of response is very sensitive in single ground motion characteristics, in consequence, it is required to carry out an analysis with more than one of ground motion. Nakazawa (2016) creates a program to calculate a simulated earthquake ground motion as known as SIMEQ [30]. When conducting the time history elastoplastic nonlinear response analysis, it is necessary to prepare the time history data as an input earthquake motion, which fits with a design response spectrum. Various methods are proposed about the production method of the time history input earthquake motion data. As a typical method, there is the method (called a sine wave synthetic method) of fitting to a target design response spectrum by stacking up sine waves.

In this method, the time history input earthquake motion $y(t)$ is expressed as,

$$y(t) = e(t) \times \sum_{i=1}^N A_i \cos(\omega_i t + \phi_i) \dots\dots\dots (3.8)$$

in which $e(t)$ is an envelope function representing the non-stationarity. N is the number of components. A_i , ω_i and ϕ_i represent an amplitude, a circle frequency and a phase angle of the i -th component. The ϕ_i is often used a uniform number that it takes randomly.

On the other hand, without using $e(t)$ function, a method to generate the simulated earthquake motion is adopted by using the phase angle ϕ_i of the observed earthquake motion data.

$$y(t) = \sum_{i=1}^N A_i \cos(\omega_i t + \phi_i) \dots\dots\dots (3.9)$$

The program, using Eq.(3.8) is a program that creates a simulated ground motion to various target spectrum.

El-Centro (Imperial Valley) in 1940, Kobe (Hanshin) in 1995, and Taft (Kern County) in 1952 are used as input ground motion in this analysis. In order to meet a target of peak ground acceleration

(PGA) in accordance with the Indonesia seismic code, a simulated ground motion method is used for scaling PGA of earthquake data to be equal with PGA of a certain location in Indonesia.

3.3. Case Study

There are two buildings made from the steel structure evaluated in this study. The first is the 6th stories building with a moment frame system for resisting seismic force, and the second is the 10th stories with a braced frame system. These buildings have been designed based on the previous Indonesia code [11, 13, 31]. The numerical model of these buildings can be seen in Figure 3.4.

Table 3.1. Summarize section property in the 6th story structure.

No	Component	Section Type	Fy (MPa)	Fu (MPa)
1	Column 1st -3rd floor	W 400.400.13.21	345	450
2	Column 4th -6th floor	W 300.300.10.15	345	450
3	Beam	W 400.200.8.13	345	450

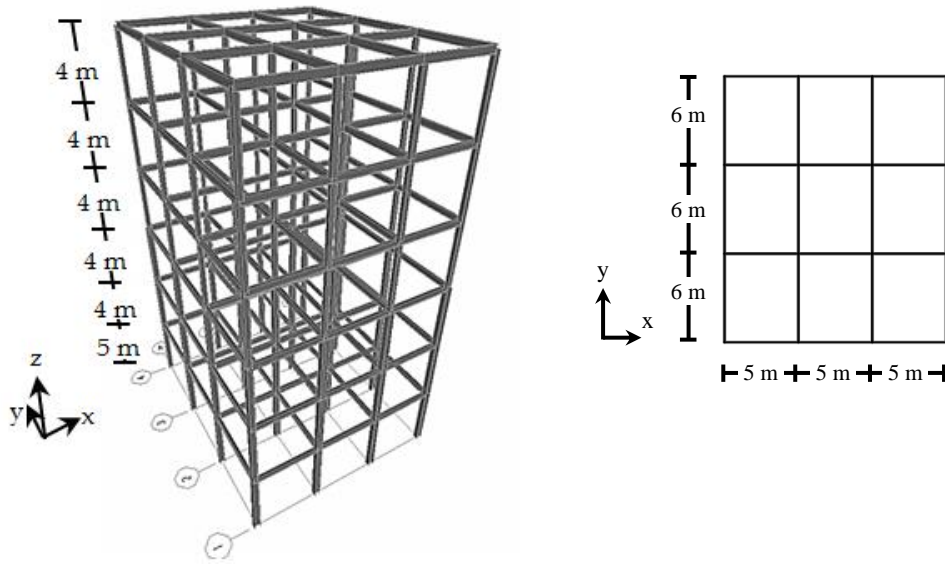
Figure 3.4a is a moment frame (MF) system of three bays in the x-direction with a uniform length of 5 m and three bays in the y-direction with a uniform length of 6 m. Table 3.1 shows the section properties of structural components.

The 10th story structure, as shown in Figure 3.4b, has two combination resisting systems, there is a moment frame in the XZ plane and a braced frame with X-bracing system in the YZ plane. The structure has five bays in the X- direction with a typical length of 5 m except in the middle span of 6 m and three bays in the Y- direction with a total length of 14 m. The height of the first story is 5 m, and the 2nd story to 10th story is 4 m uniformly. Section properties for each component element are summarised in Table 3.2.

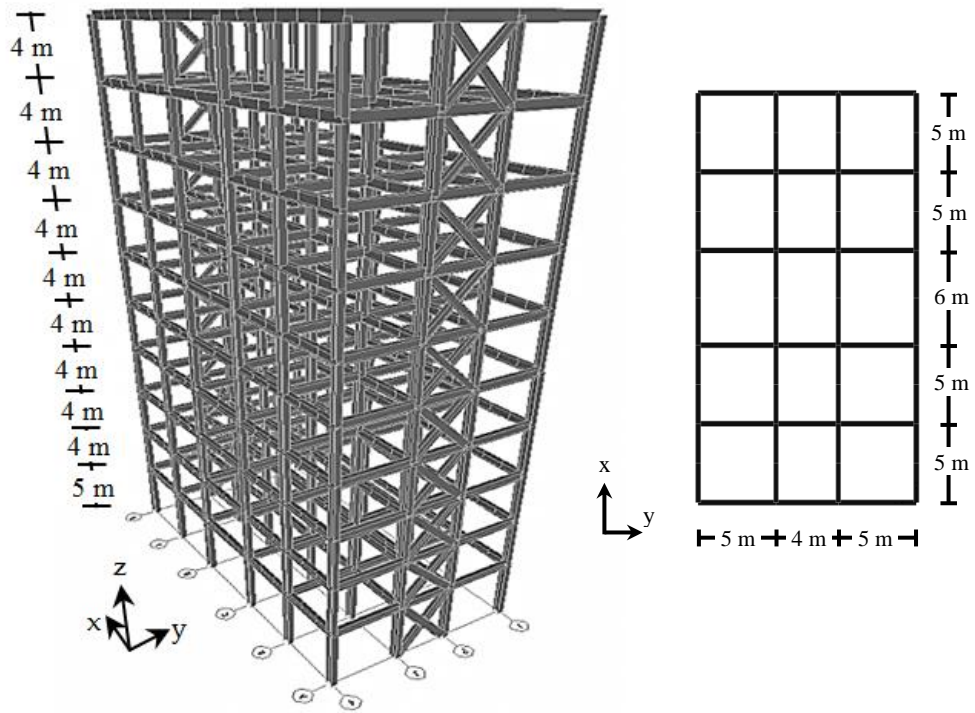
Table 3.2. Summarize section property in the 10th story structure.

No	Component	Section Type	Fy (MPa)	Fu (MPa)
1	Column 1 st floor	W 550.450.110.70	345	450
2	Column 2 nd -5 th floor	W 500.430.89.55	345	450
3	Column 6 th -10 th floor	W 450.400.70.45	345	450
4	Beam	W 700.350.70.40	345	450
5	Bracing 1 st floor	W 700.300.28.15	345	450
6	Bracing 2 nd - 5 th floor	W 610.320.25.15	345	450
7	Bracing 6 th - 10 th floor	W 500.300.18.11	345	450

Theses building are located in Padang city of Indonesia, where has a high level of seismicity based on Indonesia code, as shown in Figure 3.5. From this figure, it obtained Padang city has maximum expected ground acceleration (MCE) in the range 1.2 – 1.5g for S_S and in the area of 60% g for S_I .

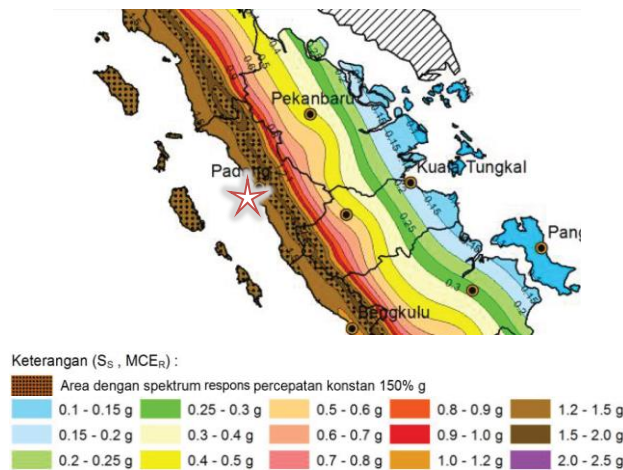


(a) The 6th stories MF steel structure model

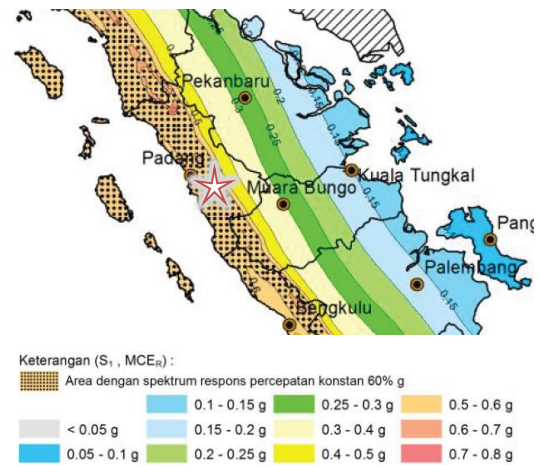


(b) The 10th stories BF steel structure model.

Figure 3.4. Perspective and floor plan



(a). S_s (0.2 of Period)



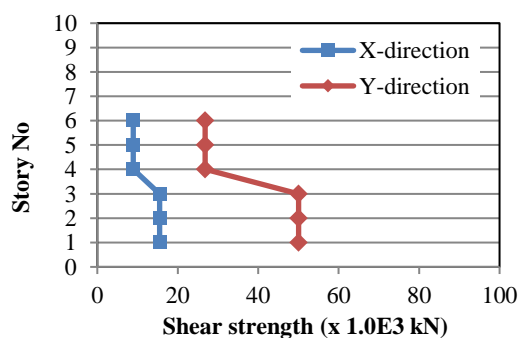
(b). S_1 (1.0 of Period)

Figure 3.5. Spectral response acceleration of Padang city (5% of critical damping) [10].

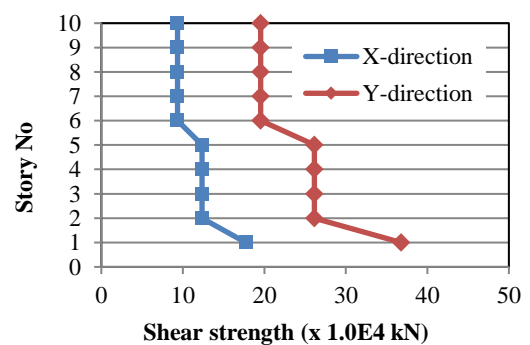
3.4. Result and Analysis

3.4.1. Screening Evaluations Result

The evaluation results of both buildings are summarized in Table 3.3. From Table 3.3, in part a, Both building is standing upright, and there is no discontinuity of resisting lateral system element. The surrounding condition of the observation result has no adjacent building at a distance of 2 meters. A mezzanine floor is also not available in both buildings. All item evaluations in Part A are compliant (C).



(a) Shear capacity of MF building



(b) Shear capacity of BF building

Figure 3.6. Total shear capacity per layer of MF and BF building

Table 3.3. Basic configuration evaluation of building A (MF) and building B (BF)

No	Description	Result	Building A (MF)	Result	Building B (BF)
			Remark		Remark
A. General					
1	Straightness of buildings	C	The building stands upright	C	The building stands upright
2	Load Path	C	There is no discontinuity of element to resist the seismic force	C	There is no discontinuity of element to resist the seismic force
3	Adjacent buildings	C	There is no building at a distance of 2 meters	C	There is no building at a distance of 2 meters
4	Mezzanines	C	No mezzanine floor	C	No mezzanine floor
B. Building Configuration					
5	Weak story	NC	The total of the shear strengths in story 4 is less than 80% of the strength in story 3	NC	The total of the shear strengths in story 2 and 6 are less than 80% of the bottom
6	Soft story	NC	In story 3 and 4, the total stiffness is less than 80%	C	No soft-story
7	Vertical irregularities	C	All vertical elements are continuous to the foundation	C	All vertical elements are continuous to the foundation
8	Geometry	C	Typical floor plan and view	C	Typical floor plan and view
9	Mass	C	Uniform mass	C	Uniform mass
10	Torsion	C	No Torsion	C	No Torsion

From Table 3.3, in part b, There were founded non-compliant (NC) in the weak story and the soft story due to shear strength and stiffness. The shear capacity of both buildings in any story can be seen in Figure 3.6. From Figure 3.6a, MF building obviously has weaker layers in the upper group of story 4,5,6 if we compare with the bottom group of story 1,2,3. The difference in shear strength in adjacent stories 3 and 4 is 58% for x-direction and 54% for y-direction. On the other side (Figure 3.6b), the upper group layer of the sixth story up to the roof story is weaker than the mid group layer of the second story up to story 5. The mid-layer is also weaker than the bottom layer of the story 1. The gap differences ratio in adjacent story 1 and 2 is 70% in the x-direction and 71% in y-direction wherein adjacent story 5 and 6 is 76% in the x-direction and 75% in the y-direction. Thus, both buildings have deficiencies in the weak story.

Figure 3.7 shows the total stiffness in any stories of both buildings. In the MF building, it found a significant difference of stiffness at adjacent stories 3 and 4 in both directions X dan Y, where the differences are around 50% from stories 3 to 4 in Y-direction (Figure 3.7a). On the other hand, the BF building has two significant differences in stiffness that is in story 1 to 2 and story 5 to 6. However,

the difference stiffness in the 6th story is more considerable compare to the 1st story, as shown in Figure 3.7b.

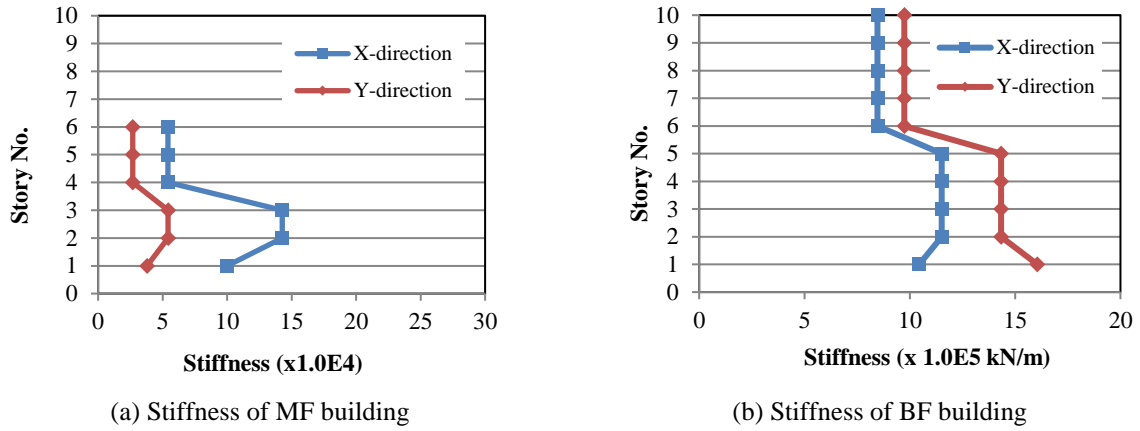


Figure 3.7. The total stiffness of MF and BF building in any stories

The result evaluation of the structural seismic resisting component summarises in Table 3.4 and Table 3.5 for MF and BF building, respectively. The axial stress of column caused by overturning forces is compliant (C) for both buildings were less than $0.3 \cdot f_y$. The result calculation use equation 1 is $2.1 \text{E}4 \text{ kN/m}^2$ for MF building and $2.0 \text{E}4 \text{ kN/m}^2$ for BF building where $0.3 \cdot f_y$ is $1,04 \text{E}5 \text{ kN/m}^2$.

Item no. 4 in Table 3.4, the MF building was founded not-compliant (NC) for non-compact sections due to column and beam sections have a slenderness ratio beyond a maximum limit. The column sections of W400.400.13.21 and W300.300.10.15 have a slenderness ratio of the flange of 9.5 and 10, respectively, where the maximum limit of a slenderness ratio is 9.4 for material with the tensile stress of 345 MPa. The beam section of W400.400.8.13 has a slenderness ratio of 15.38, which also exceeds the maximum limit. Using of non-compact members is not recommended in this procedure.

There is also NC at item no.10 in Table 3.4. The strong column weak beam (SCWB) are not satisfied in the stories 4, 5, and 6, where the total moment capacity of the beam is larger than the column.

In group section of B and C of Table 3.4, The evaluation of the connection and the diaphragm system meet the criteria. The connection has the shear studs between the metal deck and steel frames, and the diaphragm has adequate capacity to transfer seismic forces to the frame.

Table 3.4. Structural evaluation of the moment frame (MF) structure

No	Description	Result	Remarks
A. Seismic-Force-Resisting System			
1	Column axial stress	C	The axial stress of the overturning force is less than $0.3 \cdot f_y$
2	Redundancy	C	The redundant frame (more than one bays)
3	Column splices	C	No column splice
4	Compact member	NC	Non-compact section
5	Drift check	C	Story drift ratio is less than 0.015
6	Flexural stress check	C	The average flexural stress of sections is less than f_y
7	Interfering walls	C	Adequate wall isolation
8	Moment-resisting connection	C	Adequate connection
9	Panel zones	C	Panel zone can resist the shear demand at the face of the column
10	Strong column - weak beam (SCWB)	NC	There were not SCWB in the beam-column joint of story 4, 5 and 6
11	Beam penetrations	C	No web opening in beam frame
12	Girder flange continuity plates	C	Continuity plates installed
13	Bottom flange bracing	C	Bottom flange bracing installed
B. Connection			
1	Steel columns	C	Foundation and anchorage system can develop the least of the tensile capacity of the column
2	Transfer to the steel frame	C	The floor has adequate connections with frame structure (welded and shear studs)
C. Diaphragms			
1	Opening at frames	C	No diaphragm opening
2	Plan irregularities	C	Regularities
3	Diaphragm reinforcement at opening	C	No diaphragm opening

Table 3.5 presents the structural evaluation of the brace frame structure. From Table 3.5, The average axial stress on the diagonal bracing elements, as computed using Eq. (3.3), does not comply with the requirement where the axial stress is $2.8E5 \text{ kN/m}^2$ and this is greater than $0.5 \cdot F_y$ equal to $1.7E5 \text{ kN/m}^2$ (Table 3.5 point 6). The other items of evaluation are compliant for BF building.

Table 3.5. Structural evaluation of the brace frame (BF) structure

No	Description checklist	Result	Remark
A. Seismic-Force-Resisting System			
1	Column axial stress	C	The axial stress of the overturning force is less than $0.3 \cdot f_y$
2	Redundancy	C	The redundant frame (more than 1 bays)
3	Column splices	C	No column splice
4	Compact member	C	Compact section
5	Out-of-plane bracing	C	No potential out of plane buckling occurred
6	Brace axial stress	NC	Average of axial stress is greater than $0.5 F_y$
7	The slenderness of diagonal brace	C	All slenderness of brace elements less than 200
8	Tension-only braces	C	Adequate capacity
9	Concentrically braced frame joints	C	Concentrically
B. Connection			
1	Steel columns	C	Foundation and anchorage system can develop the least of the tensile capacity of the column
2	Transfer to the steel frame	C	The floor has adequate connections with frame structure (welded and shear studs)
C. Diaphragms			
1	Opening at frames	C	No diaphragm opening
2	Plan irregularities	C	Regularities
3	Diaphragm reinforcement at opening	C	No diaphragm opening

3.4.2. Result of Nonlinear Static Analysis

Nonlinear static analysis has been done to obtain the capacity curve of the structure. The static nonlinear analysis was performed under gravity and lateral load. With a particular increment, the lateral load increased until the plastic condition reached. A control displacement was performed at the roof. When it reaches a target displacement, the analysis will stop. The target displacement intends to represent the maximum displacement likely to be experienced during the design earthquake.

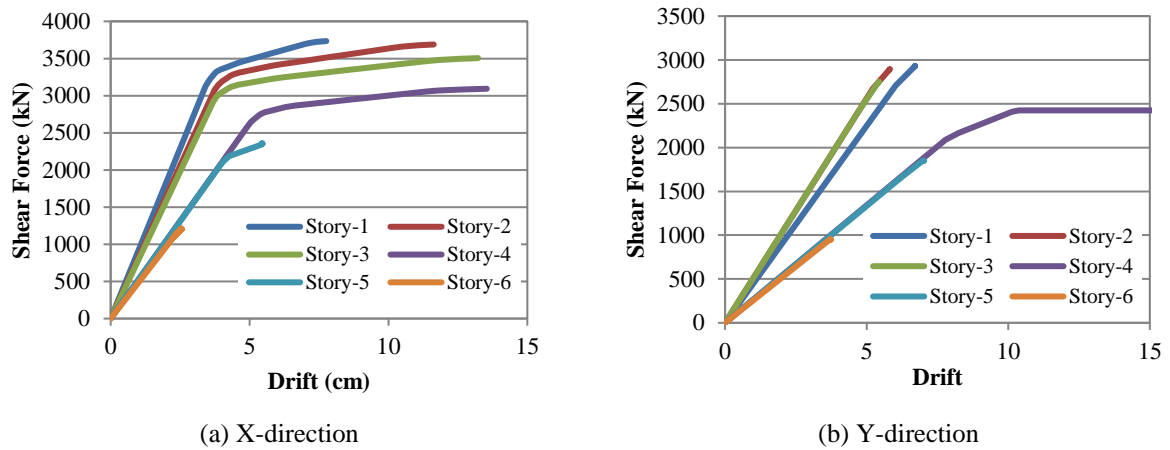


Figure 3.8. The capacity curve of MF structure in X-direction and Y-direction

Figure 3.8 shows the relationship of story drift and shear force in X and Y directions for any stories. The maximum drift occurred in the 4th story, and the minimum drift is in the 1st story. The ratio of the maximum and the yield drift called a ductility factor obtained for any stories, as shown in Table 3.6.

Table 3.6. Ductility factor in any stories of MF building

Story- <i>i</i>	X-direction			Y-direction		
	δ_{y-i}	δ_{max-i}	μ_i	δ_{y-i}	δ_{max-i}	μ_i
1	4.72	7.75	1.64	6.54	6.71	1.03
2	6.25	11.42	1.83	5.67	5.82	1.03
3	6.99	12.93	1.85	5.38	5.44	1.01
4	5.75	13.33	2.32	7.74	28.96	3.74
5	4.88	5.89	1.21	7.03	6.94	0.99
6	2.67	2.71	1.02	3.74	3.74	1.00

The capacity curves are plotted for the 1st story until the 6th story for X-direction, as shown in Figure 3.9. Following the ductility in Table 3.6, it can be seen that the 4th story has the longest drift.

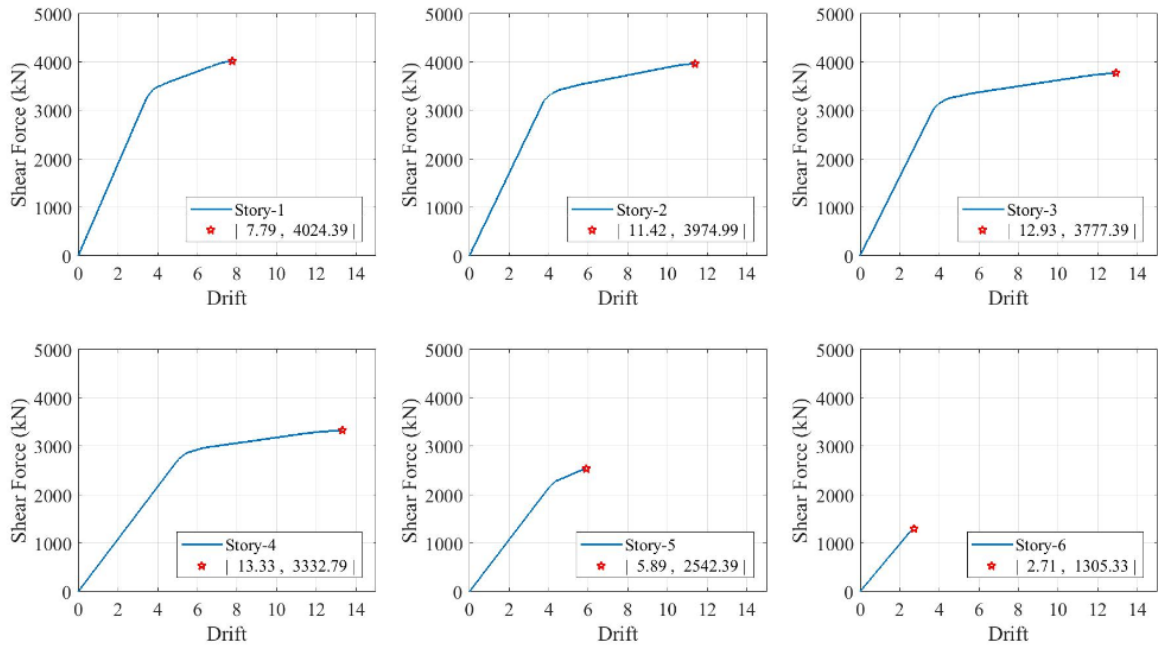


Figure 3.9. The capacity curve of MF building for any stories in X-direction

Moreover, the capacity curve for Y-direction plotted in Figure 3.10. As shown in this figure, the 4th stories have the plateau curve after beyond the yield point. It explained that the 4th story has experienced in yielding. Table 3.6. also explained that the ductility factor in the 4th story has the highest value compared to the others.

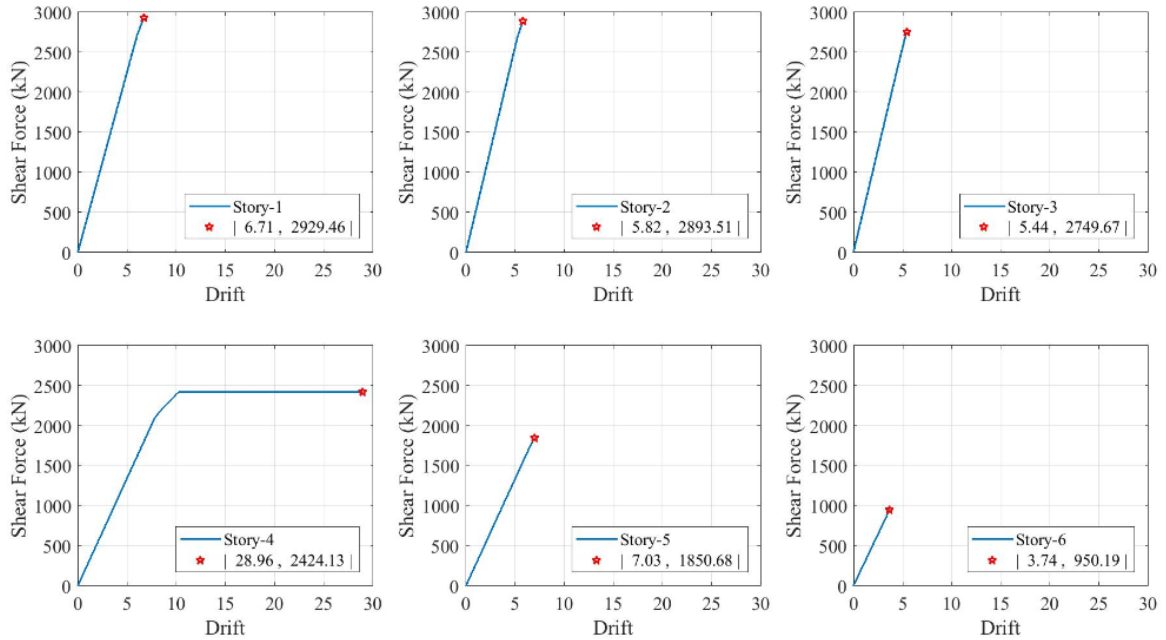


Figure 3.10. The capacity curve of MF building for any stories in Y-direction

The result of the nonlinear static analysis confirms the screening evaluation result for the case of the MF building. The screening evaluation revealed that a problem occurred in the 4th story indicated by the significant differences of the shear capacity and stiffness with the next story in Y-direction. This problem also affirmed by the nonlinear static analysis, where the drift story and the ductility factor in the 4th story have the highest value.

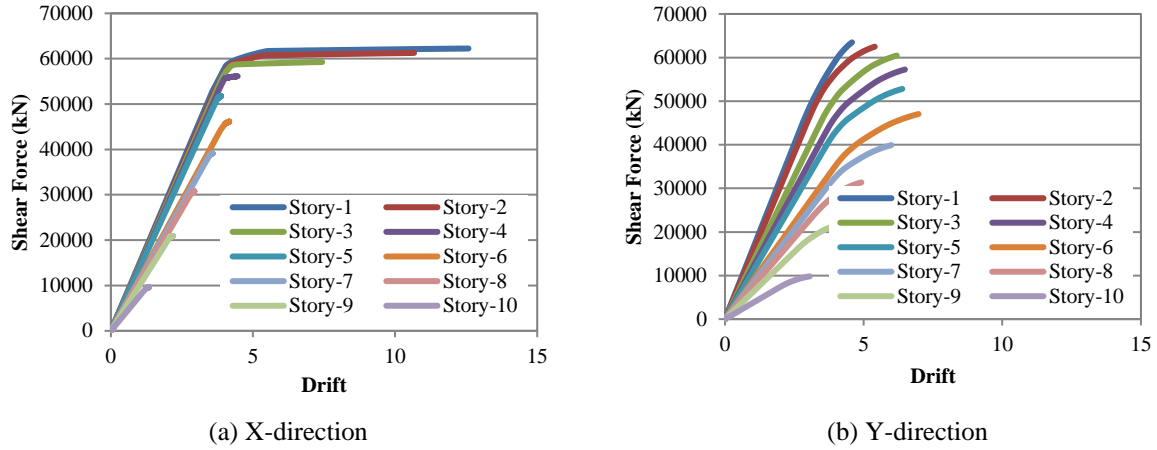


Figure 3.11. The capacity curve of BF structure in X-direction and Y-direction

For the case of the BF building, the capacity curves for the X and Y direction shown in Figure 3.11 and the calculation of ductility factors shown in Table 3.7. Obviously, the curve in the 7th story until the 10th story tends to be linear, and the ductility value is almost similar. The highest ductility occurs in the 1st story for the X direction while in the 6th story for the Y direction.

Table 3.7. Ductility factor in any stories of BF building

Story- <i>i</i>	X-direction			Y-direction		
	δ_{y-i}	δ_{max-i}	μ_i	δ_{y-i}	δ_{max-i}	μ_i
1	4.53	10.50	2.32	2.82	4.58	1.62
2	4.38	9.74	2.22	2.98	5.40	1.81
3	4.38	8.81	2.01	3.51	6.19	1.76
4	4.15	5.58	1.35	3.65	6.49	1.78
5	3.90	4.00	1.03	3.55	6.39	1.80
6	4.14	4.35	1.05	3.80	6.98	1.84
7	3.61	3.65	1.01	3.46	6.00	1.74
8	2.95	2.99	1.01	3.00	4.92	1.64
9	2.16	2.20	1.02	2.47	3.94	1.60
10	1.31	1.34	1.02	1.88	3.06	1.63

The capacity curves break down for the 1st story until the 10th story for X and Y direction, as shown in Figure 3.12 and Figure 3.13, respectively.

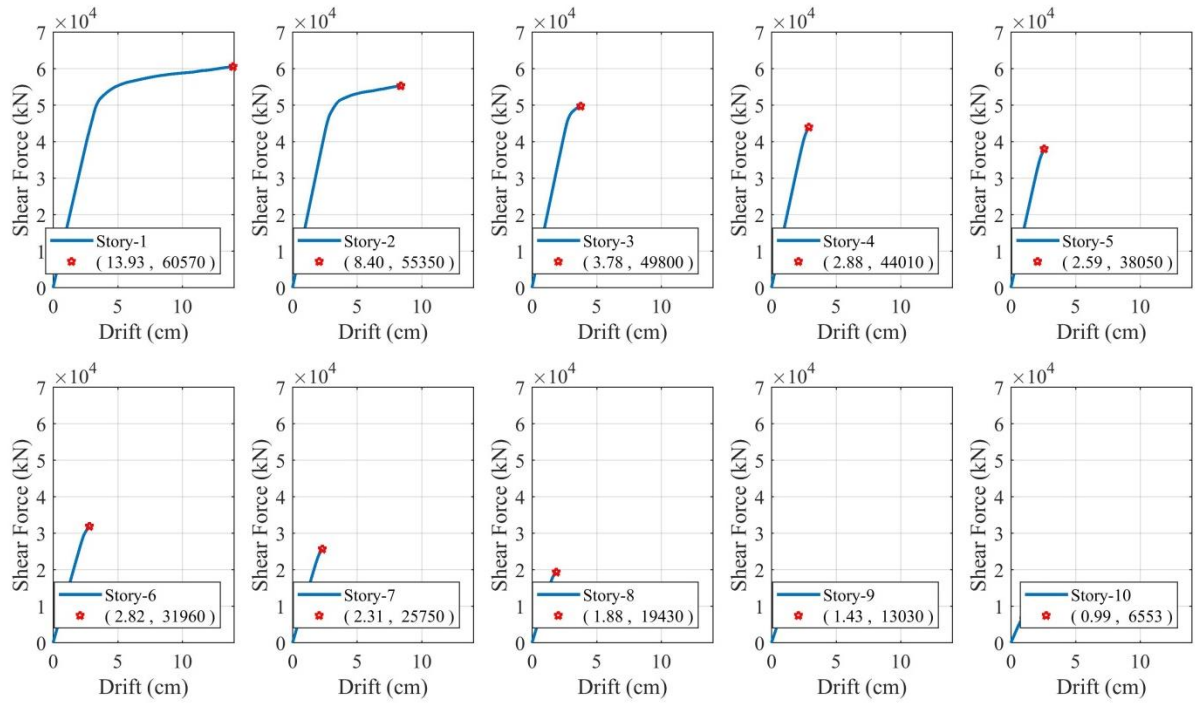


Figure 3.12. The capacity curve of BF building for any stories in X-direction

Figure 3.12, the BF in X-direction, shows the yield drifts occur in story 1, 2, and 3 while the maximum is in story 1. On the other side, Figure 3.13, the maximum drift occurs in story 6.

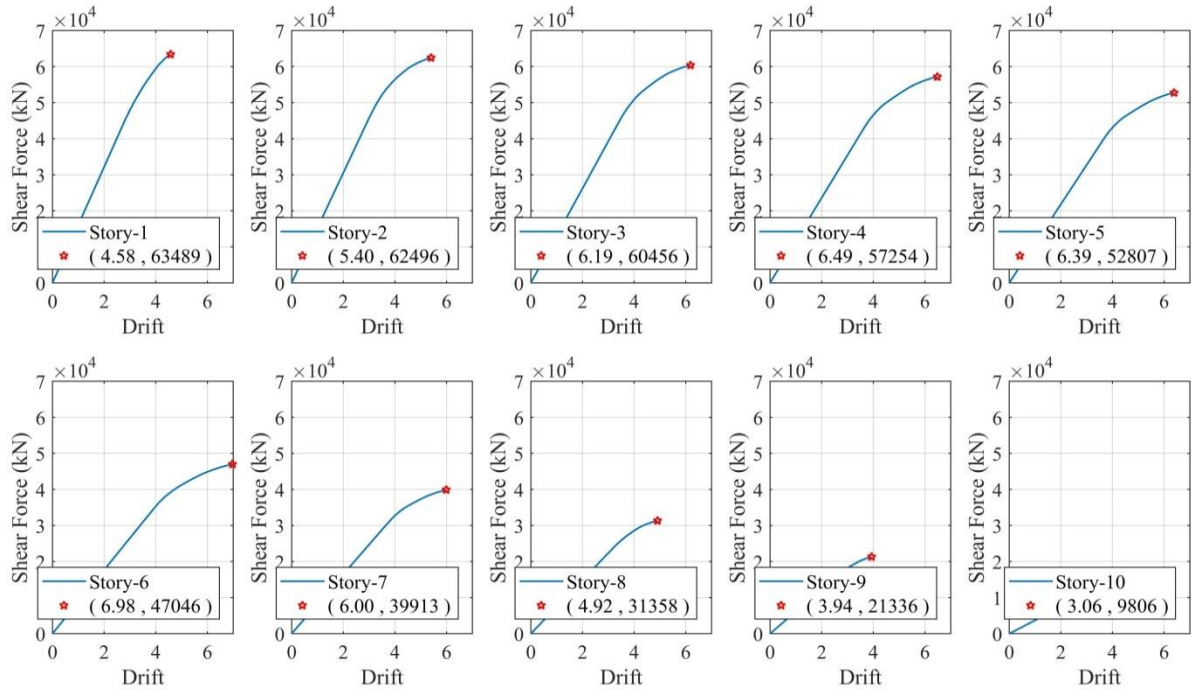


Figure 3.13. The capacity curve of BF building for any stories in Y-direction

The nonlinear static result of the BF building confirms the screening evaluation result that the problem occurred in the adjacent story 1 to 2, and the next story 5 to 6.

3.4.3. Result of Nonlinear Dynamic Analysis

Nonlinear dynamic analysis has been done for both case studies. In the beginning, modal analysis is carried out to observe the dynamic characteristic of the structures under vibration excitation. The modal analysis uses the overall mass and stiffness of a structure to find the various periods at which the structure will resonate naturally. Table 3.8 shows the dynamic properties of the MF building for the first fourth mode.

Table 3.8. Dynamic properties of MF building

Mode	X-direction		Y-direction	
	Period (Sec)	Equivalent Mass ratio (ρ)	Period (Sec)	Equivalent Mass ratio (ρ)
1	0.704	0.818	0.961	0.823
2	0.245	0.121	0.358	0.130
3	0.138	0.030	0.147	0.022
4	0.094	0.017	0.126	0.011

As shown in Table 3.8, the MF building has a fundamental period of 0.704 in X-direction and 0.961 in Y-direction. The equivalent mass ratios are larger than 80% in mode-1 for both directions. The mode shape of the displacement shows in Figure 3.14.

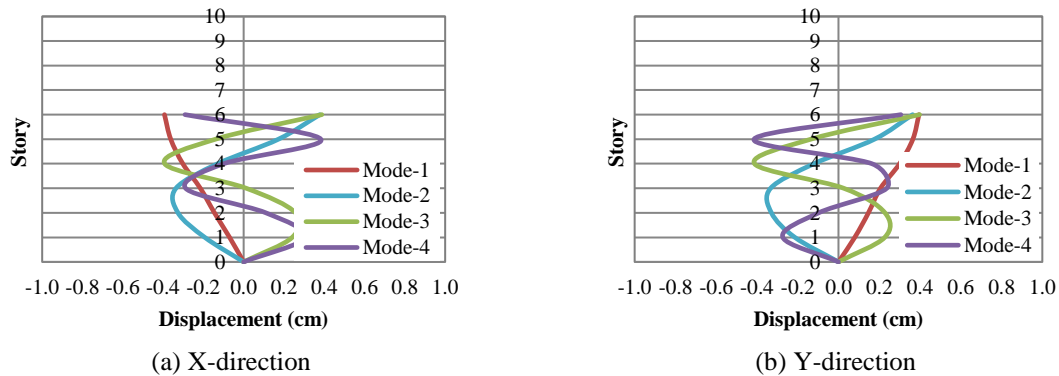


Figure 3.14. The mode shape displacement of MF building in both direction

The natural period of the BF building is smaller than the MF building, as shown in Table 3.9. The BF building has the first period of 0.729 and 0.675 in the X and Y direction, respectively. Similar to the MF building, the BF building has a dominant equivalent mass in the first mode. The mode shape displacement of the BF building can be seen in Figure 3.15.

Table 3.9. Dynamic properties of BF building

Mode	X-direction		Y-direction	
	Period (Sec)	Equivalent Mass ratio (ρ)	Period (Sec)	Equivalent Mass ratio (ρ)
1	0.729	0.780	0.675	0.822
2	0.238	0.143	0.231	0.111
3	0.130	0.041	0.132	0.032
4	0.091	0.019	0.094	0.016

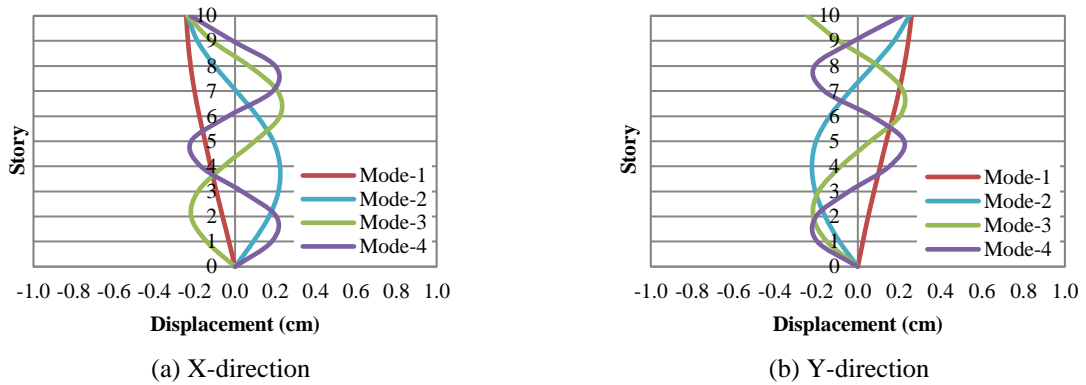


Figure 3.15. The mode shape displacement of BF building in both direction

The results of simulated ground motions are used as an input of seismic loads for dynamic analysis. A target of a response spectrum for simulating earthquake ground motion is an acceleration of 1.398 at a short period (S_s) and 0.6 at the 1.0 second of period (S_l). The site classification is soft soil clay classified as E class. The site coefficient for soil amplification is taken from Indonesian code (See Table 2.4, and 2.5 in chapter 2), which are F_a of 0.9 and F_v of 2.4. Furthermore, the design spectral response can be calculated as follow:

$$S_{DS} = \frac{2}{3} \cdot S_s \cdot F_A = \frac{2}{3} \cdot 1.398 \cdot 0.9 = 0.839$$

$$S_{D1} = \frac{2}{3} \cdot S_l \cdot F_v = \frac{2}{3} \cdot 0.60 \cdot 2.40 = 0.960 \dots\dots\dots (3.10)$$

The range of period aligns with the constant acceleration response is as follow:

$$T_0 = 0.2 \cdot (S_{D1} / S_{DS}) = 0.2 \cdot (0.960 / 0.839) = 0.229$$

$$T_s = S_{D1} / S_{DS} = 0.960 / 0.839 = 1.144 \dots\dots\dots (3.11)$$

The simulated result of the peak ground motions describes in Table 3.10.

Table 3.10. Simulated earthquake ground motions

Type of Ground Motion	Year	PGA (cm/s ²)	Simulated PGA (cm/s ²)
El Centro (Imperial Valley)	1940	341.7	309.2
Kobe (Hanshin)	1995	817.8	402.9
Taft (Kern County)	1952	175.9	310.5

The PGA simulation results show that the Kobe earthquake provides the highest PGA value compared to the others. The simulated ground motion used earthquake data of El Centro, Kobe, and Taft with scaling to a target of spectrum response can be seen in Figure 3.16.

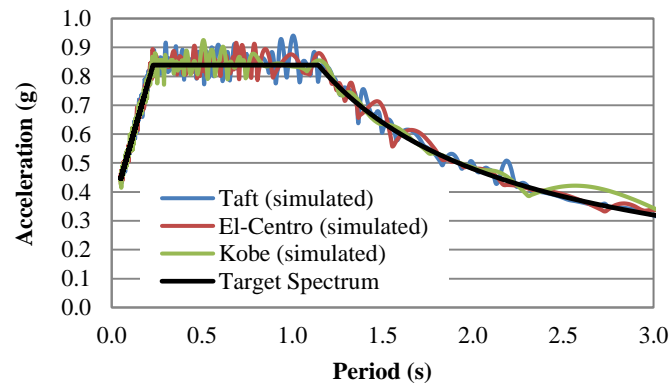
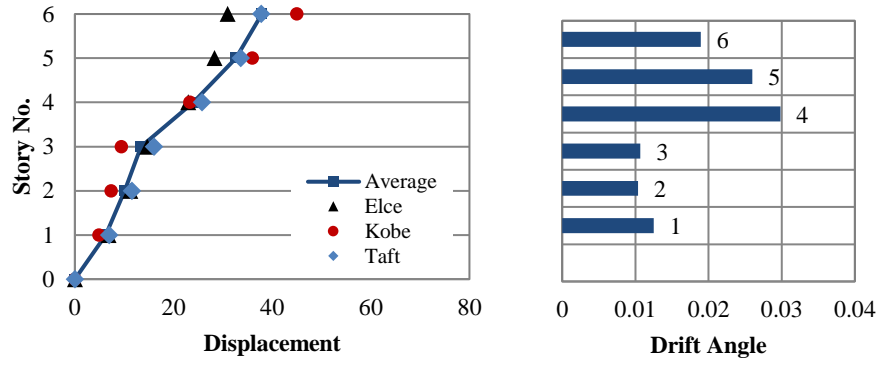
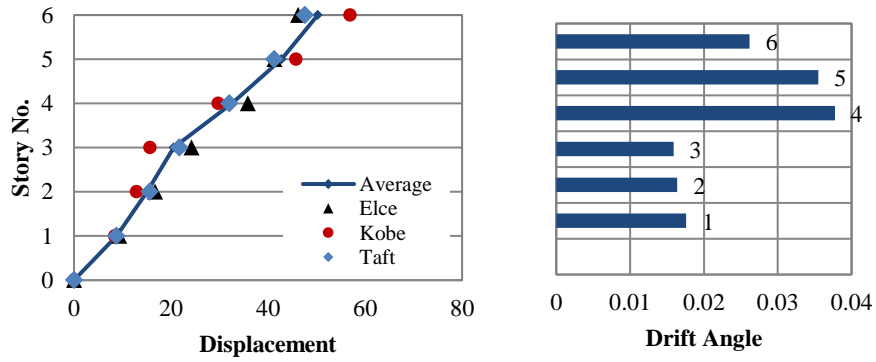


Figure 3.16. Simulated spectrum acceleration

The average maximum response is obtained from the maximum response of El Centro, Kobe, and Taft earthquake. Figure 3.17 shows the average of maximum displacement and the drift angle for each stories. The roof displacement in the X-direction is larger than the Y-direction, and this indicates that the stiffness in Y-direction is smaller than X-direction. The most significant drift angle occurred in story-4 of the MF building in X and also in Y-direction.



(a). Maximum displacement and drift angel in X-direction



(b). Maximum displacement and drift angel in Y-direction

Figure 3.17. Maximum response of MF building

The hysteresis loops of nonlinear dynamic responses in X-direction are plotted for any stories. Figure 3.18, Figure 3.19, and Figure 3.20 show the response for the 1st story until the 6th story for El Centro, Kobe, and Taft earthquake, respectively. Obviously, from all of those figures, the 4th story has the largest area of the hysteresis loop, which indicates that the 4th has experienced in yield significantly.

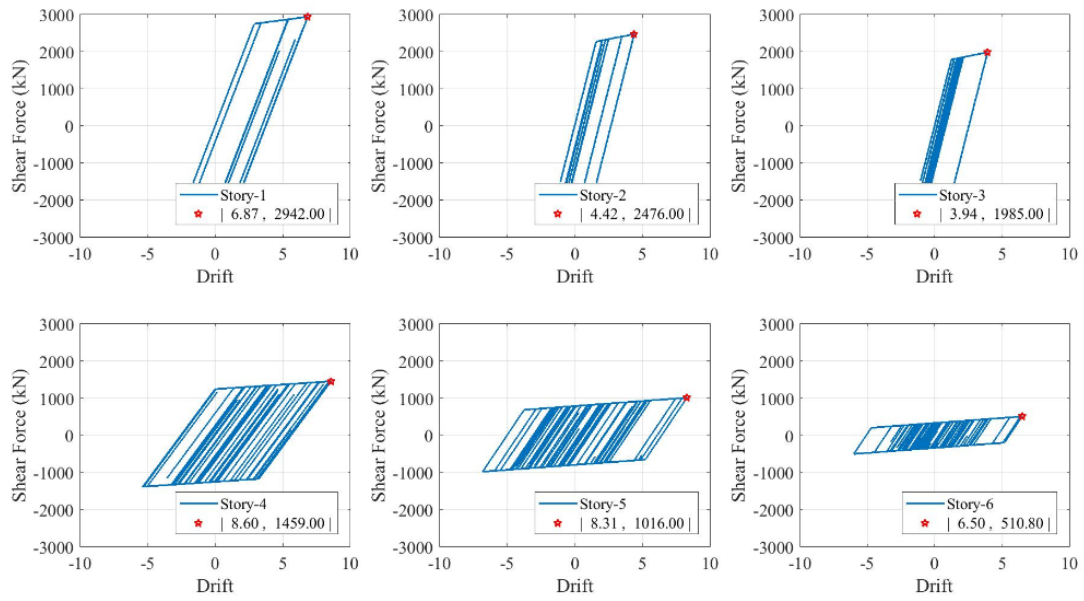


Figure 3.18. Nonlinear dynamic response due to El Centro earthquake of MF building in X-direction

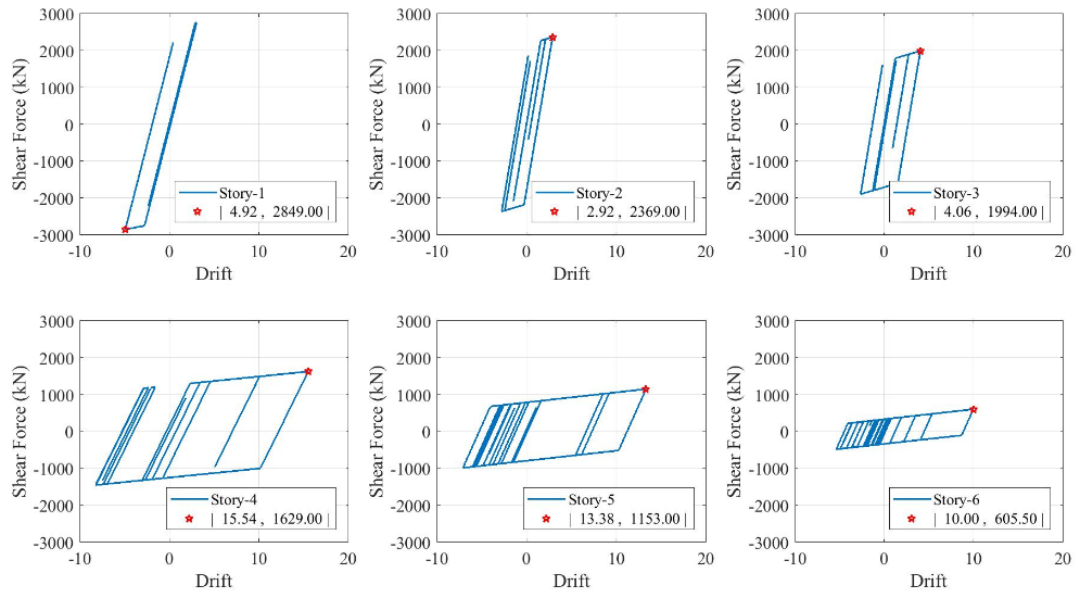


Figure 3.19. Nonlinear dynamic response due to Kobe earthquake of MF building in X-direction

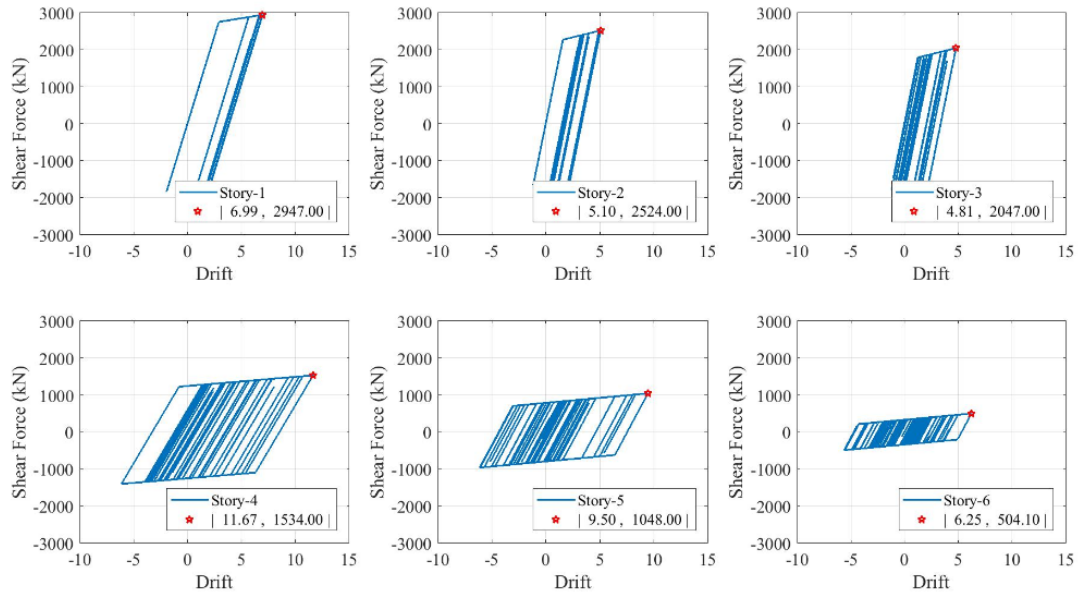


Figure 3.20. Nonlinear dynamic response due to Taft earthquake of MF building in X-direction

Figure 3.21 shows the hysteresis loop of nonlinear dynamic responses in the Y direction due to El Centro earthquake. In the 4th story, it is seen that the area of the curve is bigger than the other stories.

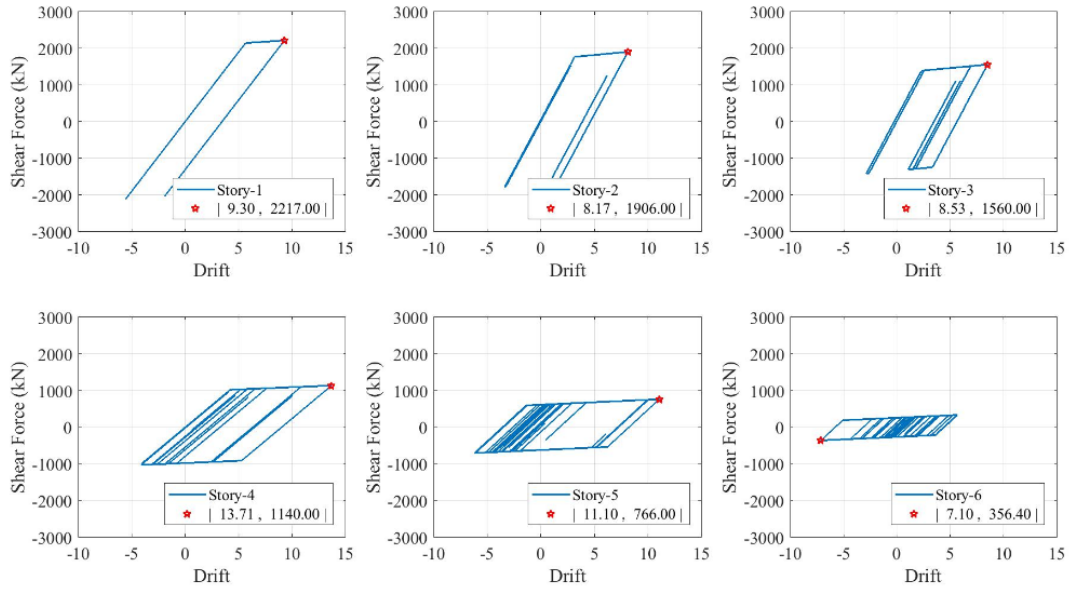


Figure 3.21. Nonlinear dynamic response due to El Centro earthquake of MF building in Y-direction

Figure 3.22 and Figure 3.23 show the hysteresis loop due to Kobe and Taft earthquake in the Y direction. Similar to El Centro earthquake, these figures indicate that the 4th story has the most significant area.

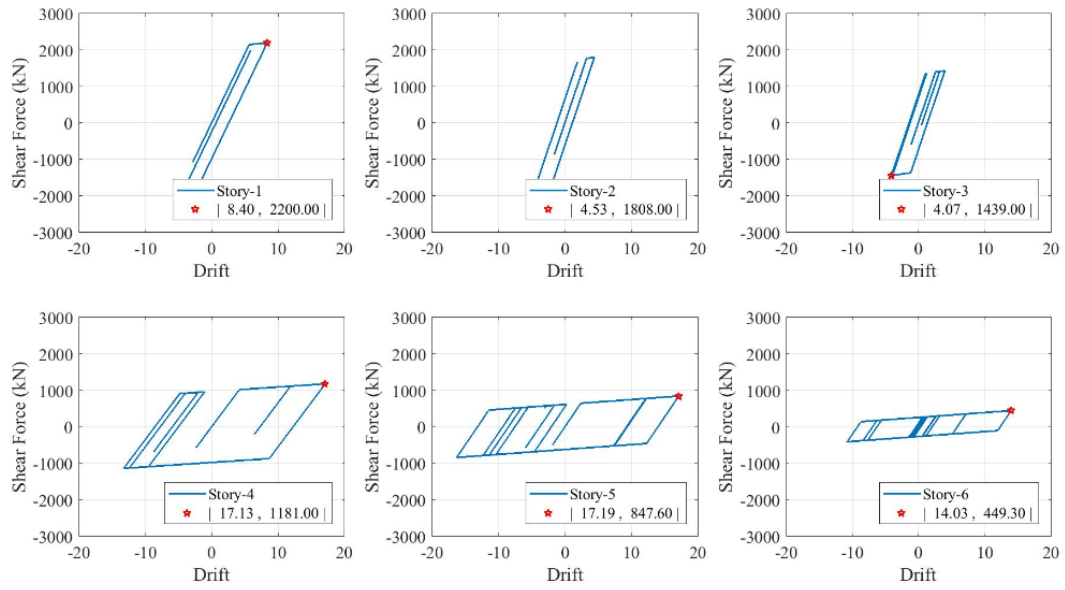


Figure 3.22. Nonlinear dynamic response due to Kobe earthquake of MF building in Y-direction

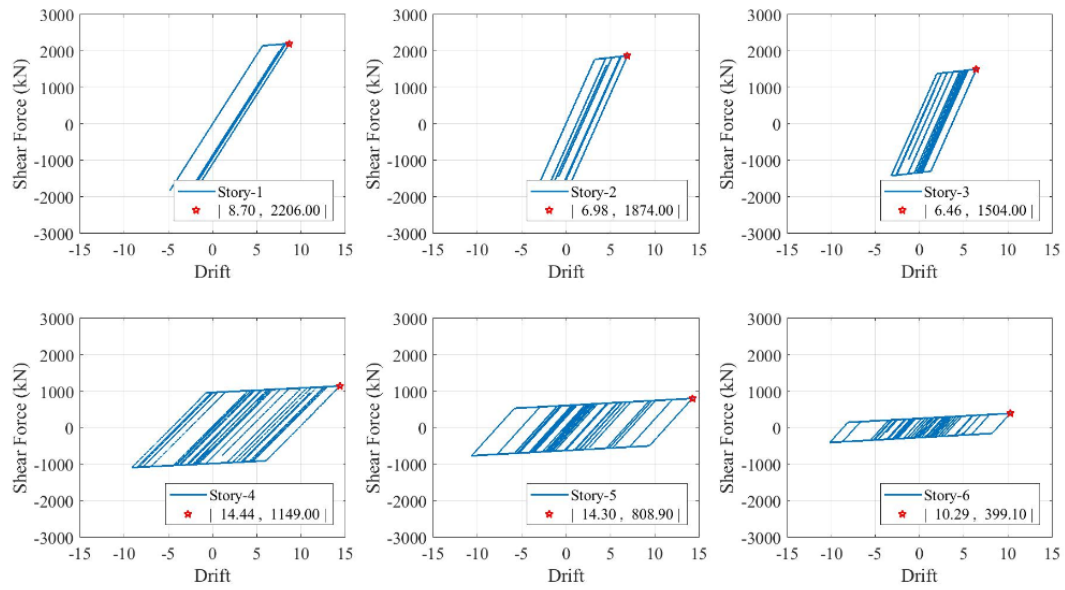
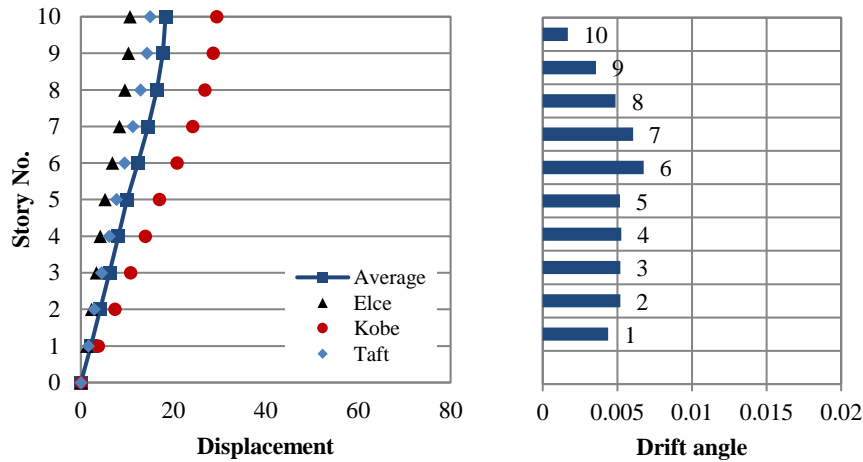


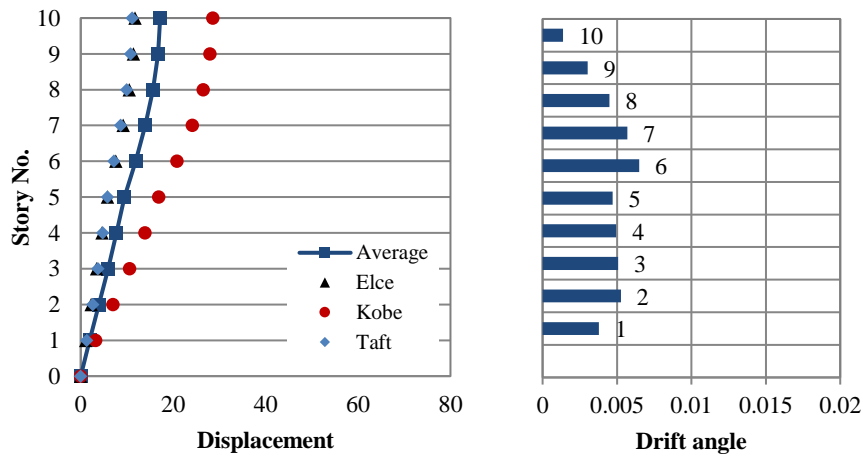
Figure 3.23. Nonlinear dynamic response due to Taft earthquake of MF building in Y-direction

The nonlinear dynamic result of the MF building confirms the screening evaluation result that the problem occurred in the 4th story, which indicated by the larger area occurs in the 4th story as well.

The average maximum response of the BF building is obtained from the maximum response of El Centro, Kobe, and Taft earthquake, as shown in Figure 3.24. It is noticed that the displacement due to Kobe earthquake is larger than the other two earthquakes because Kobe earthquake has the largest of the PGA. The highest of the drift angle occurs in the sixth story of the X and Y direction.



(a). Maximum displacement and drift angel in X-direction



(b). Maximum displacement and drift angel in Y-direction

Figure 3.24. Maximum response of BF building

The hysteresis loop of nonlinear dynamic responses in the X direction is plotted for the 1st story until the 10th story for El Centro, Kobe, and Taft earthquake in Figure 3.25, Figure 3.26 and Figure 3.27, respectively. Obviously, for all of those figures has the same pattern, the sixth story has a larger area of the hysteresis loop, which indicates that it has experienced in yield significantly. The 10th story

has the smallest area compare to the other stories. From these figures are also noticed that the lower story has a higher shear force.

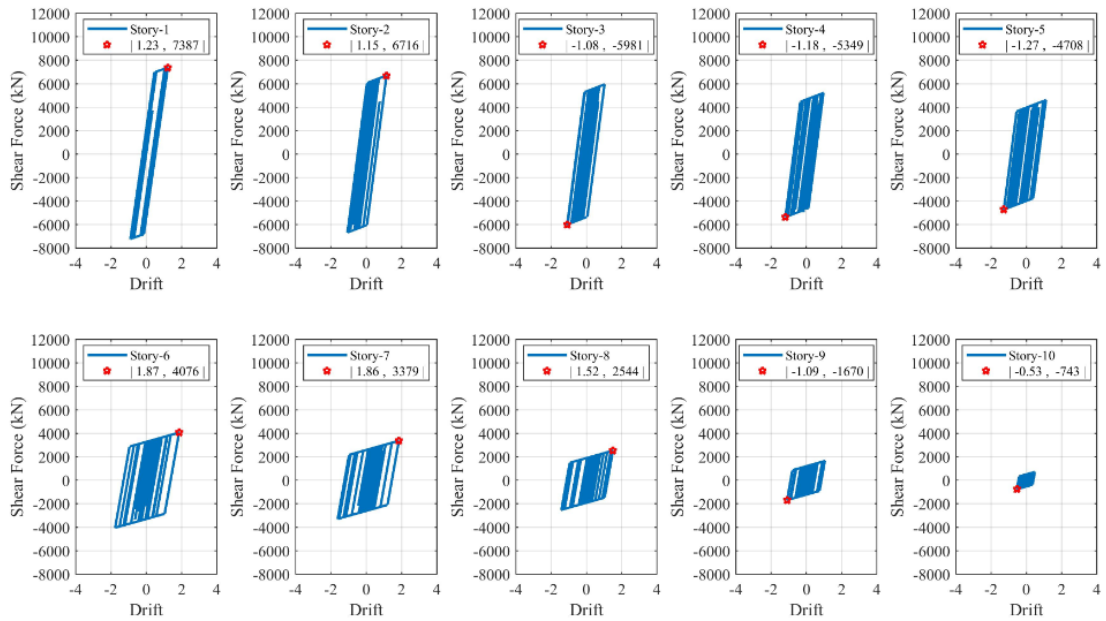


Figure 3.25. Nonlinear dynamic response due to El Centro earthquake of BF building in X-direction

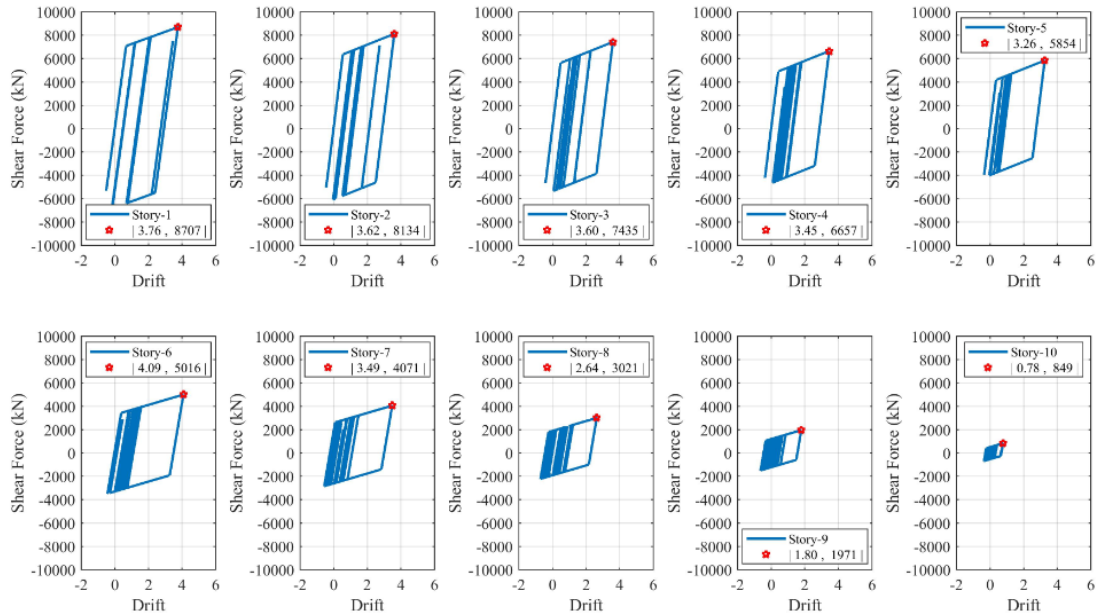


Figure 3.26. Nonlinear dynamic response due to Kobe earthquake of BF building in X-direction

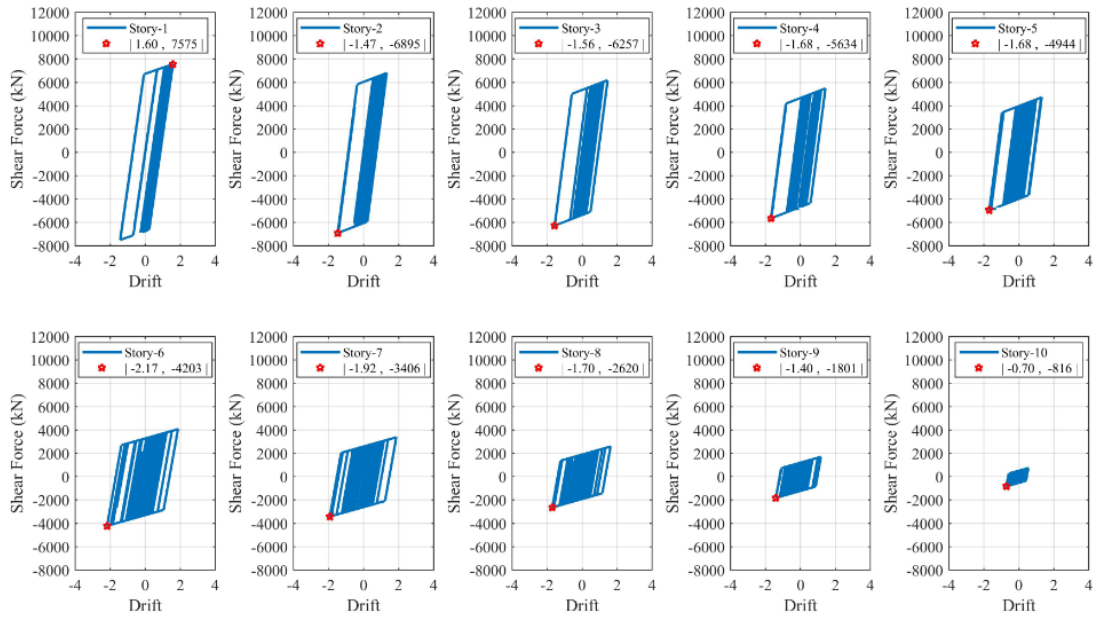


Figure 3.27. Nonlinear dynamic response due to Taft earthquake of BF building in X-direction

Figure 3.28 shows the hysteresis loop of nonlinear dynamic responses in the Y direction due to El Centro earthquake. In the 6th story, it is seen that the area of the curve is bigger than the other stories.

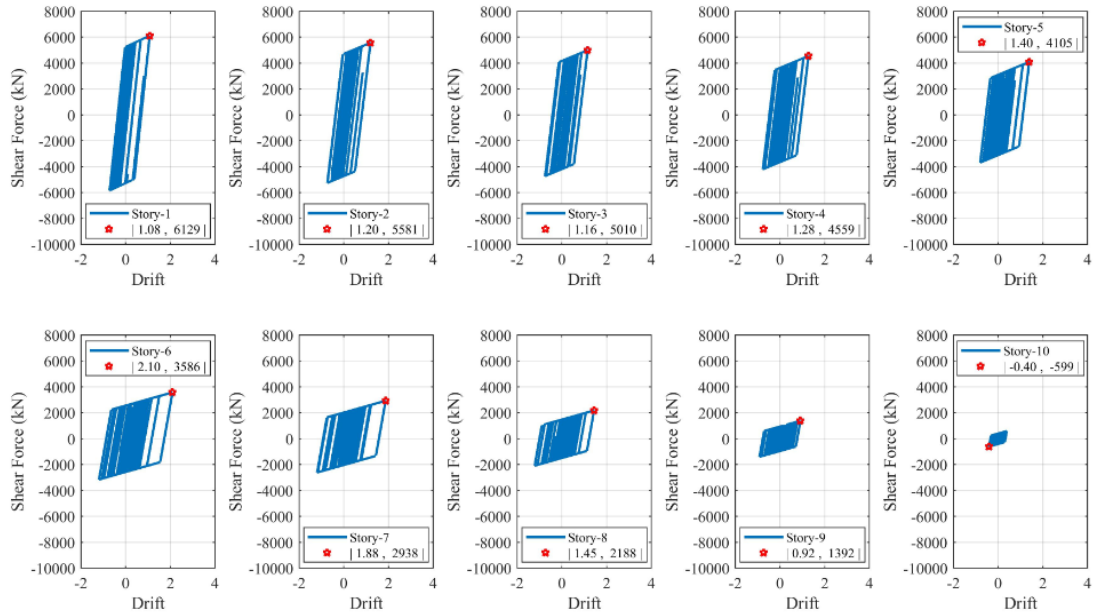


Figure 3.28. Nonlinear dynamic response due to El Centro earthquake of BF building in Y-direction

Figure 3.29 and Figure 3.30 show the hysteresis loop due to Kobe and Taft earthquake in the Y direction. Similar to El Centro earthquake, these figures indicate that the 6th story has a more significant area.

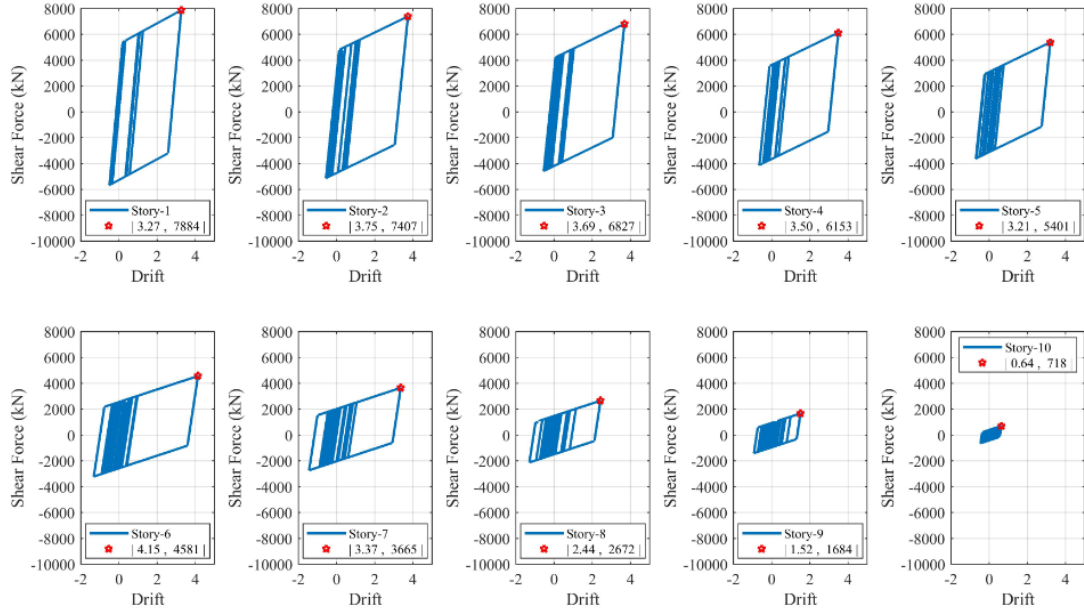


Figure 3.29. Nonlinear dynamic response due to Kobe earthquake of BF building in Y-direction

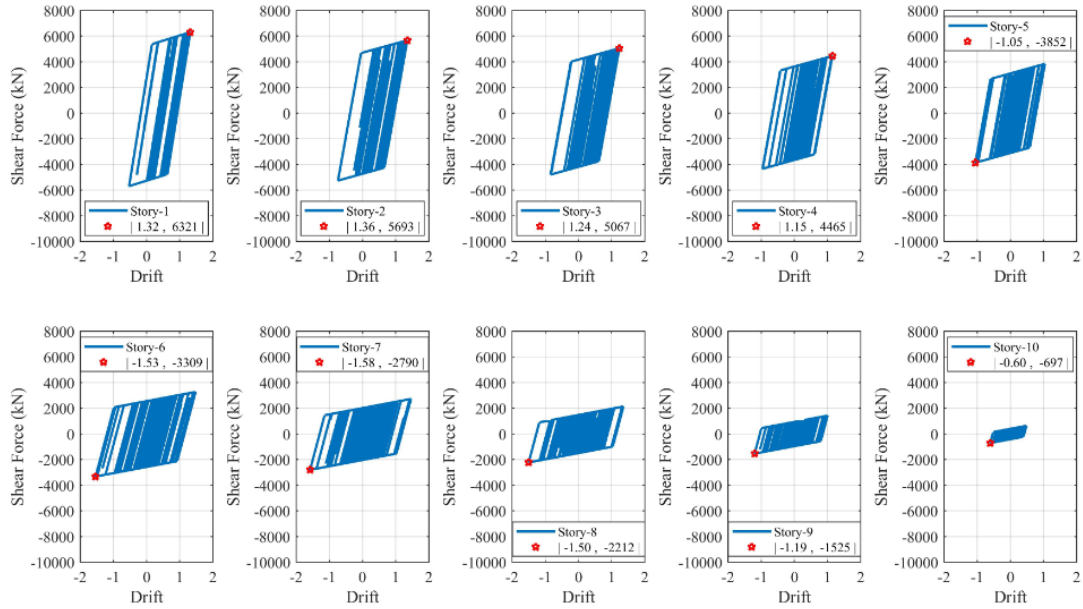


Figure 3.30. Nonlinear dynamic response due to Taft earthquake of BF building in Y-direction

The nonlinear dynamic result of the BF building confirms the screening evaluation result that the problem occurred in the 6th story, which indicated by the larger area occurs in the 6th story as well.

3.5. Conclusion

The structural evaluation has been demonstrated in this study by selecting cases of the 6th story steel moment-resisting frame (MF) system, and the 10th story braced frame (BF) system. The buildings located in Padang city were designed according to Indonesian seismic code. The evaluation was performed by applying the screening method with reference to the ASCE 41-13 standard. The nonlinear static and dynamic analyses have performed to confirm this method.

The result of the screening evaluation revealed that there are deficiencies in the basic configuration of the MF building. The MF building has the potential to occur in the weak-story and soft-story collapse mechanism. The difference in shear strength and stiffness at adjacent levels is very significant. Particularly in the lateral resisting system in the fourth story. The strong column weak beam criteria are also not satisfied in this building. The same thing also happens to the BF building, where there is potential collapse due to the weak-story in the sixth story.

The static nonlinear analyses had done to affirm this problem. The ductility factor shows that the highest ductility values occur in the fourth story of the MF building and in the sixth stories for the BF building. The capacity curves also disclose the failure likely to occur in the same stories of both buildings.

Further confirmation had carried out with the nonlinear dynamic analysis. The simulated ground motion was made under the target response spectrum set by the Indonesia code. The nonlinear dynamic results show that the potential failures arise in the fourth story of the MF building and in the sixth stories of the BF building, where indicated with the largest area of the hysteresis loop occurs in the same stories of both buildings.

This study shows that screening evaluation can be implemented to evaluate the existing structure against the risk of earthquakes.

Chapter 4

A Proposal of Seismic Index for Existing Buildings in Indonesia using Pushover Analysis

4.1. Introduction

The Japanese standards for seismic assessment of existing buildings were used as the key idea in this study. The Japan Building Disaster Prevention Association (JBDPA) published a standard for the seismic evaluation of an existing building and guidelines for the retrofitting of existing reinforced concrete buildings in 1977 [32]. In Japan, a seismic screening procedure mentioned in this guideline was used as a practical tool to identify vulnerable buildings. This tool became essential after new sets of rules and laws for the seismic design of buildings were issued in 1981, and severe earthquake damage was recorded in buildings constructed before 1981. The standard for the seismic evaluation of buildings has been widely used to evaluate the capacity of existing buildings up to now and in 2001 the English version was published to encourage engineers in a large number of countries on the issue of seismic evaluation.

However, to enable the application of this standard in other countries requires some justifications and adjustments. The estimation of structural capacity and demand loads has a different approach through this standard. In this study, the determination of the seismic index is carried out based on static non-linear analysis, also known as pushover analysis. This analysis is a widely used method for the performance evaluation buildings where the capacity of the structure is analyzed by considering its post-elastic behavior [26].

The purpose of this study is to obtain the seismic index of an existing structure based on pushover analysis as a consideration of the performance of the building and to determine the demand index by considering Indonesian seismic hazards.

4.2. Methodology

The seismic index is an index that shows the performance of a building whether the building is safe if an earthquake occurred. The index is obtained from a product of the strength index and the ductility index which is called the basic seismic index. Furthermore, the index will be compared to the demand index which is a limit of safety. Since the seismic index is greater than the demand index, the structure is considered in the safety limit.

In this study, the first analysis was carried out the determination of the seismic index in accordance with Japanese standards [32]. The demand index was also obtained based on Japanese earthquake hazards as guided in this standard. The second analysis was calculated the seismic index by using a method derived from pushover analysis. The demand index was estimated based on the Indonesian seismic hazard as indicated by the performance point of the design response spectrum and the capacity curve.

4.2.1. Seismic Index

The seismic performance of an existing building is represented by a seismic index in which denoted as I_s in Japan [32–34]. The seismic index (I_s) is calculated with Eq. (4.1) for each story and each principal orthogonal direction of the structure. The Eq. (4.1) is defined as follows:

$$I_s = E_o \cdot S_D \cdot T \dots\dots\dots (4.1)$$

In which, E_o is basic seismic index, T is time index, and S_D is irregularity index.

The basic seismic index (E_o) is given as a product of the strength index C and the ductility index F which is calculated differently in the first, second, and third levels of procedures. This study adopted the first level procedure to calculate the seismic index. Eq. (4.2) and Eq. (4.3), which are the formula for determining the basic seismic index of a shear wall structure and short column structure, are defined as follows:

$$E_o = \frac{n+1}{n+i} (C_w + \alpha_1 C_c) F_w \dots\dots\dots (4.2)$$

$$E_o = \frac{n+1}{n+i} (C_{sc} + \alpha_2 C_w + \alpha_3 C_c) F_{sc} \dots\dots\dots (4.3)$$

Where n is the number of stories, C_w is the strength index of a wall, C_c is the strength index of a column, and C_{sc} is the strength index of short columns. α_1 , α_2 , and α_3 are the effective strength factors for columns, wall, and short columns respectively. F_w is the ductility index of a wall and F_{sc} is the ductility index of a short column. C_c and C_{sc} is expressed by Eq. (4.4) and Eq. (4.5) as:

$$C_c = \frac{\tau_c \cdot A_c}{\sum W} \cdot \beta_c \dots\dots\dots (4.4)$$

$$C_{sc} = \frac{\tau_{sc} \cdot A_{sc}}{\sum W} \cdot \beta_c \dots\dots\dots (4.5)$$

In the above equation, τ_c is average shear stress at the ultimate state of columns, and it can be taken as 1.0 N/mm² or 0.7 N/mm² in the case h_o / D is larger than 6.0. h_o is a clear height of column and D is a depth of column. τ_{sc} is average shear stress at the ultimate state of short columns, which could be taken as 1.5 N/mm².

4.2.2. Pushover Analysis

Pushover analysis has been developed over the past twenty years and became the preferred analysis for designing and evaluating the structure. This method is most reliable for estimating the capacity of a structure beyond the elastic limit [26]. Pushover analysis is a method where a structure is subjected to gravity loading and a monotonic displacement-controlled lateral load pattern continuously increases through elastic and inelastic behavior until an ultimate condition or a collapsed state of the structure is reached. The lateral load may represent the range of base shear induced by earthquake loading, and its configuration may be proportional to the distribution of mass along with building height, mode shapes, or other practical means. The output will generate a capacity curve that plots a strength-based parameter against deflection. For example, performance may relate the strength level achieved in certain members to the lateral displacement at the top of the structure, or a bending moment may be plotted against plastic rotation. The results will provide insight into the ductile

capacity of the structural system, and indicate the mechanism, load level, and deflection at which failure occurs.

The application of the conventional pushover procedure, described in ATC-40 [26], has some limitations. This procedure generates a capacity curve representing the first mode response of the structure based on the assumption that the fundamental mode of vibration is the predominant response. The eigen-value analysis should be considered to confirm the dominant first mode for irregular structures. Besides, it is important to take into account the effects of irregularities on seismic performance evaluations. Many researchers proposed a pushover method with considering the structure irregularity and the higher mode effect [35–38]. This method could be used as an alternative method to determine the capacity curve and then calculate the seismic index as proposed in this study.

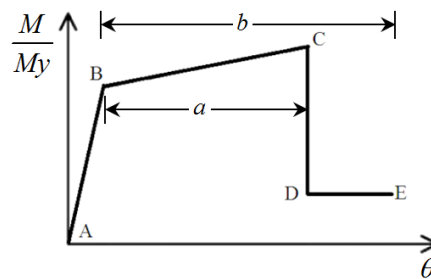


Figure 4.1. Moment-rotation relationship of typical plastic hinge

When analyzing frame objects, material nonlinearity is assigned to discrete hinge locations where plastic rotation occurs [27, 39]. Beam and column components are modeled as nonlinear frame elements by defining plastic hinges at both ends of the elements. As shown in Figure 4.1, The plastic hinges properties have five points, labeled A, B, C, D, and E, which define the force-deformation behavior. The same type of curve is also used for moment and rotation relationship. The value assigned to each of these points varies depending on the type element, material properties, and section size.

A linear response is related to a line between point A and an effective yield point B. The slope from point B to point C is typically a small percentage (0% to 10%) of the elastic slope and is included to represent phenomena such as strain hardening. Point C has an ordinate that represents the strength of the element and an abscissa value equal to the deformation at which significant strength degradation begins (line CD). Beyond point D, the element responds with substantially reduced strength until point E. At deformations greater than point E, the seismic element strength is essentially zero [39].

This study proposes a procedure of seismic calculation index by using the capacity curve of a pushover. The left side of Figure 4.2 shows a capacity curve and an idealized bilinear elastoplastic curve, and the right side shows a curve that describes the constant energy principle to get the relationship between ductility factor (F) and ductility index (μ).

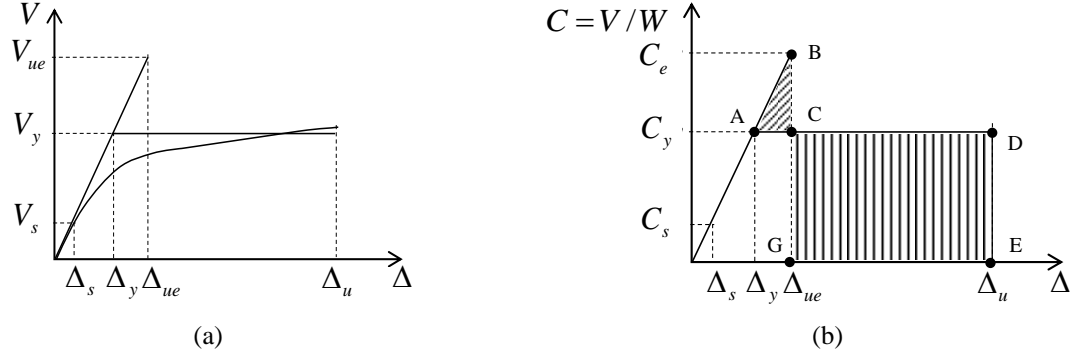


Figure 4.2. Converting the capacity curve to be an elastoplastic curve by the constant energy principle

By the constant energy principle, the area of triangle ACB is similar to the area of rectangle CDEG. The ductility index is derived as follows,

$$\begin{aligned} \frac{1}{2}(\Delta_{ue} - \Delta_y) \cdot (C_e - C_y) &= C_y \cdot (\mu \Delta_y - \Delta_{ue}) \\ \frac{1}{2}(F \Delta_y - \Delta_y) \cdot (F C_y - C_y) &= C_y \cdot (\mu \Delta_y - F \Delta_y) \\ \frac{1}{2} \Delta_y \cdot C_y (F - 1)^2 &= C_y \cdot \Delta_y (\mu - F) \\ F &= \sqrt{2\mu - 1} \dots\dots\dots (4.6) \end{aligned}$$

The step by step procedure of the calculation describes as follows:

Converted a capacity curve to be an elastoplastic curve based on the concept of equal energy,

- Calculated elastic stiffness (K_e) based on the ratio between shear strength and displacement at elastic conditions $K_e = V_s / \Delta_s$.
- Calculated displacement of Δ_y at an intersection of a linear curve with a gradient of K_e , in which $\Delta_y = V_y / K_e$. In the bilinear elastoplastic idealization, an elastic shear strength (V_y) is considered to be equal an ultimate shear strength (V_u).
- Determined the ductility factor (μ) at the displacement of maximum shear strength (Δ_u) over (Δ_y), $\mu = \Delta_u / \Delta_y$.
- Calculated ductility index (F) with a concept of constant energy by Eq. (4.6), $F = \sqrt{2\mu - 1}$.

- e. Estimated the ultimate elastic shear strength (V_{ue}) by using ductility index (F) with equation $V_{ue} = F.V_y$ and calculate displacement on ultimate shear strength elastic (V_{ue}) with the equation $\Delta_{ue} = V_{ue} / K_e$.
- f. Determined the total weight of a structure and convert shear strength to be a shear ratio. In which V_y , V_{ue} will be C_y , C_{ue} respectively.
- g. Calculated the basic seismic index (E_o) with the equation $E_o = C_y.F$.
- h. Determined the seismic index of a structure by using Eq. (4.1).

4.3. Case Study

Calculations of the seismic index based on the JBPDA method and pushover analysis will analyze the following case study. Two buildings were evaluated in this study. Both buildings are located in Indonesia and were designed using the Indonesian standard. These buildings were selected to be evaluated because these buildings were designed based on the old standard design [13, 31], and now, the standard has updated [10]. The earthquake-resistant standard design for the building has a potency to be updated again due to the development of new seismic hazard maps of Indonesia [3, 40–42]. Therefore, a re-evaluation of the existing building against the new earthquake load regulation is needed.

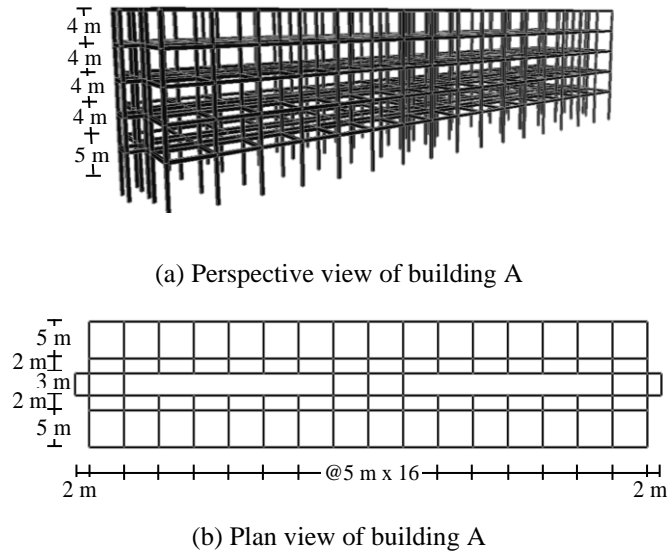


Figure 4.3. Perspective and plan view of building A.

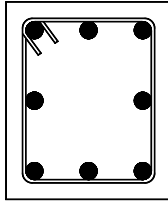
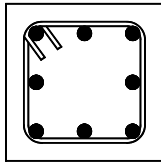
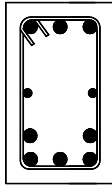
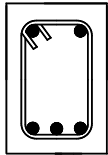
The first case study is a five-story apartment building, which is referred to as building A. While the second, referred to building B, is a four-story office building. The building A has an area of 1360 m² per floor. The structure is a space frame that has compressive strength concrete (f_c') of 25 MPa, as shown in Table 4.1.

Table 4.1. Material properties of building A and B

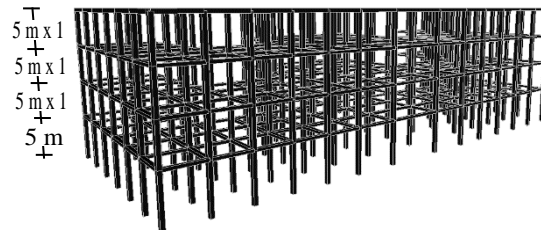
Concrete		Longitudinal rebar			Transversal rebar		
f_c' (MPa)	E_c (MPa)	f_y (MPa)	f_u (MPa)	E_s (MPa)	f_y (MPa)	f_u (MPa)	E_s (MPa)
25	2.0E4	390	560	2.0E5	235	382	2.0E5

There are two types of columns in this building where type 1 is a rectangular section of 500x600 mm², and type 2 is a square section of 350x350 mm². The layout of the building has a typical plan in every story. The floor height is equal in the 1st until the 5th floor as shown in Figure 4.3. The detailed dimension of beams and columns can be seen in Table 4.2.

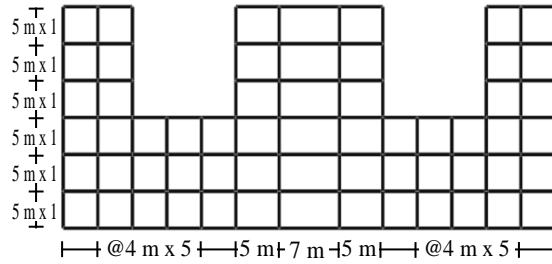
Table 4.2. Beam and column dimension of the building A

Column (C1) 500 x 600 mm	Column (C2) 350 x 350 mm	Beam (B1) 300 x 500	Beam (B2) 200 x 300
			
Longitudinal rebar: 8.D19	Longitudinal rebar: 8.D16	Longitudinal rebar: Top 3.D19 Bottom 5.D19	Longitudinal rebar: Top 2.D16 Bottom 3.D16
Transversal rebar: D10 – 100 mm	Transversal rebar: D10 – 100 mm	Transversal rebar: D10 – 100/150 mm	Transversal rebar: D10 – 100/150 mm

Building B has an irregular floor plan, as shown in Figure 4.4. Although it has a planar irregularity, the torsional effect is not considered since the estimated distance between the story center of mass (CM) and the story center of rigidity (CR) is less than 20% of the building width in either plan dimension according to ASCE 41-13. In this case, the distance of CM-CR is 0.29, 0.55, 0.68, and 0.77 m in story-1 to story-4, respectively and the 20% of building width is 2.4 m as a distance limit. The floor plan area is 1008 m² uniformly on each floor. The structure is a reinforced concrete using a space frame system with f_c' of 25 MPa.



(a) Perspective view of building B

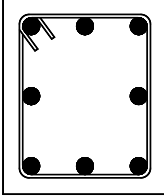
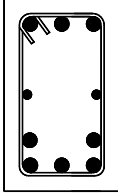
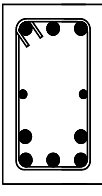


(b) Plan view of building B

Figure 4.4. Perspective and plan view of building B.

The column of building B has a typical rectangular section of 400x500 mm². The detailed dimensions of beams and columns can be seen in Table 4.3.

Table 4.3. Beam and column dimension of the building B

Column (C1) 400 x 500 mm	Beam (B1) 300 x 500	Beam (B2) 250 x 400
		
Longitudinal rebar: 8.D19	Longitudinal rebar: Top 3.D19 Bottom 5.D19	Longitudinal rebar: Top 3.D16 Bottom 5.D16
Transversal rebar: D10 – 100 mm	Transversal rebar: D10 – 100/150 mm	Transversal rebar: D10 – 100/150 mm

4.4. Results of the Seismic Evaluation

4.4.1. Seismic Index

Two existing buildings were evaluated in this paper. The calculation of the seismic index of buildings A and B was determined based on the Japanese standard. The seismic index was calculated in each story and multiplied by a story modification factor. As an example, the modification story factor for the 5th floor (C_5) can be calculated by Eq. (4.7) as follows:

$$C_5 = \frac{n+1}{n+i} = \frac{5+1}{5+5} = 0.6 \dots\dots\dots (4.7)$$

Where n is the number of stories in the building and i is an observed story. A similar method could be applied to the other floors. Secondly, the strength index of the vertical element was determined. In the case of building A, the vertical element for resisting lateral load only has a column. Since there were two types of the column, the total strength index can be calculated as shown in Eq. (4.8):

$$C_c = \frac{1.0 \times 2.0E07}{1.6E07} \times 1.12 + \frac{0.7 \times 4.2E07}{1.6E07} \times 1.12 = 1.61 \dots\dots\dots (4.8)$$

The basic seismic index of the structure E_o of the 5th floor was determined from Eq. (4.2), was calculated in Eq. (4.9) as follows:

$$E_{o5} = 0.6(0 + 1.0 \times 1.61) \times 1.0 = 0.97 \dots\dots\dots (4.9)$$

Irregularity index S_D was taken as 1.0 and also time index T was taken 1.0 since no reduction factor was considered. The seismic index for the 5th floor of building A following Eq. (4.1) is described in Eq. (4.10):

$$I_{s5} = 0.97 \times 1.0 \times 1.0 = 0.97 \dots\dots\dots (4.10)$$

The same procedure as shown in Eq. (4.7 - 4.10) could be applied to other floors in buildings A and B.

Table 4.4 and Table 4.5 shows the seismic index of building A and B respectively. In Table 4.4, the maximum seismic index for both directions takes place in story 5. The dominant parameter in determining the seismic index was the basic seismic index E_o , then an irregularity index (S_D) and time index (T) was taken as 1.0. The result of a seismic index in the transversal direction is greater than the longitudinal direction. It is because the ratio h_o/D in the transversal directions is smaller than 6, but otherwise to the longitudinal direction, the ratio is larger than 6. Therefore, the average shear

stress of columns in the transversal direction is 1 N/mm² and in the longitudinal direction is 0.7 N/mm².

Table 4.4. Seismic index of building A

Direction	Story	E_o	S_D	T	I_s
Transverse	5	0.97	1.00	1.00	0.97
	4	0.54	1.00	1.00	0.54
	3	0.40	1.00	1.00	0.40
	2	0.35	1.00	1.00	0.35
	1	0.32	1.00	1.00	0.32
Longitudinal	5	0.89	1.00	1.00	0.89
	4	0.49	1.00	1.00	0.49
	3	0.37	1.00	1.00	0.37
	2	0.32	1.00	1.00	0.32
	1	0.30	1.00	1.00	0.30

Meanwhile, building B (Table 4.5) has an identical basic seismic index in both directions. The average shear stress of a column is equivalent in the transversal direction and the longitudinal direction.

Table 4.5. Seismic index of building B

Direction	Story	E_o	S_D	T	I_s
Transverse	4	0.66	1.00	1.00	0.66
	3	0.38	1.00	1.00	0.38
	2	0.29	1.00	1.00	0.29
	1	0.26	1.00	1.00	0.26
Longitudinal	4	0.66	1.00	1.00	0.66
	3	0.38	1.00	1.00	0.38
	2	0.29	1.00	1.00	0.29
	1	0.26	1.00	1.00	0.26

Figures 4.5(a) and 4.5(b) show the seismic index graphs for each story in buildings A and B. The strength index is similar for both directions in building B. Therefore, the graph of longitudinal direction coincides with transversal as shown in Figure 4.5(b).

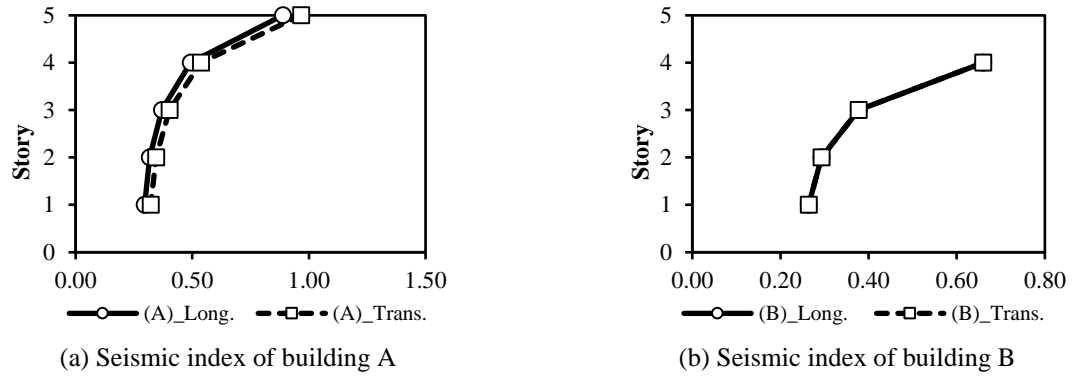


Figure 4.5. Seismic index of building A and B

4.4.2. Seismic Index Base on Pushover Analysis

Pushover analysis of a structure produces a capacity curve. A capacity curve plots the displacement of the top floor in the x-axis and the base shear in the y-axis. Modeling parameters for nonlinear hinge properties use generalized force-deformation relation of concrete elements where the flexural type of deformation controlled behavior is considered for both beam and column. The plastic rotation angle at maximum plastic capacity (see Figure 4.1) was taken as 0.025 radians for beams and 0.035 radians for columns [39].

Table 4.6. The lateral force in building A and B

Story	Building A		Building B	
	Height (m)	Lateral Force (kN)	Height (m)	Lateral Force (kN)
5	21	4,308.75		
4	17	3,369.58	17	2975.95
3	13	2,466.16	13	2134.47
2	9	1,607.71	9	1353.45
1	5	811.33	5	653.42

A target of displacement magnitude of both buildings is equal to the allowable story drift multiplied by the total height of the structure. The allowable story drift was taken as 0.025 with considering as risk category I based on ASCE 7-10. Equivalent seismic load in accordance with SNI 1726-2002 and ASCE 7-10 [43] was used as the lateral force on both buildings. An equivalent static acceleration, which is modified by a seismic coefficient depending on the seismicity of the location, soil properties, and the natural period, was multiplied by the total mass of the structure to give the base

7shear force [44, 45]. Table 4.6 shows the detail of the lateral load. The lateral load was given equal in both directions in this analysis.

In order to determine the seismic index based on the capacity curve, the capacity curve was initially converted to a bilinear curve (elastoplastic) using the procedure in section 3.2. A linear line with a gradient equal to elastic stiffness (K_e) can be determined by the value of step-1 of the pushover data, as shown in Table 4.7.

Table 4.7. The capacity curve of building A and building B

(A) Longitudinal		(A) Transversal		(B) Longitudinal		(B) Transversal	
Displ.	Base Force	Displ.	Base Force	Displ.	Base Force	Displ.	Base Force
(m)	(kN)	(m)	(kN)	(m)	(kN)	(m)	(kN)
0.0	0.0	0.0	0.0	0.00	0.0	0.00	0.0
0.06	7,248.1	0.05	7,578.0	0.06	2,771.8	0.06	3,361.5
0.08	9,717.7	0.06	9,341.5	0.13	5,961.0	0.12	6,954.1
0.11	11,003.8	0.10	11,247.8	0.22	7,748.6	0.22	9,487.9
0.16	11,775.0	0.13	11,944.6	0.28	8,374.8	0.31	10,578.1
0.20	12,019.4	0.33	14,231.0	0.31	8,529.3	0.35	10,892.9
0.42	12,707.4	0.38	14,676.7	0.35	8,793.1	0.41	11,240.8
0.58	13,116.6	0.57	15,325.7	0.43	9,126.9	0.42	11,283.7

Maximum strength elastic (V_y) was divided by the total weight of a structure to obtain the strength index (C_y). Calculation of the seismic index for building A in the longitudinal direction are described as follow:

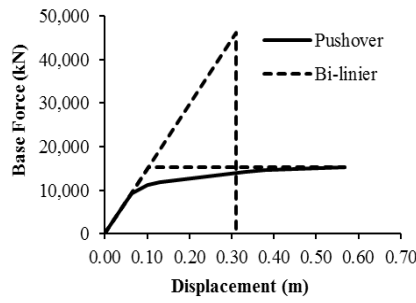
$$K_e = \frac{V_s}{\Delta_s} = 7,248.1 / 0.06 = 131,418.6 \text{ [kN/m]}$$

$$\mu = \frac{\Delta_u}{\Delta_y} = 0.56 / 0.09 = 5.83$$

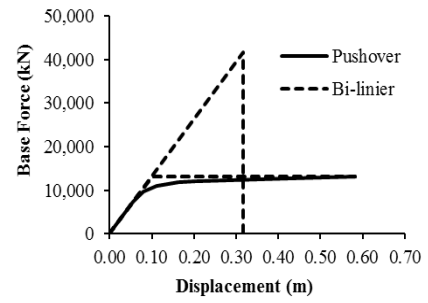
$$F = \sqrt{2\mu - 1} = \sqrt{2 \times 5.83 - 1} = 3.27$$

$$C_y = \frac{V_y}{W} = 12,730 / 80,240 = 0.16$$

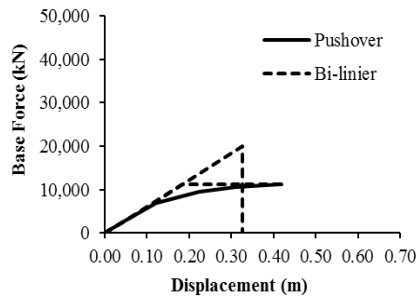
$$E_o = C_y \times F = 0.16 \times 3.27 = 0.52$$



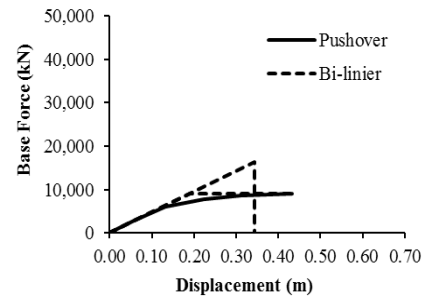
(a) I_s of building A in the longitudinal direction



(b) I_s of building A in the transversal direction



(c) I_s of building B in the longitudinal direction



(d) I_s of building B in the transversal direction

Figure 4.6. Seismic index (I_s) of building A and B

Table 4.8 shows the summarises calculation for buildings A and B for both directions. The bilinear curve for buildings A and B in both directions from Table 4.8 are plotted in graphs as shown in Figure 4.6.

Table 4.8. Seismic index using pushover analysis

Case	K_e (kN/m)	μ	F	C_y	$E_o = C_y \cdot F$
A_Long	1.31E+05	5.83	3.27	0.16	0.52
A_Trans	1.49E+05	5.50	3.16	0.18	0.58
B_Long	4.78E+04	2.26	1.88	0.18	0.34
B_Trans	6.11E+04	2.27	1.88	0.22	0.42

A seismic index comparison using procedure level-1 of Japanese standard and a seismic index based on pushover analysis can be seen in Table 4.9. The seismic index value for the entire structure can be represented by the index on the 1st floor in the calculation of level-1. As shown in Table 4.9, the result of the seismic index results from pushover analysis is larger than the results of the seismic index based on the Japanese standard. Due to the fact that the calculation of structural capacity was carried out until post elastic conditions and stopped when ultimate capacity was achieved. While the calculation based on the Japanese standard on level - 1 was only based on Eq. (4.2) and Eq. (4.3). Furthermore, the shear stress value used an average value of 0.7 to 1.0 N / mm².

Table 4.9. Seismic index comparison

Case	I_s	I_s
	(Level-1)	(Pushover)
A_Long	0.30	0.52
A_Trans	0.32	0.58
B_Long	0.26	0.34
B_Trans	0.26	0.42

4.4.3. Evaluation of Structure Performance

The seismic demand index (I_{so}) was taken as 0.8 based on the Japanese standard. This demand index is estimated based on hazard conditions due to earthquake loads in Japan. The response spectrum at specific locations other than Japan can be determined based on the code of that location. The response spectrum then becomes a demand curve and it will be compared to the capacity curve in the acceleration-displacement response spectrum (ADRS) format. The intersection of these two curves is the approximation of the performance point of the structure.

In this study, the performance point of buildings A and B were investigated based on the Indonesian seismic load. The demand response spectrum of spectral acceleration is 1.4 at 0.2 seconds and 0.6 at 1 second in Padang city. The site coefficient is taken as 1.0 and 1.5. Figure 4.7 shows the performance point of buildings A and B.

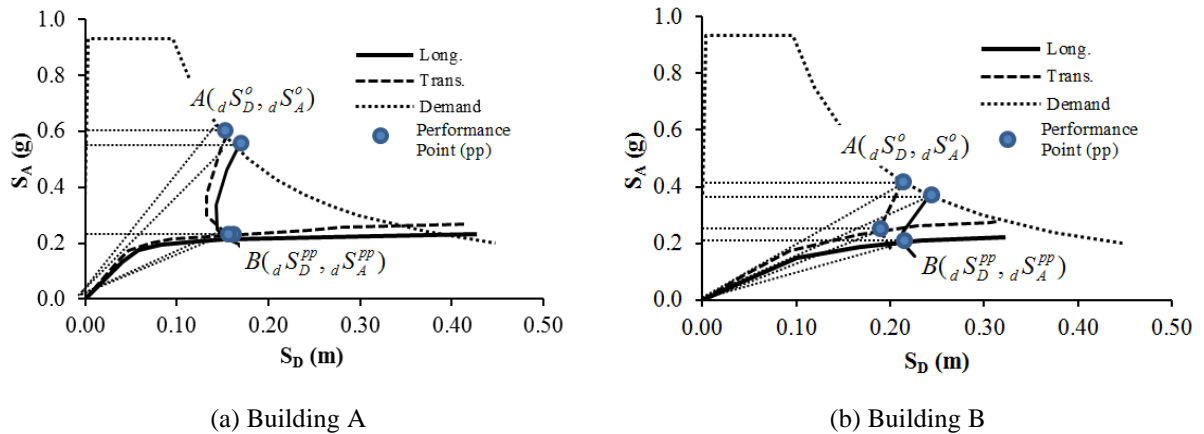


Figure 4.7. Performance point of Building A and B

A similar procedure for determining the seismic index can also be applied in determining the seismic demand index. The seismic demand index is given by the product of the strength index (C_y) and the ductility index (F). The ductility index (F) is equal to a ratio between $A(dS_D^o, dS_A^o)$ and

$B({}_d S_D^o, {}_d S_A^o)$ as shown in Figure 4.7. The point A is an acceleration response at the demand curve and B is acceleration response at the performance point. The seismic demand index, I_{so} , is taken equal to E_{so} since no reduction factor is considered. By this method, the seismic demand index is smaller than the seismic demand base on the Japanese standard. The seismic index value (I_s) as shown in Table 4.9 is larger than the seismic demand index (I_{so}) of Table 4.10, so that the building is in a safe condition.

Table 4.10. Evaluation of the structure performance

Case	A (${}_d S_D^o, {}_d S_A^o$)	B (${}_d S_D^o, {}_d S_A^o$)	F (A/B)	C_y	I_{so} ($E_{so} = F \cdot C_y$)
A_Long	0.540	0.210	2.57	0.16	0.41
A_Trans	0.580	0.225	2.58	0.18	0.47
B_Long	0.370	0.195	1.90	0.18	0.35
B_Trans	0.420	0.255	1.65	0.22	0.36

4.5. Conclusion

Two existing buildings were evaluated in this chapter. The first building consisted of five stories and the second has four stories. Both buildings were moment-resisting frame system and reinforced concrete material. An index represented the seismic performance of the existing building in the Japanese standard. This index was called by a seismic index which a function of strength and ductility parameters. The structure has the difference seismic indexes in lateral and transversal directions because of the differences in the stiffness in both directions. The evaluation result, building A has a seismic index in transversal direction larger than in a longitudinal direction. Meanwhile, building B has the same seismic index in both directions of the structure.

The application of a seismic index based on the Japanese standard needs adjustment for other countries. In this study, a set procedure was proposed to determine the seismic index based on the result of the pushover analysis. The result of the seismic index was higher than it obtained by the Japanese standard, due to the calculation of structural capacity was carried out until post elastic conditions. While the calculation based on the Japanese standard on level - 1 was based on the average shear stress on the resisting elements of lateral force. Furthermore, the seismic demand index was smaller compared to the Japanese seismic demand index. The final assessment of the structural performance of this proposed method indicated that both buildings were in a safe condition.

Chapter 5

The Dynamic Seismic Performance Index of Building in Indonesia

5.1. Introduction

Indonesia is an earthquake-prone country that often experiences earthquakes. The main cause is that it is located on the interface of three tectonic plates: Eurasian, Pacific, and Indo-Australian. These plates continue to move and collide with each other. A series of earthquake events have occurred in Indonesia, such as the 1797 collision of the Sumatran-Andaman plate, with a magnitude of 8.9. In 2004, a huge earthquake occurred in Simeulue Island, Banda Aceh, with a magnitude of 9.1 and was followed by a devastating tsunami. There was an earthquake of magnitude 8.5 in Mentawai island in September 2007, and an earthquake of magnitude 7.6 hit Padang in 2009 due to the subducting plate and caused considerable damage to the city. Again on Mentawai island, an earthquake of magnitude 7.8 occurred in 2010, which caused a tsunami on the west coast of those islands [1, 29].

A standard for the seismic evaluation of an existing building was published by The Japan Building Disaster Prevention Association (JBDPA) in 1977 [32]. From this, an index to determine the performance of buildings due to earthquake loads, known as the seismic index, was created and is widely used in Japan. Nakazawa et al. proposed a seismic performance evaluation method for steel gymnasiums using a dynamic structural seismic index corresponding to the critical deformation of a member based on the nonlinear seismic response analysis [8, 9, 46, 47]. This method has a more complex analysis in determining the performance index than the seismic index of the JBDPA which determined their index without performing dynamic analysis [29, 32].

Until now, there have been no guidelines that can be used to evaluate the performance of an existing structure in Indonesia, although regulations regarding the design of earthquake-resistant structures continue to be updated [3, 41]. This paper proposes a method to obtain the performance of an existing structure with the dynamic seismic index dI_s considering Indonesia's seismic hazard and the dynamic ductility index dF that represents a modification factor (R). To estimate the dynamic ductility factor dF two methods are proposed. The first is the average energy principle with a constant value of 1.0, and the average energy and displacement principle. The second is the equivalent linearization method by considering Indonesia's response spectrum design.

5.2. Numerical Model

In the past, a lot of buildings collapsed during an earthquake with the ground floor being destroyed while the above floor still existed. This kind of collapse is known as a soft-story phenomenon. In a multi-story building where the upper level is more rigid than the first floor, plastic hinges will occur at the top column, as shown in Figure 5.1a. A lumped mass method may be used to model the 3D structures in which the mass is concentrated in the center of mass. The mechanism of collapse and the inter-story drift of MDOF system that are dominant in the first mode can be presented in an SDOF system. In this study, the soft-story phenomenon where the adjacent floor is stiffer than the first floor is modeled as an SDOF system for simplification as shown in Figure 5.1b. The effective weight and the stiffness of the SDOF system can vary by setting the parameters of the fundamental period T_0 , which are selected from 0.1 to 2.0. The shear force yield coefficient C_y varies from 0.1 to 0.5. The critical ductility factor μ_{cr} is taken from low ductility until high ductility with μ_{cr} of 1.0 until 10. In order to get nonlinear conditions, seismic intensity λ_E increases step by step from 1.0 until ten or more, in increments of 1.0. Nonlinear behavior is modeled as a bilinear hysteretic model, which assumes a second stiffness ratio k_2 of 0.05.

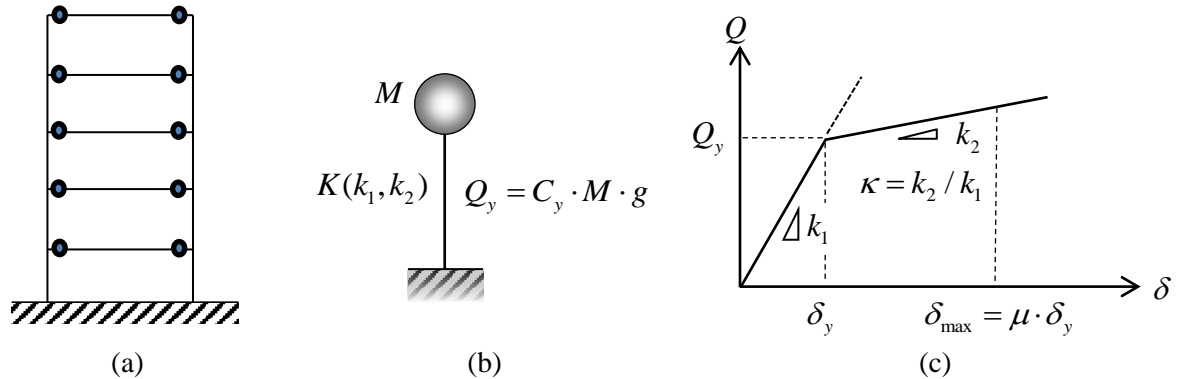


Figure 5.1. SDOF system with bilinear hysteretic model

5.3. Methodology

The dynamic response characteristic of inelastic systems with respect to earthquake ground motion is one of the fundamental themes in earthquake-resistant structure design. Nonlinear analysis was carried out, varying the magnitude of the maximum input ground motion by certain increments to measure the continuous response from elastic to yield until nonlinear conditions were reached. This method, known as incremental dynamic analysis, has been used in previous research [48, 49]. The dynamic seismic index is obtained from an incremental dynamic analysis that shows the response of a structure as performance due to earthquake load.

In this study, the first step was carried out by a simulated ground motion that fit into Indonesia's seismic condition and conformed to Indonesia's seismic code [10]. Then, dynamic analysis was performed using these simulated ground motions. A shear force coefficient at elastic condition (C_0) was calculated by linear dynamic analysis at a seismic intensity (λ_E) of 1.0. The next stage, the nonlinear dynamic analysis was carried out by amplifying λ_E with an increment of 1.0 for each step. This was conducted 20 times or more until each model reached a nonlinear condition. Afterward, a linear interpolation was calculated to get the response for each critical ductility (μ_{cr}) to obtain the result of the dynamic seismic index (dI_s) and the ductility index (dF). Each of the above calculations was carried out on each earthquake ground motions.

A total of 1500 combination analyses were carried out by nonlinear dynamic methods, as tabulated in Table 5.1. The value of the fundamental period (T_0) depends on the stiffness and mass. In general, the low rise and high rise buildings except the base isolation structure will have a period in the range of 0.1 to 2.0 seconds. Earthquake resistant buildings have inelastic state design that generally uses response modification coefficient (R) values ranging from 2.0 to 8.0 based on code. The shear force coefficient at the initial yield (C_y) is the ratio of the maximum shear coefficient at the elastic condition (C_e) and the response modification. It can be expressed as $C_y = C_e / R$. The value of the shear coefficient can be calculated from the elastic response spectrum based on code. If the structure is at the elastic condition with C_e equal to 1.0 and $R = 2.0$, so C_y will be 0.5. The C_y value will be less than 0.5 for $R = 8.0$. When the structure is designed at the inelastic condition, then the value of C_e will be smaller, so the C_y value will be smaller as well. In this study, the C_y value is taken in the range of 0.1 to 0.5.

Table 5.1. Selected ductility factor when varying T_0 and C_y

$T_0 [sec] \backslash C_y$	0.1	0.2	0.3	0.4	0.5
0.1	1, 2, 3, ..., 10	1, 2, 3, ..., 10	1, 2, 3, ..., 10	1, 2, 3, ..., 10	1, 2, 3, ..., 10
0.2	1, 2, 3, ..., 10	1, 2, 3, ..., 10	1, 2, 3, ..., 10	1, 2, 3, ..., 10	1, 2, 3, ..., 10
\vdots	1, 2, 3, ..., 10	1, 2, 3, ..., 10	1, 2, 3, ..., 10	1, 2, 3, ..., 10	1, 2, 3, ..., 10
1.0	1, 2, 3, ..., 10	1, 2, 3, ..., 10	1, 2, 3, ..., 10	1, 2, 3, ..., 10	1, 2, 3, ..., 10
1.2	1, 2, 3, ..., 10	1, 2, 3, ..., 10	1, 2, 3, ..., 10	1, 2, 3, ..., 10	1, 2, 3, ..., 10
\vdots	1, 2, 3, ..., 10	1, 2, 3, ..., 10	1, 2, 3, ..., 10	1, 2, 3, ..., 10	1, 2, 3, ..., 10
2.0	1, 2, 3, ..., 10	1, 2, 3, ..., 10	1, 2, 3, ..., 10	1, 2, 3, ..., 10	1, 2, 3, ..., 10

Note : 1, 2, 3, ..., 10 are μ_{cr}

5.3.1. Input Earthquake Motions

The objective buildings were assumed to be located in Padang city, Indonesia. The demand acceleration spectrum S_A at the ground surface is determined by the Indonesian code and is considered as:

$$S_A(T, h, \lambda_E) = \lambda_E \times S_{A0}(T) \times F_h(h) \quad (5.1)$$

in which T was the natural period of the structure, h was the damping factor, λ_E was seismic intensity. This gave an index representing the strength of an earthquake's ground motion. $\lambda_E = 1.0$ represents a design basis earthquake (DBE) level and corresponds to an extremely rare earthquake with a return period interval of 500 years, while $\lambda_E = 1.5$ represents a risk-targeted maximum considered earthquake (MCER) level and corresponds to the largest possible earthquake expected to occur in the next 2,500 years.

$F_h(h)$ is a numerical coefficient of the response spectrum reduction corresponding to the damping factor h of a structure. Various equations have been proposed for $F_h(h)$. The building standard law (BSL) of Japan adopted the following equation [50, 51]:

$$F_h(h) = \frac{1.5}{1 + 10.h} \quad (5.2)$$

The Architectural Institute of Japan (AIJ) recommends the following equation, where a is 75 and h_0 is 5% as initial elastic damping [9]:

$$F_h(h) = \sqrt{\frac{1+a \cdot h_0}{1+a \cdot h_{eq}}} \dots\dots\dots (5.3)$$

The International Building Code (IBC) proposed a very close approximation to the reduction coefficient related to the damping ratio (h) in the following equation [43, 52]:

$$F_h(h) = 0.25 \cdot (1 - \ln h) \dots\dots\dots (5.4)$$

$S_{A0}(T)$ is a demand acceleration response spectrum with $\lambda_E = 1.0$ and damping factor $h = 5\%$ at the ground surface and takes into account the amplification of the surface soil layer.

$$S_{A0}(T) = \begin{cases} S_{DS} \left(0.4 + 0.6 \frac{T}{T_0} \right) & \dots \quad T \leq T_0 \\ S_{DS} & \dots \quad T_0 < T \leq T_s \\ \frac{S_{D1}}{T} & \dots \quad T > T_s \end{cases} \dots\dots\dots (5.5)$$

where, $T_0 = 0.2 \frac{S_{D1}}{S_{DS}}$, $T_s = \frac{S_{D1}}{S_{DS}}$

Here, S_{D1} is the design spectral response acceleration parameter at 1.0 second, and S_{DS} is the design spectral response acceleration parameter at short periods. Figure 5.2 shows the design response spectrum as it conforms to Indonesian code SNI 1726 [10].

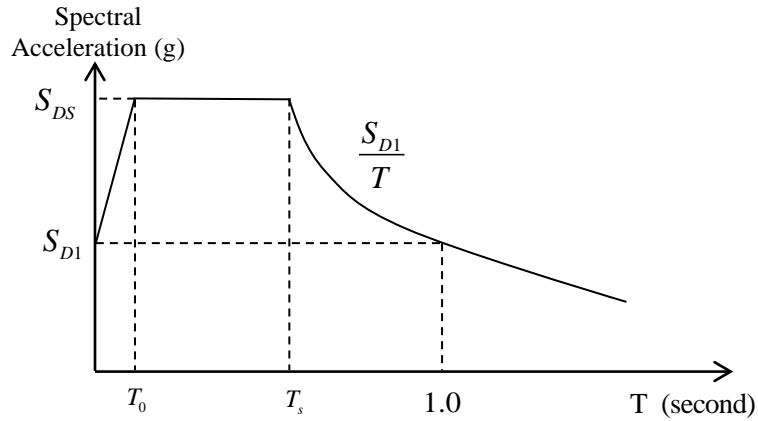


Figure 5.2. The design response spectrum of Indonesian code

In order to carry out the time history nonlinear seismic response analysis, the ground motions were simulated to fit the target design of the response spectrum by referring to Equation (5.5).

5.3.2. Simulated Ground Motions

A nonlinear dynamic method performs analysis with subjected to earthquake ground motions to obtain the result on forces and displacements. The calculation response can be sensitive to the characteristics of single ground motion, so more than ground motion was required [53–55]. In Indonesian code it is specified that the dynamic analysts must use at least three ground motion data. Indonesia has no recorded the ground acceleration time history for the strong earthquakes that ever occurred. The ground acceleration record can be selected from events of magnitudes that comply with the maximum considered earthquake of Indonesian code. Six of ground motion consisting of El-Centro, Kobe, and Taft waves were used as input ground motion in this analysis. The average of these six data must be close to the response spectrum target.

In order to meet the target of peak ground acceleration (PGA) conforming to Indonesia's seismic code, a simulated ground motion method was used for scaling PGA of earthquake data to be equal with PGA in a certain location in Indonesia. The results of the simulated earthquake ground motions were used as the input of seismic loads for dynamic analysis. One target of a response spectrum for simulation is Padang city, located in the west part of Indonesia, because this is the most earthquake-prone city in Indonesia. The risk-targeted maximum considered earthquake (MCER) had an acceleration of 1.39 over a short period (S_s) and 0.6 at the 1.0 second period of period (S_I). The site soil properties were soft soil and the site coefficients were 0.9 in the short period and 2.4 at the 1.0 second period. Therefore, in the DBE level, the response spectra design at the short period (S_{DS}) became 0.834 second and 0.96 at the 1.0 second period (S_{DI}). Results of the simulated peak ground motion can be seen in Table 5.2.

Table 5.2. Simulated earthquake ground motions

Type of Ground Motion	Year	PGA [cm/s ²]	Simulated PGA [cm/s ²]
El Centro – NS	1940	341.6	309.2
El Centro – EW		210.1	259.9
Kobe – NS	1995	817.8	403.0
Kobe – EW		617.1	418.3
Taft – NS	1952	152.7	362.9
Taft – EW		175.9	310.5

The simulated ground motions of El Centro, Kobe, and Taft earthquakes were scaled into the Indonesia response spectrum, as shown in Figure 5.3. Figure 5.3(a) shows the acceleration response

spectrum based on the original earthquake motions; and Figure 5.3(b) shows the acceleration response spectrum base on the simulated earthquake motions at the design basis earthquake (DBE) level. The simulated earthquake motions will be used in every dynamic analysis in this study.

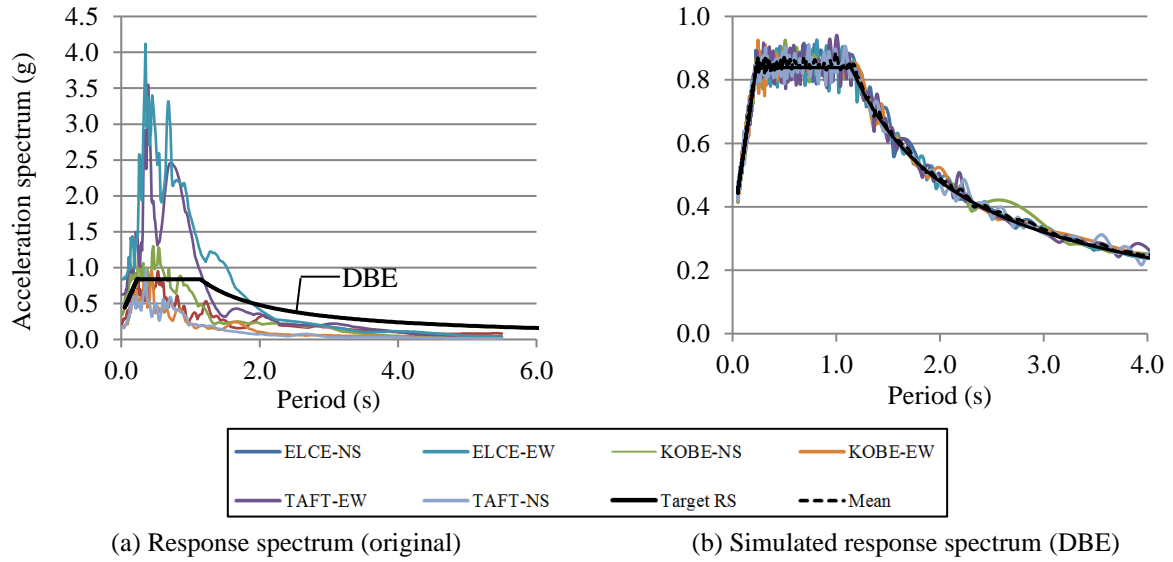


Figure 5.3. Simulation of the acceleration response spectrum

5.3.3. Dynamic Seismic Index and Ductility Index

Seismic intensity λ_E is represented as an index identifying the magnitude of the seismic input wave to the objective structure. The maximum input ground acceleration A_{\max} is defined as an index representing the magnitude of the input seismic motion to the objective structure. Nonlinear response analyses were performed while gradually increasing the seismic intensity, and the maximum deformation of the objective structure for each input level was calculated. Figure 5.4 shows the concept of a dynamic ductility index and dynamic seismic performance index. The relationship between shear force Q (shear force coefficient C) and maximum deformation δ_{\max} (ductility factor μ) is shown.

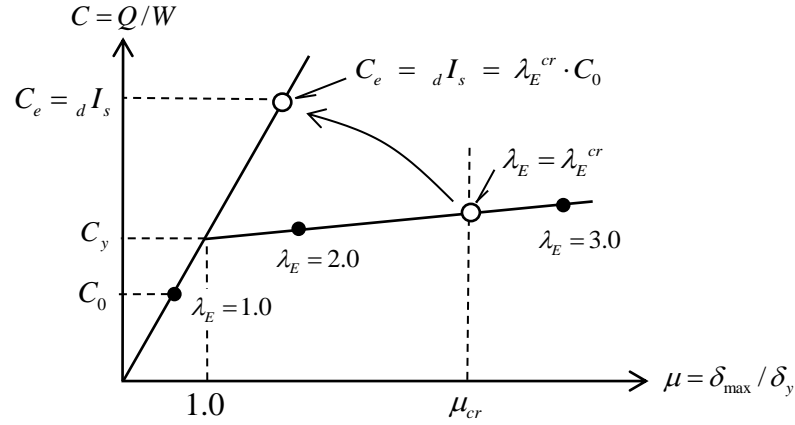


Figure 5.4. Relationship between shear force coefficient C and ductility factor μ

As illustrated in Figure 5.4, the critical deformation is defined in order to evaluate the limit state of structures. The critical seismic intensity λ_E^{cr} is obtained when the maximum deformation reaches the critical deformation by nonlinear analysis method. A shear force coefficient at elastic condition C_0 is obtained with respect to $\lambda_E^{cr} = 1.0$. The maximum of shear force coefficient at elastic condition C_e , as expressed as a dynamic seismic performance index ${}_dI_s$, corresponding to λ_E^{cr} , when the structure is elastic, can be expressed as

$$C_e = {}_dI_s = \lambda_E^{cr} \cdot C_0 \dots\dots\dots (5.6)$$

The response modification factor (R) of a structure can be estimated not only from the code of a building's seismic design but also from dynamic analysis. The dynamic ductility index ${}_dF$ represents the R -value, which explains the margin of the initial yield to the limit state. The value of ${}_dF$ is determined by the dynamic seismic index ${}_dI_s$ dividing the yielding shear coefficient C_y .

$${}_dF = \frac{{}_dI_s}{C_y} = \frac{\lambda_E^{cr} \cdot C_0}{C_y} \dots\dots\dots (5.7)$$

In general, the value of C_y is a shear force coefficient corresponding to the ultimate shearing force of a structure.

5.3.4. Estimation Method of Ductility Index

The dynamic ductility index can be estimated without conducting a dynamic analysis. Two methods were investigated in this paper. The first method was based on the characteristic of maximum displacement, and the second on the equivalent linearization of nonlinear response.

5.3.4.1. The Characteristic Displacement Response Method

The value of the dynamic ductility index can be estimated based on the characteristic of maximum displacement response. The values of dF are highly dependent on the critical deformation or critical ductility factor μ_{cr} . In previous studies, Newmark & Hall proposed rules concerning the relation of maximum displacement and yield strength on the inelastic earthquake response of bilinear systems, as shown in Figure 5.5 [56, 57]. Over a relatively short period, the maximum potential energy of an elastic system (area OAD in Figure 5.5(a)) and the inelastic potential energy for a system with the same initial period (area OBCE in Figure 5.5(a)), are almost the same irrespective of the yield strength. This is called the constant energy principle. The relationship of ductility index is closer to:

$$F = \frac{Q_e}{Q_y} = \sqrt{2\mu - 1} \dots\dots\dots (5.8)$$

Over a relatively long period, the maximum displacement of inelastic systems and the maximum displacement of elastic systems in the same initial period, are almost the same if the yield strength is larger than a certain limiting value. This is called the constant displacement principle or property of displacement conservation. The ductility index equation as follows:

$$F = \frac{Q_e}{Q_y} = \mu \dots\dots\dots (5.9)$$

For a structure with a very short period, the maximum displacement of systems is an elastic condition. The ductility is ineffective in reducing the required elastic seismic force. The ductility index is a constant of 1.0.

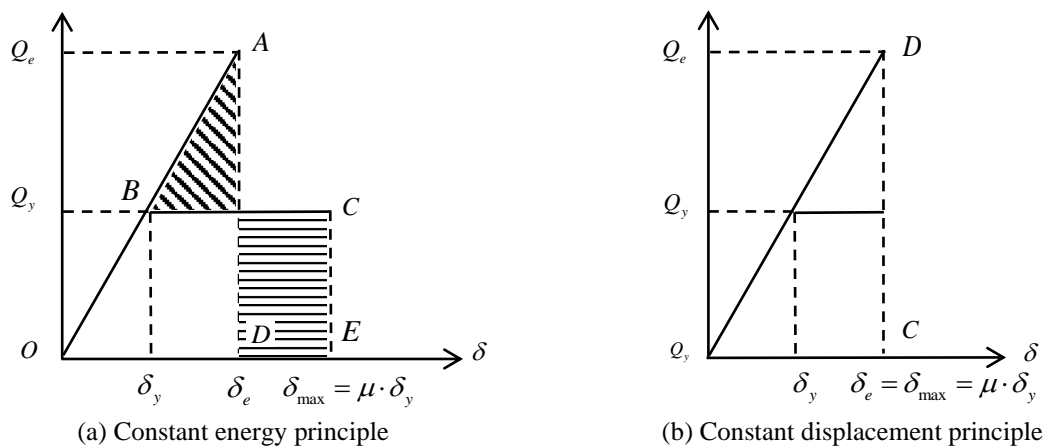


Figure 5.5. Characteristics of maximum displacement

This study proposes a transition estimation formula that has a period in between the very short period and short period range. The transition estimation forecasts an average value of the constant energy principle and constant ductility index of 1.0 as follows:

$$F = \frac{Q_e}{Q_y} = \left(1 + \sqrt{2\mu_{cr} - 1}\right) / 2 \dots\dots\dots(5.10)$$

The transition estimation of the ductility index is also proposed for the period range in between a short period and long period. The forecast formula is an average value of the constant energy principle and constant displacement principle as follows:

$$F = \frac{Q_e}{Q_y} = \left(\mu_{cr} + \sqrt{2\mu_{cr} - 1}\right) / 2 \dots\dots\dots(5.11)$$

5.3.4.2. The Equivalent Linearization Method

In 2017, Nakazawa et al. investigated an estimation method to obtain a seismic performance index for a steel gymnasium structure using the Japanese seismic code [9]. The implementation of this method needed adjustment for the Indonesian seismic code. In this study, the equivalent linearization method proposed by changes the response spectrum parameter by using Indonesia response spectrum design as described in Eq. (5.5). The maximum deformation δ_{\max} base on the equivalent linearization method, considering the seismic intensity λ_E can be expressed as:

$$\delta_{\max} = \mu \cdot \delta_y = S_D(\lambda_E, T_{eq}, h_{eq}) = \frac{T_{eq}^2}{4\pi^2} \lambda_E \times S_{AG0}(T_{eq}) \times F_h(h_{eq}) \dots\dots\dots(5.12)$$

Therefore, the equivalent damping factor h_{eq} and equivalent period T_{eq} for the bilinear restoring force can be obtained as follows.

$$h_{eq} = h_0 + \frac{2}{\pi \mu \kappa} \ln\left(\frac{1 - \kappa + \mu \kappa}{\mu \kappa}\right), \quad T_{eq} = \sqrt{\frac{\mu}{1 + \kappa(\mu - 1)}} T_0 \dots\dots\dots(5.13)$$

The critical seismic intensity λ_E^{cr} corresponding to the critical ductility factor μ_{cr} is given as

$$\lambda_E^{cr} = \frac{g C_y T_0^2}{S_{AG0}(T_{eq}) \times F_h(h_{eq}) T_{eq}^2} \cdot \mu_{cr} \dots\dots\dots(5.14)$$

Also, the base shear coefficient C_0 of the elastic system at the damage limit level ($\lambda_E = 1.0$) can be obtained from the following equation using the response spectrum:

$$C_0 = \frac{S_{AG0}(T_0) \times F_h(h_0)}{g} \dots\dots\dots(5.15)$$

Substituting Eq. (5.14) and (5.15) into the definition of ${}_dF$ in Eq.(5.7), the estimated value ${}_dF^{est}$ of the dynamic ductility index obtained by the equation as follows

$${}_dF^{est} = \left(\frac{S_{AG0}(T_0)}{S_{AG0}(T_{eq})} \right) \cdot \left(\frac{F_h(h_0)}{F_h(h_{eq})} \right) \cdot (1 + \kappa(\mu_{cr} - 1)) \dots\dots\dots(5.16)$$

Here, S_{AG0} with respect to T_0 and T_{eq} is determined based on the acceleration response spectrum design conforming to Indonesia's seismic code. Several reduction factors for this acceleration, as explained in Eq (5.2),(5.3) and (5.4) are investigated in this study.

5.4. Analysis Result

5.4.1. Dynamic Seismic Index

Dynamic linear analysis with a seismic intensity λ_E of 1.0 was carried out to obtain the elastic shear force coefficient of C_0 . C_0 is the shear force at λ_E of 1.0 over the weight of the structure (W) as in by following Eq (5.17). The result of C_0 is presented in Table 5.3.

$$C_0 = Q(\lambda_E = 1.0) / W \dots\dots\dots(5.17)$$

Table 5.3. The shear coefficient of C_0

T_0 (sec)	δ_{max} (cm)	Q_{max} (kN)	C_0
0.10	0.01	4352.50	0.453
0.20	0.06	5686.83	0.592
0.30	0.13	5642.17	0.587
0.40	0.24	5777.83	0.602
0.50	0.39	6025.17	0.627
0.60	0.59	6301.67	0.656
0.70	0.78	6150.83	0.640
0.80	1.07	6463.00	0.673
0.90	1.28	6124.33	0.638
1.00	1.66	6404.83	0.667
1.20	2.24	6028.67	0.628
1.40	2.43	4790.33	0.499
1.60	2.80	4224.67	0.440
1.80	3.18	3797.83	0.395
2.00	3.54	3420.00	0.356

Figure 5.6 shows the spectrum of the dynamic seismic index, which is the relationship between natural periods and the dynamic seismic index (dI_s) for each critical ductility (μ_{cr}). Linear interpolation was done to estimate the dI_s index at each incremental of μ_{cr} .

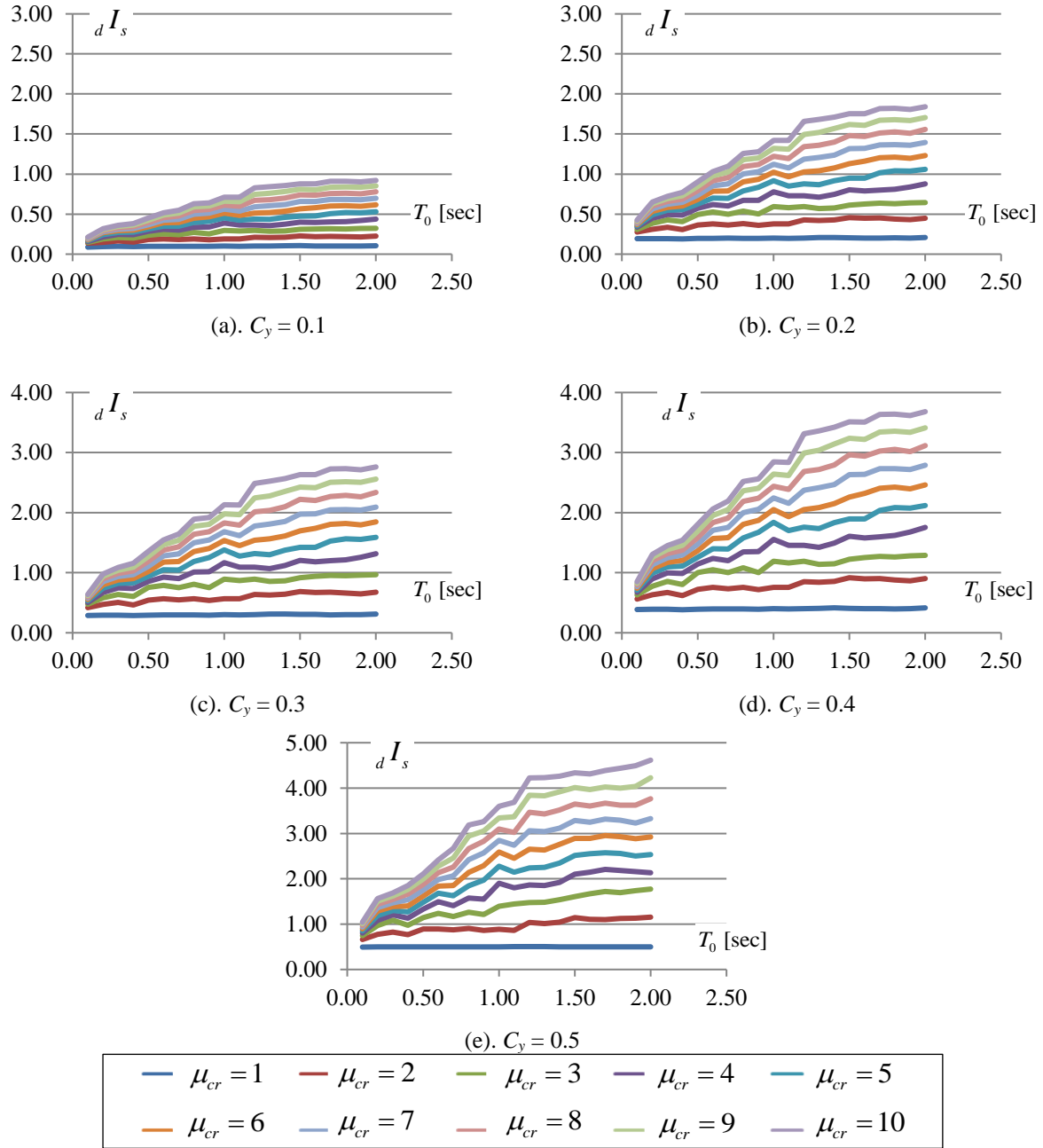


Figure 5.6. The spectrum of the dynamic seismic index (dI_s)

In Figure 5.6, the values of dI_s tends to increase with an increasing μ_{cr} . At low μ_{cr} , the increase of dI_s value is not too significant with increasing periods, but at higher μ_{cr} , it is.

5.4.2. Dynamic Ductility Index

The dynamic ductility index is defined as the ratio between the elastic shear coefficient at the initial yielding C_y and the maximum of shear coefficient at elastic condition C_e . Figure 5.7 shows the relationship between the dynamic ductility index (dF) and critical ductility (μ_{cr}) from a period of 0.1 until 2.0 seconds.

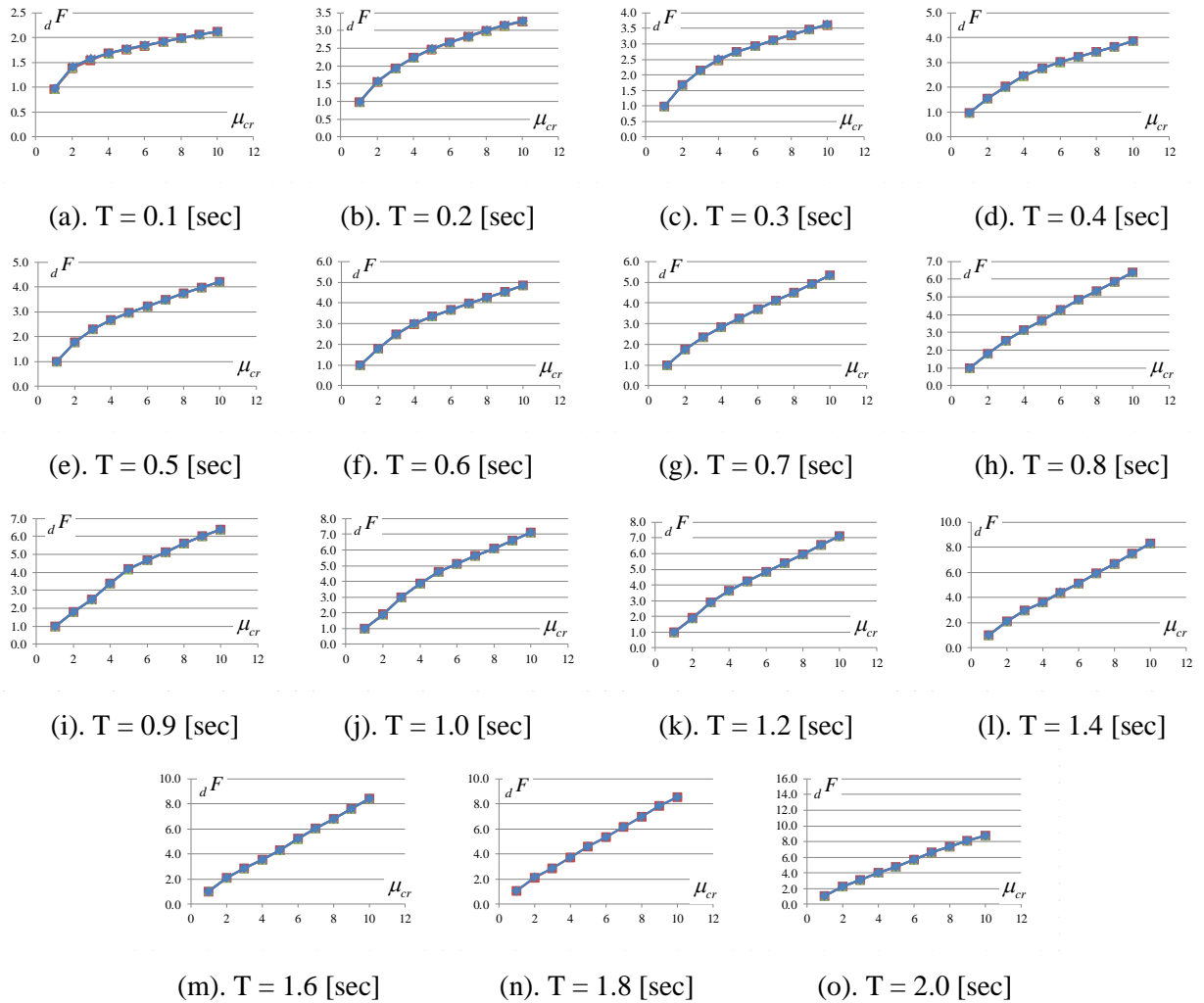


Figure 5.7. Relationship dynamic ductility index (dF) and critical ductility (μ_{cr})

Figure 5.7 indicates that the value of dF increases with an increase μ_{cr} value. The dF value for all variations of C_y is similar. This indicates that dF is independent of C_y .

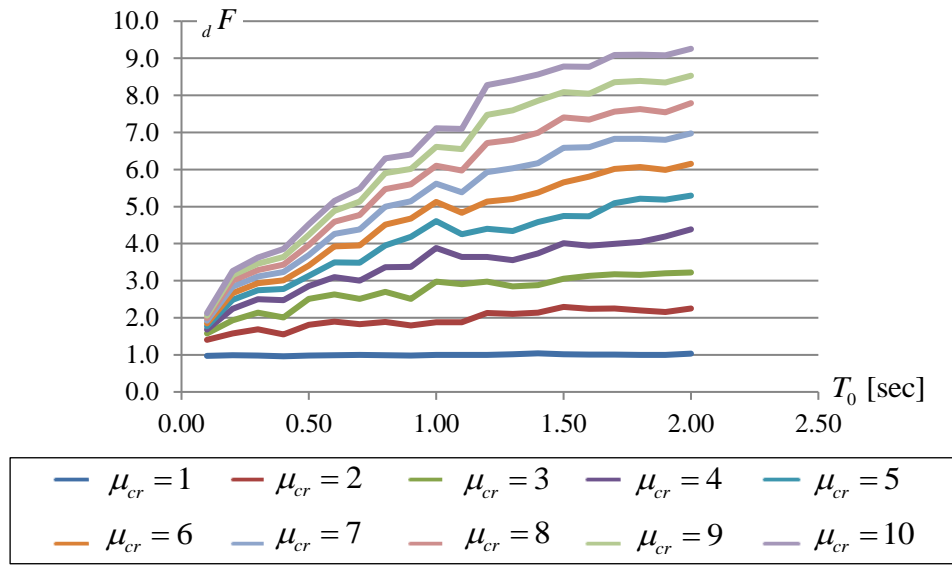


Figure 5.8. Spectrum of dynamic ductility index (dF)

Figure 5.8 shows the spectrum of the dynamic ductility index. The spectrum of dF for C_y of 0.1, 0.2, 0.3, 0.4, and 0.5 are equal with each other due to dF being independent of C_y . In Figure 5.8, the structure with high ductility produces greater dF at a high natural period. On the other hand, a structure with low ductility produces small dF values over an increasing period.

5.4.3. Estimation of Ductility Index

Dynamic analysis was done using a simulated earthquake load base on the Indonesian response spectrum.

5.4.3.1. Characteristic Displacement Estimation Method

The dynamic ductility index (dF) for several critical ductility factors (μ_{cr}) from low to high was calculated. The ductility index was estimated based on the proposal equation (5.8), (5.9), (5.10), and (5.11) as follows:

$$\begin{aligned}
 {}_dF_{est_1} &= \sqrt{2\mu - 1} \\
 {}_dF_{est_2} &= \mu_{cr} \\
 {}_dF_{est_3} &= \left(1 + \sqrt{2\mu_{cr} - 1}\right) / 2 \\
 {}_dF_{est_4} &= \left(\mu_{cr} + \sqrt{2\mu_{cr} - 1}\right) / 2 \dots\dots\dots(5.18)
 \end{aligned}$$

The ratio of dynamic ductility index (dF) and estimated ductility index (dF_{est}) was obtained in order to observe the accuracy of the estimation. When the ratio of dF/dF_{est} was close to 1.0, it meant that the estimation was more accurate. A horizontal line marker, which has a constant gradient of 1.0, was plotted to mark the accuracy of the ratio.

Figure 5.9 shows the relationship between the critical ductility factor (μ_{cr}) and the ratio of dF/dF_{est} . As shown in Figure 5.9.a, at a period of 0.1, the chart of dF_{est_3} is close to the horizontal line of 1.0 compared to the other charts. However, the estimation method changed at period 0.3, and the chart of dF_{est_1} was closer than the others (Figure 5.9.b). In Figure 5.9.c, the estimation of dF_{est_4} was closer to the horizontal line. The estimation of dF_{est_2} was closer from 1.2 up to 2.0 (Figure 5.9.e and 5.9.f).

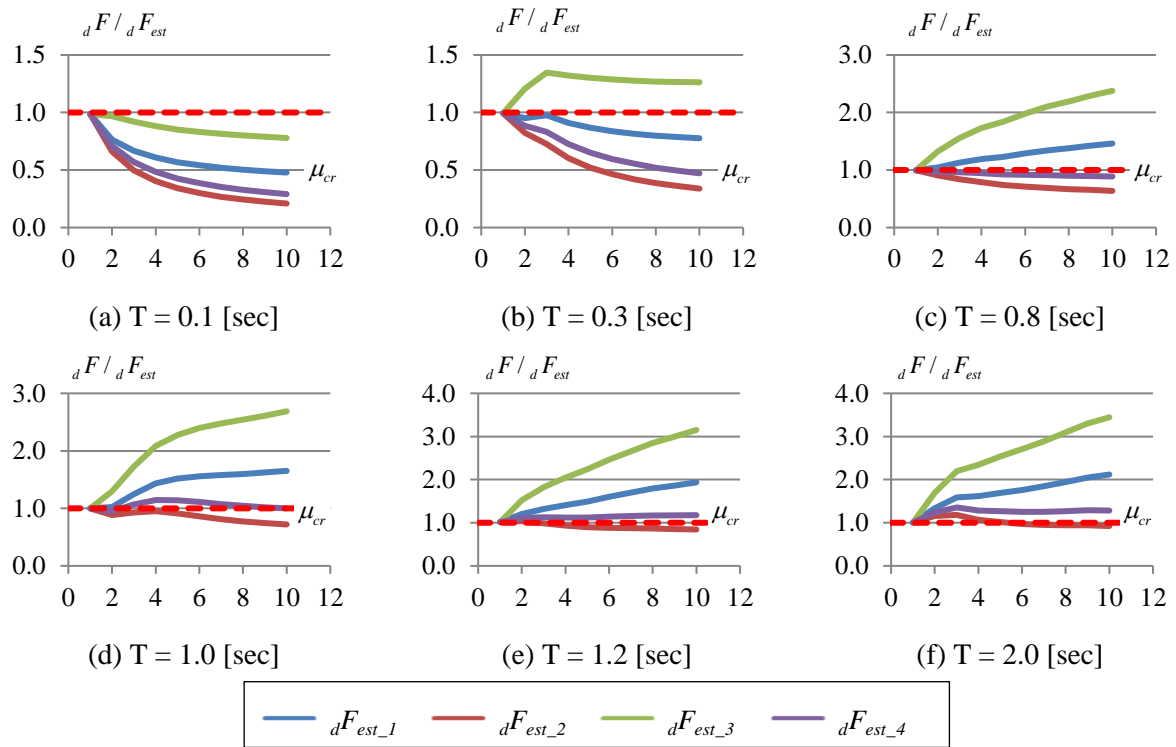


Figure 5.9. Relationship dynamic ductility index and estimation ductility index

The accuracy of all estimation methods of Figure 5.9 is summarised in Table 5.4. An average error for the whole critical ductility (μ_{cr}) was calculated for each period. The accurate estimation method was selected based on minimum error. Table 5.4 shows the minimum error for each estimation method.

Table 5.4. The percentage of error estimation for each dF estimation

T_0 [sec]	% Error					$dF_{est_#}$
	dF_{est_1}	dF_{est_2}	dF_{est_3}	dF_{est_4}	Min	
0.1	38.7%	58.7%	13.8%	51.6%	13.8%	dF_{est_3}
0.2	19.1%	47.4%	16.0%	37.4%	16.0%	dF_{est_3}
0.3	12.9%	43.6%	25.3%	32.8%	12.9%	dF_{est_1}
0.4	12.8%	44.3%	26.0%	33.2%	12.8%	dF_{est_1}
0.5	1.0%	37.2%	43.5%	24.5%	1.0%	dF_{est_1}
0.6	9.1%	31.7%	59.1%	17.4%	9.1%	dF_{est_1}
0.7	10.4%	31.5%	61.6%	16.9%	10.4%	dF_{est_1}
0.8	24.8%	23.7%	83.9%	6.9%	6.9%	dF_{est_4}
0.9	28.1%	22.3%	89.3%	4.9%	4.9%	dF_{est_4}
1.0	42.4%	14.1%	111.0%	5.5%	5.5%	dF_{est_4}
1.1	39.6%	15.7%	106.8%	3.4%	3.4%	dF_{est_4}
1.2	53.2%	8.1%	127.6%	13.1%	8.1%	dF_{est_2}
1.3	52.5%	8.7%	126.5%	12.4%	8.7%	dF_{est_2}
1.4	56.6%	6.2%	132.7%	15.5%	6.2%	dF_{est_2}
1.5	64.1%	1.6%	143.8%	21.1%	1.6%	dF_{est_2}
1.6	63.9%	1.6%	143.5%	21.1%	1.6%	dF_{est_2}
1.7	66.7%	0.0%	147.7%	23.1%	0.0%	dF_{est_2}
1.8	66.1%	0.3%	146.7%	22.7%	0.3%	dF_{est_2}
1.9	65.7%	0.5%	146.2%	22.4%	0.5%	dF_{est_2}
2.0	69.5%	1.5%	151.9%	25.0%	1.5%	dF_{est_2}

From Table 4, the estimation of the ductility index, dF_{est} , can be formulated with respect to the range of period shown in this following equation:

$$dF_{est} = \begin{cases} 1 & , T < 0.1 \text{ [sec]} \\ \left(1 + \sqrt{2\mu_{cr} - 1}\right)/2 & , 0.1 \leq T < 0.3 \text{ [sec]} \\ \sqrt{2\mu_{cr} - 1} & , 0.3 \leq T < 0.8 \text{ [sec]} \\ \left(\mu_{cr} + \sqrt{2\mu_{cr} - 1}\right)/2 & , 0.8 \leq T < 1.2 \text{ [sec]} \\ \mu_{cr} & , 1.2 \leq T < 2.0 \text{ [sec]} \end{cases} \dots\dots\dots(5.19)$$

Equation (5.19) consists of 5 groups covering different periods. The first group is for a period of less than 0.1. The ductility index can be estimated with a constant value of 0.1. In the second group, for a period between 0.1 and 0.3, the ductility index can be estimated with the average of energy principle and 1.0, Eq. (5.10). The energy principle can estimate the ductility index in the range 0.3 to 0.8 in the third group. The average of the energy and displacement principle, Eq. (5.11), can estimate

the ductility index at 0.8 until less than 1.2 in the fourth group. In the last group, at a period greater than 1.2, the ductility index is close to the critical ductility value, which corresponds to the displacement principle.

5.4.3.2. Equivalent Linearization Estimation Method

Figure 5.10 shows the relationship ductility factor and dynamic ductility index at any certain period of several estimation methods.

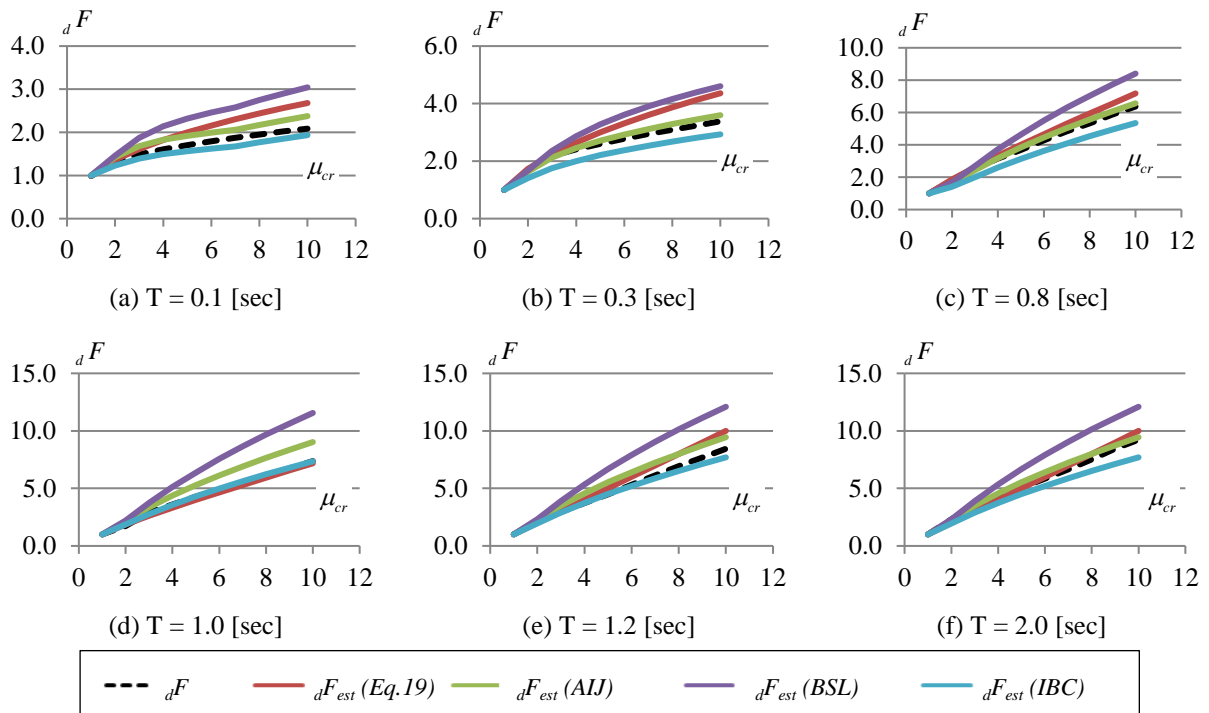


Figure 5.10. Relationship ductility factor and dynamic ductility index on several estimation methods

Figure 5.10, it can be seen, the estimation method using BSL's reduction at the top of the chart, or overestimated, and the estimation using IBC's reduction is at the bottom or slightly underestimated. The estimation method using the AIJ reduction factor gives the closest estimate to the dynamic ductility index (dF). In order to make observation easier, the ratio of estimation method and dynamic analysis with eliminating BSL and IBC are calculated in Table 5.5.

Table 5.5. The percentage of error comparison for both estimation method

T_0 [sec]	% Error		Min error estimation
	dF_est_AIJ	$dF_eq(5.19)$	
0.1	9.6%	13.8%	dF_est_AIJ
0.2	3.2%	16.0%	dF_est_AIJ
0.3	3.1%	12.9%	dF_est_AIJ
0.4	2.7%	12.8%	dF_est_AIJ
0.5	7.3%	1.0%	$dF_eq(5.19)$
0.6	8.0%	9.1%	dF_est_AIJ
0.7	1.9%	10.4%	dF_est_AIJ
0.8	0.9%	6.9%	dF_est_AIJ
0.9	8.5%	4.9%	$dF_eq(5.19)$
1.0	7.9%	5.5%	$dF_eq(5.19)$
1.2	12.8%	8.1%	$dF_eq(5.19)$
1.4	11.0%	6.2%	$dF_eq(5.19)$
1.5	6.8%	1.6%	$dF_eq(5.19)$
1.6	6.9%	1.6%	$dF_eq(5.19)$
1.7	5.4%	0.0%	$dF_eq(5.19)$
1.8	5.7%	0.3%	$dF_eq(5.19)$
1.9	5.8%	0.5%	$dF_eq(5.19)$
2.0	3.9%	1.5%	$dF_eq(5.19)$

As shown in Table 5.5, the accuracy of the estimation using the equivalent linearization method is more accurate for the lower period, but for the higher period, since the period of 0.9 until 2.0, the characteristic displacement estimation method gives the closest estimate. Both of the estimation methods can be used as alternatives to estimate the dynamic ductility index and dynamic seismic index of a structure without carrying out a nonlinear dynamic analysis, which is very complex and takes a long time.

5.5. Conclusion

This study dealt analytically with the dynamic seismic index dI_s and the dynamic ductility index dF in order to evaluate the seismic performance of a structure. A collection of simulated ground motions was used in linear and nonlinear dynamic analysis, which had Indonesia's response spectrum code as the target. The values of dI_s and dF were analyzed for a structure that had critical ductility factor μ_{cr} at a low ductility and at high ductility.

The relationship between dI_s and critical ductility factor μ_{cr} showed that the values of dI_s tended to increase with increasing μ_{cr} . Similar to dI_s , the dF value increases with an increase in the value of μ_{cr} ,

but the dF is independent of C_y . A structure with a high natural period and high ductility will produce a greater dF value.

The ductility index could be estimated by the estimation method without conducting the dynamic analysis. Two estimation methods were introduced in this paper. First, was the characteristic displacement response method, formulated from the relationship of the critical ductility factor μ_{cr} and the ductility index, as shown in Equation (5.19). Second was the equivalent linearization method.

The accuracy of the estimation method using equivalent linearization is more accurate in the lower period, but in the higher period, the proposed method using the characteristic displacement estimation response gave the closest estimate.

Chapter 6

Conclusion

6.1. Summary

An earthquake is not killing people but the collapse of building around the people can potentially kill them. Indonesia has often suffered major damaging earthquakes due to Indonesia located between the Eurasian plate, Pacific plate and Indo-Australian plate. Many big cities in Indonesia, with a large numbers of buildings, are in earthquake prone areas. Therefore, the main objective of this research is to develop a systematic evaluation of existing buildings in Indonesia.

In order to achieve the objective, in this research is conducted the study of the possibility of screening evaluation in preliminary stage. There are fifteenth buildings in evaluating in this study. The whole building is located in Pekanbaru city of Indonesia and these were designed by using Indonesian code. These buildings are evaluated by Rapid Visual Screening (RVS) and then the static non-linear analysis is used to confirm the result of the RVS. Only one building is recommended for further evaluation while the rest does not need further evaluation because there is no risk of facing earthquake hazards base on the RVS method. This is confirmed by comparing with the non-linear static analysis method where the results of the roof drift ratio show that buildings that require further evaluation have a roof drift ratio that is greater than the drift limit. Therefore this RVS method can be used for the preliminary evaluation for the large numbers of buildings in a city against the earthquake risk.

The next stage of system evaluation is proposed as a rapid evaluation method (REM). The reliability of this method is described in Chapter 3 of this study. The rapid evaluation has been

demonstrated in this study by selecting cases of the 6th story steel moment-resisting frame (MF) system, and the 10th story braced frame (BF) system. The structures located in Padang city were designed according to Indonesian seismic code. The evaluations apply a screening method with referring to ASCE 41-13 standard. Nonlinear static and dynamic analysis is performed to confirm this method. The result of screening evaluation, there are deficiencies in the basic configuration of the MF building indicated with non-compliant (NC) of weak story and soft story. The strong column weak beam criteria are not fulfilled in this building. It is confirmed by non-linear static and dynamic analysis, where the story failure likely to occur in the same stories with the screening result. The same evaluation method is also implemented in BF building. There is no soft-story effect in this building but the requirement of the strength capacity in adjacent story is not sufficed. Even though the deficiencies exist in this building, the result of static and dynamic analysis shows that the entire floor has drift angle smaller than the drift limit. This study shows that the screening evaluation can be implemented to evaluate the existing structure against the risk of earthquake.

An index for evaluating the existing building performance is also proposed in this study. Two existing buildings were evaluated in Chapter 4. The first building consisted of five stories and the second has four stories. Both buildings were moment-resisting frame system and reinforced concrete material. An index represented the seismic performance of the existing building in the Japanese standard. This index was called by a seismic index, which a function of strength and ductility parameters. The structure has the difference seismic indexes in lateral and transversal directions because of the differences in the stiffness in both directions. The evaluation result, building A has a seismic index in transversal direction larger than in a longitudinal direction. Meanwhile, building B has the same seismic index in both directions of the structure.

The application of a seismic index based on the Japanese standard needs adjustment for other countries. In this study, a set procedure was proposed to determine the seismic index based on the result of the pushover analysis. The result of the seismic index was higher than it obtained by the Japanese standard, due to the calculation of structural capacity was carried out until post elastic conditions. While the calculation based on the Japanese standard on level - 1 was based on the average shear stress on the resisting elements of lateral force. Furthermore, the seismic demand index was smaller compared to the Japanese seismic demand index. The final assessment of the structural performance of this proposed method indicated that both buildings were in a safe condition.

The dynamic seismic index dI_s and the dynamic ductility index dF are more accurately in order to evaluate the seismic performance of a structure. A collection of simulated ground motions was used in linear and nonlinear dynamic analysis, which had Indonesia's response spectrum code as the target. The ductility index could be estimated by the estimation method without conducting the dynamic analysis in this study. Two estimation methods were introduced that the first was the characteristic displacement response method which formulated from the relationship of the critical ductility factor μ_{cr} and the ductility index. The second was the equivalent linearization method.

Finally, this study concludes that several stages can be carried out to overcome the problem in evaluating the performance of existing buildings. Seismic index methods such as those conducted in Japan, with some adjustments, can be used as guidelines to be applied in Indonesia to assess the performance of the building.

6.2. Future works

Although the comprehension evaluation strategies are already explained in this study, some improvements can still be made. There are some ideas that I would have like to try for future works concerns as follow:

- The dynamic seismic performance index estimation method that was derived with the linearization method using the bilinear hysteretic model for inelastic force-displacement relationship. It could be interesting to consider the other hysteretic models for various structural types. For instance: Reinforced concrete with bending type structures. In modeling the force-displacement relation of reinforced concrete structures, many factors have to be considered such as cracking, yielding, stiffness reduction in the unloading region after yielding, the orientation towards the maximum displacement point after load reversal, the effects of repeated cycles, the effects of axial forces and shear forces. Previous researchers have proposed the Takeda model and the degraded trilinear model.
- The characteristic of the displacement response method that was proposed in this study to approach the ductility index with the various structures period could be interesting to take over the energy principle for converting the elasto-plastic curve in chapter 4.

- To estimate the ductility factor of the existing structure precisely is very difficult. Future investigations are necessary to validate the approach method with experimental research.

In addition, information disseminating is needed to make stakeholders aware of the risk that will arise if an earthquake occurs and the existing building is unable to deal with it.

References

- [1] Kurniawandy et al., *Structural Building Screening and Evaluation*, AIP Conferences Proceedings, 1892, (5 pages), 2017.
- [2] *USGS National Earthquake Information Center, Regional Information*. [Online]. Available: <https://earthquake.usgs.gov/earthquakes/eventpage/us2000cmwz#region-info>. [Accessed: 25-Jan-2018].
- [3] M. Irsyam and et al., *Development of New Seismic Hazard Maps of Indonesia 2017*, in Proceedings of the 19th International Conference on Soil Mechanics and Geotechnical Engineering, pp. 1525–1528, 2017.
- [4] W. H. Asrurifak, M.; Irsyam, M.; Budiono, B.; Triyoso, *Development of Spectral Hazard Map for Indonesia with a Return Period of 2500 Years using Probabilistic Method*, Civil Engineering Dimension, vol. 12, no. 1, 2010.
- [5] Ministry of public works of Indonesia, *Indonesia Earthquake Hazard Map 2010 as a Basic References of Earthquake Resistant Infrastructure Design (in Indonesian)*, 2010.
- [6] Pusgen, *The source and seismic hazards map of Indonesia in 2017 (in Indonesian)*, Ministry of public works of Indonesia, 2017.
- [7] S. Nakazawa, *Evaluation of Dynamic Ductility Index of a School Gymnasium*, in IASS 2011, pp. 1–8, 2011.
- [8] S. Nakazawa, T. Yanagisawa, and S. Kato, *Evaluation of dynamic ductility index of steel gymnasiums based on pushover analysis*, Journal of Structural Construction Engineering, vol. 78, no. 683, pp. 111–118, 2013.
- [9] S. Nakazawa and H. Maeda, *Estimation method for dynamic ductility index of steel structures by using equivalent linearization method*, AIP Conferences Proceedings, vol. 1892, pp. 2–9, 2017.
- [10] Indonesian Code, *SNI 1726:2012 Earthquake Resistant Design Code for Building and non-Building of Indonesia (in Indonesian)*, Standardization Agency of Indonesia (BSN), Jakarta, 2012.
- [11] Indonesian code., *SNI 03-1729-2002, The Design Procedure of Steel Structures for Buildings*, Standardization Agency of Indonesia (BSN), Jakarta, 2002.
- [12] Farzad Naeim, H. Bhatia, and R. M. Lobo, *Performance Base Seismic Engineering, The Seismic Design Handbook*. Los Angeles, California, 2000.
- [13] Indonesian code, *SNI 03-1726-2002, Earthquake Resistant Design Code for Building*, Standardization Agency of Indonesia (BSN), Jakarta, 2002.
- [14] N. Ramly, M. Ghafar, M. Alel, and A. Adnan, *Rapid Visual Screening Method for Seismic Vulnerability Assessment of Existing Buildings in Bukit Tinggi, Pahang, Malaysia*, International Conference on Advances in Civil, Structural and Mechanical Engineering, vol. 1, no. 2, pp. 978–981, 2014.
- [15] M. F. Shah, A. Ahmed, G. . Kegyes, A. Al-Ghamadi, and R. . Ray, *A Case Study Using Rapid Visual Screening Method to Determine the Vulnerability of Buildings in two Districts of Jeddah, Saudi Arabia*, 15th International Symposium on New Technology for Urban Safety of Mega Cities Asia, 2016.
- [16] Applied Technology Council ATC, *FEMA 154, Rapid Visual Screening of Buildings for Potential Seismic Hazards*, 2nd ed., Washington DC, 2002.

- [17] Applied Technology Council ATC, *FEMA 154, Rapid Visual Screening of Buildings for Potential Seismic Hazards: A Handbook*, 3rd ed., Washington DC, 2016.
- [18] S. K. Jain, K. Mitra, M. Kumar, and M. Shah, *A Proposed Rapid Visual Screening Procedure for Seismic Evaluation of RC-Frame Buildings in India*, *Earthq. Spectra*, vol. 26, no. 3, pp. 709–729, 2010.
- [19] Applied Technology Council ATC, *FEMA 155, Rapid Visual Screening of Buildings for Potential Seismic Hazards: Supporting Documentation*, Washington DC, 2002.
- [20] Jagmohan L. Humar, *Dynamics of Structures*, Carleton University, Ottawa, Canada, 2002.
- [21] A. Ghali, A. M. Neville, and T. G. Brown, *Structural Analysis, Unified classical and matrix approach*, Spon Press, United States of America, 2009.
- [22] A. K. Chopra, *Dynamics of Structures, Theory and Applications to Earthquake Engineering*, Person, Berkley, 2007.
- [23] R. W. Clough and J. Penzein, *Dynamic of Structures*, Computers & Structures, Inc., Berkley, 1995.
- [24] M. Paz and Y. H. Kim, *Structural Dynamics*, Springer, New York, 2004.
- [25] Akenori Shibata., *Dynamic Analysis of Earthquake Resistance Structures*, Tohoku University Press, Sendai, Japan, 2010.
- [26] Applied Technology Council ATC 40, *Seismic Evaluation and Retrofit of Concrete Buildings*, vol. 1. California, USA, 1996.
- [27] M. H. Serror and M. N. Abdelmoneam, *Seismic Performance Evaluation of Egyptian Code-Designed Steel Moment Resisting Frames*, *HBRC J.*, vol. 14, no. 1, pp. 37–49, 2016.
- [28] American Society of Civil Engineers., *ASCE/SEI 41-13 Seismic Evaluation and Retrofit of Existing Building*, The United States of America, 2014.
- [29] A. Kurniawandy and S. Nakazawa, *Seismic performance evaluation of existing building using Seismic Index method*, in *International Conference on Advances in Civil and Environmental Engineering*, 2019, vol. 276.
- [30] S. Nakazawa, *SIMEQ Program for Creating Simulated Earthquake Motions*, in *Toyohashi University of Technology*, Ver 1.2., Japan, 2016.
- [31] Indonesian code, *SNI 03-1727-1989 Design Load Procedure for Homes and Buildings*. Standardization Agency of Indonesia (BSN), Jakarta, 1989.
- [32] JBDPA, *Standard for Seismic Evaluation of Existing Reinforced Concrete Buildings (English Version)*, Japan Building Disaster Prevention Association, Tokyo, Japan, 2001.
- [33] Y. Nakano, M. Maeda, H. Kuramoto, and M. Murakami, *Guideline for post-earthquake damage evaluation and rehabilitation of buildings in Japan*, in the 13th World Conference on Earthquake Engineering, no. 124, pp. 1–15, Canada, 2004,
- [34] Y. Mehani, R. Taleb, and H. Bechtoula, *Seismic Vulnerability Evaluation of Existing Reinforced Concrete Building Retrofitted with RC Wing Walls*, 15th World Conf. Earthq. Eng. Lisbon Port., vol. 2000, 2012.
- [35] T. Azuhata, T. Saito, M. Takayama, and K. Nagahara, *Seismic Performance Estimation of Asymmetric Buildings Based On the Capacity Spectrum Method*, in *Proc. 12th World Conference on Earthquake Engineering*, vol. 02, pp. 1–8, 2000.
- [36] E. Kalkan and S. K. Kunnath, *Method of Modal Combinations for Pushover Analysis of Buildings*, in 13th World Conference on Earthquake Engineering, Canada, no. 2713, 2004.
- [37] R. C. Barros; and R. Almeida, *Pushover Analysis of Asymmetric Three-dimensional Building*

- Frames*, Journal of Civil Engineering and Management, vol. XI, pp. 3–12, 2005.
- [38] S. Viti, M. Tanganelli, M. De Stefano, and E. Engineering, *Seismic Behaviour and Design of Irregular and Complex Civil Structures*, in *Geotechnical, Geological and Earthquake Engineering*, vol. 24, Springer Dordrecht Heidelberg New York London, pp. 149–158, 2013.
 - [39] American Society of Civil Engineers, *ASCE 41-13, Seismic Evaluation and Retrofit of Existing Buildings*, The United State of America, 2014.
 - [40] M. Irsyam, M. Asrurifak, R. Mikhail, I. I. Wahdiny, S. Rustiani, and M. Munirwansyah, *Development of Nationwide Vs30 Map and Calibrated Conversion Table for Indonesia using Automated Topographical Classification*, J. Eng. Technol. Sci., vol. 49, no. 4, 2017.
 - [41] I. W. Sengara, I. D. Sidi, A. Mulia, M. Asrurifak, and D. Hutabarat, *Development of Risk Coefficient for Input to New Indonesian Seismic Building Codes*, J. Eng. Technol. Sci., vol. 48, no. 1, pp. 49–65, 2016.
 - [42] P. R. Rahmat, J. Kiyono, Y. Ono, and H. R. Parajuli, *Seismic Hazard Analysis for Indonesia*, J. Nat. Disaster Sci., vol. 33, no. 2, pp. 59–70, 2012.
 - [43] ASCE 7-10, *Minimum Design Loads for Building and other Structures*, American Society of Civil Engineers, 2010.
 - [44] S. H. Helou and I. Muhammad, *Equivalent Lateral Load Method vs Response Spectrum Analysis Which Way is Forward*, Asian Journal of Engineering Technology, vol. 02, no. 05, pp. 2321–2462, 2014.
 - [45] R. K. Mohammadi and H. El Naggar, *Modifications on Equivalent Lateral Force Method*, in 13th World Conference on Earthquake Engineering, Canada, 2004.
 - [46] T. Oya, S. Nakazawa, K. Kashiwai, and K. Shiro, *Evaluation of Seismic Capacity of Sports Halls Based on Elasto-plastic Earthquake Response Analysis – Dynamic ductility index and demand strength of braces on longitudinal direction*, J. Struct. Eng., vol. Vol.56B, p. pp.469–480, 2010.
 - [47] S. Nakazawa, S. Kato, and Y. Toshimasa, *Evaluation of Dynamic Ductility Index of a School Gymnasium*, IASS 2011, pp. 1–8, 2011.
 - [48] D. Vamvatsikos and C. A. Cornell, *Applied Incremental Dynamic Analysis*, Earthquake Spectra, vol. 20, no. 2, pp. 523–553, 2004.
 - [49] Sang Whan Han and A. K. Chopra, *Approximate Incremental Dynamic Analysis using The Modal Pushover Analysis Procedure*, Earthquake Engineering Structural Dynamic, no. 35, pp. 1853–1873, 2006.
 - [50] M. Midorikawa, I. Okawa, I. Masanori, and M. Teshigawara, *Performance-based Seismic Design Code for Buildings in Japan*, Earthquake Engineering and Engineering Seismology, vol. 4, pp. 15–25, 2003.
 - [51] M. Itabashi and H. Fukuda, *The Japanese Building Standard Law and a Series of Steels for Earthquake-resistant Building Structures*, Technology Law Insurance, vol. 4, 1999.
 - [52] R. L. Mayes and F. Naem, *Design of Structures with Seismic Isolation*, in *The Seismic Design Handbook*, p. 740, 2000.
 - [53] E. Kalkan and A. K. Chopra, *Practical Guidelines to Select and Scale Earthquake Records for Nonlinear Response History Analysis of Structure*, U.S. Geological Survey Open-File Report, 2010.
 - [54] Mulchandani et al., *Ground Motion Selection and Scaling using ASCE 7-16 , Case Study on Town Alipur in Delhi Region*, in 16th Symposium on Earthquake Engineering, no. 371, pp. 1–9, 2018.

- [55] J. C. Reyes, A. C. Riaño, E. Kalkan, O. A. Quintero, and C. M. Arango, *Assessment of Spectrum Matching Procedure for Nonlinear Analysis of Symmetric and Asymmetric-plan Buildings*, Eng. Struct., vol. 72, pp. 171–181, 2014.
- [56] Newmark NM ; Hall WJ, *Earthquake Spectra and Design*, in Earthquake Engineering Research Institute (EERI), 1982.
- [57] N. Lam, J. Wilson, and G. Hutchinson, *The Ductility Reduction Factor in the Seismic Design of Buildings*, Earthquake Engineering Structure Dynamic, vol. 27, no. 7, 1998.

Appendix

Survey form of Rapid Visual Screening

HIGH Seismicity

Sketch :

Address : Kampus Bina Widya
Universitas Riau

Other Identifiers KW

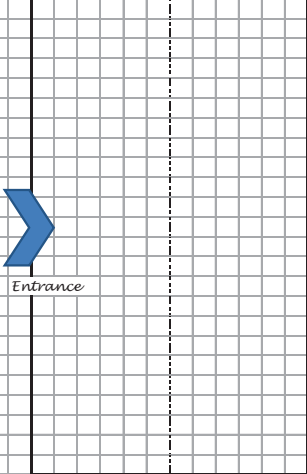
No. Stories 2 Year +/- 1995

Screener tbn Date 2016


Total Floor Area (sq. ft.) _____

Building Name FMIPA UR

Use Pendidikan (Education building)



Entrance



OCCUPANCY SOIL		TYPE		FALLING HAZARDS											
Assembly	Govt	Office	Number of Persons	A	B	C	D	E	F	Unreinf.	Parapets	Cladding	Other		
Commercial	Historic	Residential	0 - 10	Hard	Avg.	Dense	Stiff	Soft	Poor	Chimneys					
Emer. Services	Industrial	School	101 - 1000	Rock	Rock	Soil	Soil	Soil	Soil						
BASIC SCORE, MODIFIERS, AND FINAL SCORE, S															
BUILDING TYPE	W1	W2	S1	S2	S3	S4	S5	C1	C2	C3	PC1	PC2	RM1	RM2	URM
			(MRF)	(BR)	(LM)	(RC SW)	(URM INF)	(MRF)	(SW)	(URM INF)	(TU)	(FD)	(RD)		
Basic Score	4.4	3.8	2.8	3	3.2	2.8	2	2.5	2.8	1.6	2.6	2.4	2.8	2.8	1.8
Mid Rise (4 to 7 stories)	N/A	N/A	0.2	0.4	N/A	0.4	0.4	0.4	0.4	0.2	N/A	0.2	0.4	0.4	0
High Rise (>7 stories)	N/A	N/A	0.6	0.8	N/A	0.8	0.6	0.8	0.3	N/A	0.4	N/A	0.6	N/A	N/A
Vertical Irregularity	-2.5	-0.2	-1	-1.5	N/A	-1	-1	-1.5	-1	-1	N/A	-1	-1	-1	-1
Plan Irregularity	-0.5	-0.5	-0.5	-0.5	-0.5	-0.5	-0.5	-0.5	-0.5	-0.5	-0.5	-0.5	-0.5	-0.5	0.5
Pre - Code	0	-1	-1	-0.8	-0.6	-0.8	-0.2	-1.2	-1	-2	-0.8	-0.8	-1	-0.8	-0.2
Post- Benchmark	2.4	2.4	1.4	1.4	N/A	1.6	N/A	1.4	2.4	N/A	2.4	2.8	2.6	N/A	N/A
Soil Type C	0	-0.4	-0.4	-0.4	-0.4	-0.4	-0.4	-0.4	-0.4	-0.4	-0.4	-0.4	-0.4	-0.4	-0.4
Soil Type D	0	-0.8	-0.6	-0.6	-0.6	-0.6	-0.4	-0.6	-0.6	-0.4	-0.6	-0.6	-0.6	-0.6	-0.6
Soil Type E	0	-0.8	-1.2	-1.2	-1	-1.2	-0.8	-1.2	-0.8	-0.8	-0.4	-1.2	-0.4	-0.6	0.8
FINAL SCORE, S															
2.7															
COMMENTS												Detail Evaluation Required			
> No Irregularity in vertical and horizontal (plan) direction > Final score >= 2, No detail evaluation needed												YES			
												NO			

HIGH Seismicity

Sketch :

Address : Kampus Bina Widya
Universitas Riau

Other Identifiers KW

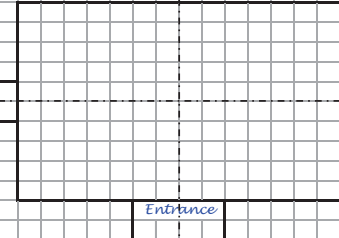
No. Stories 5 Year +/- 2014

Screener tbn Date 2016


Total Floor Area (sq. ft.) _____

Building Name Rusunawa

Use Asrama Mahasiswa (Residential)



Entrance



OCCUPANCY SOIL		TYPE		FALLING HAZARDS											
Assembly	Govt	Office	Number of Persons	A	B	C	D	E	F	Unreinf.	Parapets	Cladding	Other		
Commercial	Historic	Residential	0 - 10	Hard	Avg.	Dense	Stiff	Soft	Poor	Chimneys					
Emer. Services	Industrial	School	101 - 1000	Rock	Rock	Soil	Soil	Soil	Soil						
BASIC SCORE, MODIFIERS, AND FINAL SCORE, S															
BUILDING TYPE	W1	W2	S1	S2	S3	S4	S5	C1	C2	C3	PC1	PC2	RM1	RM2	URM
			(MRF)	(BR)	(LM)	(RC SW)	(URM INF)	(MRF)	(SW)	(URM INF)	(TU)	(FD)	(RD)		
Basic Score	4.4	3.8	2.8	3	3.2	2.8	2	2.5	2.8	1.6	2.6	2.4	2.8	2.8	1.8
Mid Rise (4 to 7 stories)	N/A	N/A	0.2	0.4	N/A	0.4	0.4	0.4	0.4	0.2	N/A	0.2	0.4	0.4	0
High Rise (>7 stories)	N/A	N/A	0.6	0.8	N/A	0.8	0.6	0.8	0.3	N/A	0.4	N/A	0.6	N/A	N/A
Vertical Irregularity	-2.5	-0.2	-1	-1.5	N/A	-1	-1	-1.5	-1	-1	N/A	-1	-1	-1	-1
Plan Irregularity	-0.5	-0.5	-0.5	-0.5	-0.5	-0.5	-0.5	-0.5	-0.5	-0.5	-0.5	-0.5	-0.5	-0.5	0.5
Pre - Code	0	-1	-1	-0.8	-0.6	-0.8	-0.2	-1.2	-1	-2	-0.8	-0.8	-1	-0.8	-0.2
Post- Benchmark	2.4	2.4	1.4	1.4	N/A	1.6	N/A	1.4	2.4	N/A	2.4	2.8	2.6	N/A	N/A
Soil Type C	0	-0.4	-0.4	-0.4	-0.4	-0.4	-0.4	-0.4	-0.4	-0.4	-0.4	-0.4	-0.4	-0.4	-0.4
Soil Type D	0	-0.8	-0.6	-0.6	-0.6	-0.6	-0.4	-0.6	-0.6	-0.4	-0.6	-0.6	-0.6	-0.6	-0.6
Soil Type E	0	-0.8	-1.2	-1.2	-1	-1.2	-0.8	-1.2	-0.8	-0.8	-0.4	-1.2	-0.4	-0.6	0.8
FINAL SCORE, S															
3.1															
COMMENTS												Detail Evaluation Required			
> No Irregularity in vertical and horizontal (plan) direction > Final score >= 2, No detail evaluation needed												YES			
												NO			

HIGH Seismicity

Sketch :

Address : Kampus Bina Widya Universitas Riau

Other Identifiers xx

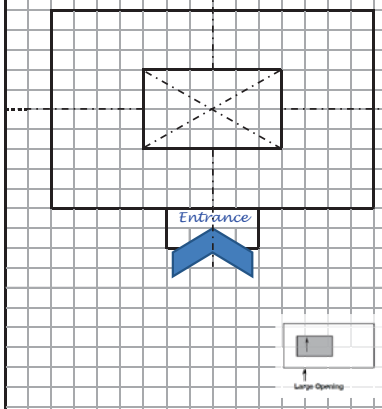
No. Stories 2 Year +/- 2010

Screener tbn Date 2016


Total Floor Area (sq. ft.) _____

Building Name Fisipol

Use School and office room



Entrance



OCCUPANCY SOIL		TYPE		FALLING HAZARDS									
Assembly	Govt	Office	Number of Persons	A	B	C	D	E	F	Unreinf.	Parapets	Cladding	Other
Commercial	Historic	Residential	0 - 10	Hard	Avg.	Dense	Stiff	Soft	Poor	Chimneys			
Emer. Services	Industrial	School	101 - 1000	Rock	Rock	Soil	Soil	Soil	Soil				

BASIC SCORE, MODIFIERS, AND FINAL SCORE, S

BUILDING TYPE	W1	W2	S1	S2	S3	S4	S5	C1	C2	C3	PC1	PC2	RM1	RM2	URM
Basic Score	4.4	3.8	2.8	3	3.2	2.8	2	2.5	2.8	1.6	2.6	2.4	2.8	2.8	1.8
Mid Rise (4 to 7 stories)	N/A	N/A	0.2	0.4	N/A	0.4	0.4	0.4	0.4	0.2	N/A	0.2	0.4	0.4	0
High Rise (>7 stories)	N/A	N/A	0.6	0.8	N/A	0.8	0.8	0.6	0.8	0.3	N/A	0.4	N/A	0.6	N/A
Vertical Irregularity	-2.5	-0.2	-1	-1.5	N/A	-1	-1	-1.5	-1	-1	N/A	-1	-1	-1	-1
Plan Irregularity	-0.5	-0.5	-0.5	-0.5	-0.5	-0.5	-0.5	-0.5	-0.5	-0.5	-0.5	-0.5	-0.5	-0.5	0.5
Pre - Code	0	-1	-1	-0.8	-0.6	-0.8	-0.2	-1.2	-1	-2	-0.8	-0.8	-1	-0.8	-0.2
Post- Benchmark	2.4	2.4	1.4	1.4	N/A	1.6	N/A	1.4	2.4	N/A	2.4	2.8	2.6	N/A	N/A
Soil Type C	0	-0.4	-0.4	-0.4	-0.4	-0.4	-0.4	-0.4	-0.4	-0.4	-0.4	-0.4	-0.4	-0.4	-0.4
Soil Type D	0	-0.8	-0.6	-0.6	-0.6	-0.6	-0.4	-0.6	-0.6	-0.4	-0.6	-0.6	-0.6	-0.6	-0.6
Soil Type E	0	-0.8	-1.2	-1.2	-1	-1.2	-0.8	-1.2	-0.8	-0.8	-0.4	-1.2	-0.4	-0.6	0.8

FINAL SCORE, S **2.2**

COMMENTS

> Irregularity in horizontal (plan) direction due to large opening

> Final score >= 2, No detail evaluation needed

Detail Evaluation Required

YES **NO**

HIGH Seismicity

Sketch :

Address : Kampus Bina Widya Universitas Riau

Other Identifiers xx

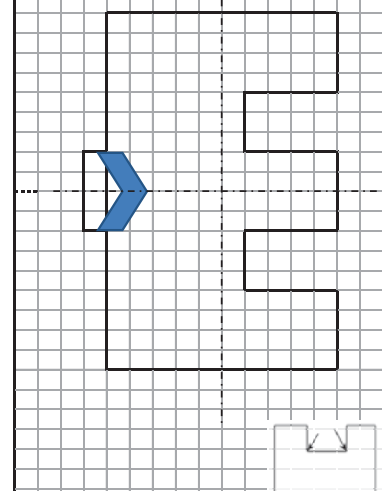

No. Stories 2 Year +/- 2010

Screener tbn Date 2016

Total Floor Area (sq. ft.) _____

Building Name Fkip

Use School and office room

OCCUPANCY SOIL		TYPE		FALLING HAZARDS									
Assembly	Govt	Office	Number of Persons	A	B	C	D	E	F	Unreinf.	Parapets	Cladding	Other
Commercial	Historic	Residential	0 - 10	Hard	Avg.	Dense	Stiff	Soft	Poor	Chimneys			
Emer. Services	Industrial	School	101 - 1000	Rock	Rock	Soil	Soil	Soil	Soil				

BASIC SCORE, MODIFIERS, AND FINAL SCORE, S

BUILDING TYPE	W1	W2	S1	S2	S3	S4	S5	C1	C2	C3	PC1	PC2	RM1	RM2	URM
Basic Score	4.4	3.8	2.8	3	3.2	2.8	2	2.5	2.8	1.6	2.6	2.4	2.8	2.8	1.8
Mid Rise (4 to 7 stories)	N/A	N/A	0.2	0.4	N/A	0.4	0.4	0.4	0.4	0.2	N/A	0.2	0.4	0.4	0
High Rise (>7 stories)	N/A	N/A	0.6	0.8	N/A	0.8	0.8	0.6	0.8	0.3	N/A	0.4	N/A	0.6	N/A
Vertical Irregularity	-2.5	-0.2	-1	-1.5	N/A	-1	-1	-1.5	-1	-1	N/A	-1	-1	-1	-1
Plan Irregularity	-0.5	-0.5	-0.5	-0.5	-0.5	-0.5	-0.5	-0.5	-0.5	-0.5	-0.5	-0.5	-0.5	-0.5	0.5
Pre - Code	0	-1	-1	-0.8	-0.6	-0.8	-0.2	-1.2	-1	-2	-0.8	-0.8	-1	-0.8	-0.2
Post- Benchmark	2.4	2.4	1.4	1.4	N/A	1.6	N/A	1.4	2.4	N/A	2.4	2.8	2.6	N/A	N/A
Soil Type C	0	-0.4	-0.4	-0.4	-0.4	-0.4	-0.4	-0.4	-0.4	-0.4	-0.4	-0.4	-0.4	-0.4	-0.4
Soil Type D	0	-0.8	-0.6	-0.6	-0.6	-0.6	-0.4	-0.6	-0.6	-0.4	-0.6	-0.6	-0.6	-0.6	-0.6
Soil Type E	0	-0.8	-1.2	-1.2	-1	-1.2	-0.8	-1.2	-0.8	-0.8	-0.4	-1.2	-0.4	-0.6	0.8

FINAL SCORE, S **2.2**

COMMENTS

> Irregularity in horizontal (plan) direction

> Final score >= 2, No detail evaluation needed

Detail Evaluation Required

YES **NO**

HIGH Seismicity

Sketch :

Address : Kampus Bina Widya
Universitas Riau

Other Identifiers KW

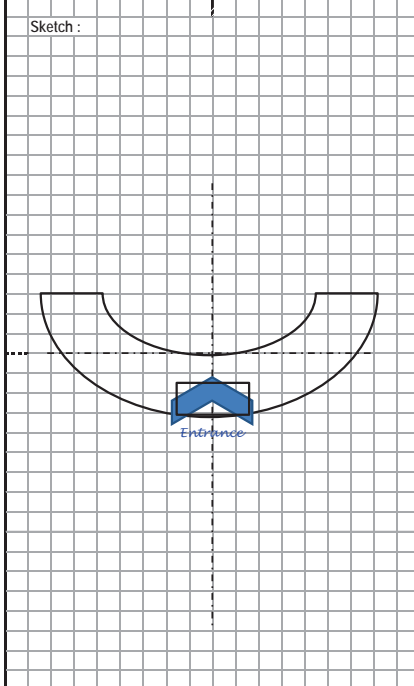

No. Stories 3 Year +/- 2004

Screener tbn Date 2016

Total Floor Area (sq. ft.) _____

Building Name FT

Use School and office room

OCCUPANCY		SOIL	TYPE		FALLING HAZARDS								
Assembly	Govt	<u>Office</u>	Number of Persons	A	B	C	D	<u>E</u>	F	<input type="checkbox"/> Unreinf.	<input checked="" type="checkbox"/> Parapets	<input type="checkbox"/> Cladding	<input checked="" type="checkbox"/> Other
Commercial	Historic	<u>Residential</u>	0 - 10	Hard	Avg.	Dense	Stiff	<u>Soft</u>	Poor	<input type="checkbox"/> Chimneys	<input type="checkbox"/> Roof		
Emer. Services	Industrial	<u>School</u>	101 - 1000	Rock	Rock	Soil	Soil		Soil				

BASIC SCORE, MODIFIERS, AND FINAL SCORE, S

BUILDING TYPE	W1	W2	S1	S2	S3	S4	S5	<u>C1</u>	C2	C3	PC1	PC2	RM1	RM2	URM
			(MRF)	(BR)	(LM)	(RC SW)	(URM INF)	(MRF)	(SW)	(URM INF)	(TU)	(FD)	(RD)		
Basic Score	4.4	3.8	2.8	3	3.2	2.8	2	<u>2.5</u>	2.8	1.6	2.6	2.4	2.8	2.8	1.8
Mid Rise (4 to 7 stories)	N/A	N/A	0.2	0.4	N/A	0.4	0.4	0.4	0.2	N/A	0.2	0.4	0.4	0	
High Rise (>7 stories)	N/A	N/A	0.6	0.8	N/A	0.8	0.6	0.8	0.3	N/A	0.4	N/A	0.6	N/A	
Vertical Irregularity	-2.5	-0.2	-1	-1.5	N/A	-1	-1	-1.5	-1	-1	N/A	-1	-1	-1	-1
Plan Irregularity	-0.5	-0.5	-0.5	-0.5	-0.5	-0.5	-0.5	<u>-0.5</u>	-0.5	-0.5	-0.5	-0.5	-0.5	-0.5	0.5
Pre - Code	0	-1	-1	-0.8	-0.6	-0.8	-0.2	-1.2	-1	-2	-0.8	-1	-0.8	-0.2	
Post - Benchmark	2.4	2.4	1.4	1.4	N/A	1.6	N/A	<u>1.4</u>	2.4	N/A	2.4	2.8	2.6	N/A	
Soil Type C	0	-0.4	-0.4	-0.4	-0.4	-0.4	-0.4	-0.4	-0.4	-0.4	-0.4	-0.4	-0.4	-0.4	-0.4
Soil Type D	0	-0.8	-0.6	-0.6	-0.6	-0.6	-0.4	-0.6	-0.6	-0.4	-0.6	-0.6	-0.6	-0.6	-0.6
Soil Type E	0	-0.8	-1.2	-1.2	-1	-1.2	-0.8	<u>-1.2</u>	-0.8	-0.8	-0.4	-1.2	-0.4	-0.6	0.8

FINAL SCORE, S 2.2

COMMENTS

- > Irregularity in horizontal (plan) direction
- > Final score >= 2, No detail evaluation needed

Detail Evaluation Required

YES ☐ NO ☒

HIGH Seismicity

Sketch :

Address : Kampus Bina Widya
Universitas Riau

Other Identifiers KW

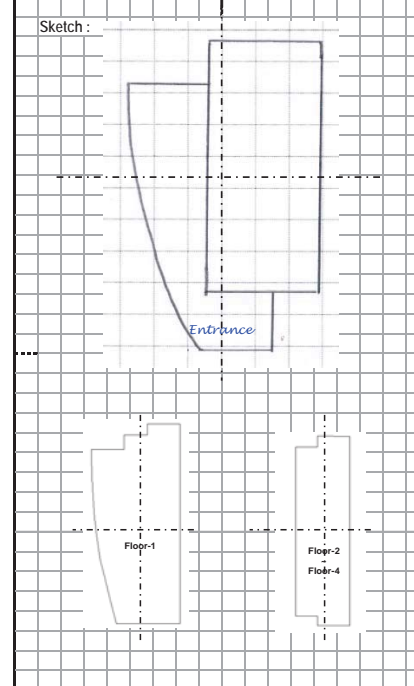

No. Stories 5 Year +/- 2014

Screener tbn Date 2016

Total Floor Area (sq. ft.) _____

Building Name Gedung Surya Dumai

Use Hospital

OCCUPANCY		SOIL	TYPE		FALLING HAZARDS								
Assembly	Govt	<u>Office</u>	Number of Persons	A	B	C	D	<u>E</u>	F	<input type="checkbox"/> Unreinf.	<input checked="" type="checkbox"/> Parapets	<input type="checkbox"/> Cladding	<input type="checkbox"/> Other
Commercial	Historic	<u>Residential</u>	0 - 10	Hard	Avg.	Dense	Stiff	<u>Soft</u>	Poor	<input type="checkbox"/> Chimneys	<input type="checkbox"/> Roof		
Emer. Services	Industrial	<u>School</u>	101 - 1000	Rock	Rock	Soil	Soil		Soil				

BASIC SCORE, MODIFIERS, AND FINAL SCORE, S

BUILDING TYPE	W1	W2	S1	S2	S3	S4	S5	<u>C1</u>	<u>C2</u>	C3	PC1	PC2	RM1	RM2	URM
			(MRF)	(BR)	(LM)	(RC SW)	(URM INF)	(MRF)	(SW)	(URM INF)	(TU)	(FD)	(RD)		
Basic Score	4.4	3.8	2.8	3	3.2	2.8	2	<u>2.5</u>	<u>2.8</u>	1.6	2.6	2.4	2.8	2.8	1.8
Mid Rise (4 to 7 stories)	N/A	N/A	0.2	0.4	N/A	0.4	0.4	<u>0.4</u>	<u>0.4</u>	0.2	N/A	0.2	0.4	0.4	0
High Rise (>7 stories)	N/A	N/A	0.6	0.8	N/A	0.8	0.6	0.8	0.3	N/A	0.4	N/A	0.6	N/A	
Vertical Irregularity	-2.5	-0.2	-1	-1.5	N/A	-1	-1	-1.5	-1	-1	N/A	-1	-1	-1	-1
Plan Irregularity	-0.5	-0.5	-0.5	-0.5	-0.5	-0.5	-0.5	<u>-0.5</u>	<u>-0.5</u>	-0.5	-0.5	-0.5	-0.5	-0.5	0.5
Pre - Code	0	-1	-1	-0.8	-0.6	-0.8	-0.2	-1.2	-1.0	-2.0	-0.8	-0.8	-1	-0.8	-0.2
Post - Benchmark	2.4	2.4	1.4	1.4	N/A	1.6	N/A	<u>1.4</u>	<u>2.4</u>	N/A	2.4	N/A	2.8	2.6	N/A
Soil Type C	0	-0.4	-0.4	-0.4	-0.4	-0.4	-0.4	-0.4	-0.4	-0.4	-0.4	-0.4	-0.4	-0.4	-0.4
Soil Type D	0	-0.8	-0.6	-0.6	-0.6	-0.6	-0.4	-0.6	-0.6	-0.4	-0.6	-0.6	-0.6	-0.6	-0.6
Soil Type E	0	-0.8	-1.2	-1.2	-1	-1.2	-0.8	<u>-1.2</u>	<u>-0.8</u>	-0.8	-0.4	-1.2	-0.4	-0.6	0.8

FINAL SCORE, S 2.6 4.3

COMMENTS

- > There are two system of structure, i.e: MRF and SW
- > Irregularity in horizontal (plan) direction
- > Final score >= 2, No detail evaluation needed

Detail Evaluation Required

YES ☐ NO ☒

HIGH Seismicity

Sketch :

Address : Sudirman street
Pekanbaru City

Other Identifiers KV

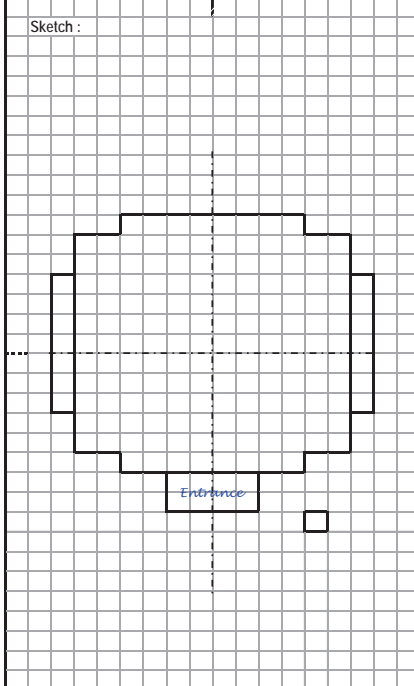

No. Stories 10 Year +/- 1995

Screener tbn Date 2016

Total Floor Area (sq. ft.)

Building Name Building - A, RS-UR

Use Hospital

OCCUPANCY		SOIL	TYPE		FALLING HAZARDS								
Assembly	Govt	<u>Office</u>	Number of Persons	A	B	C	D	<u>E</u>	F	<input type="checkbox"/> Unreinf.	<input checked="" type="checkbox"/> Parapets	<input type="checkbox"/> Cladding	<input type="checkbox"/> Other
Commercial	Historic	Residential	0 - 10	Hard	Avg.	Dense	Stiff	Soft	Poor	<input type="checkbox"/> Chimneys			
Emer. Services	Industrial	School	101 - 1000	Rock	Rock	Soil	Soil	Soil	Soil				

BUILDING TYPE	W1	W2	S1	S2	S3	S4	S5	C1	C2	C3	PC1	PC2	RM1	RM2	URM
Basic Score	4.4	3.8	2.8	3	3.2	2.8	2	<u>2.5</u>	<u>2.8</u>	1.6	2.6	2.4	2.8	2.8	1.8
Mid Rise (4 to 7 stories)	N/A	N/A	0.2	0.4	N/A	0.4	0.4	0.4	0.2	N/A	0.2	0.4	0.4	0	
High Rise (>7 stories)	N/A	N/A	0.6	0.8	N/A	0.8	0.8	<u>0.6</u>	<u>0.8</u>	0.3	N/A	0.4	N/A	0.6	N/A
Vertical Irregularity	-2.5	-0.2	-1	-1.5	N/A	-1	-1	-1.5	-1	-1	N/A	-1	-1	-1	-1
Plan Irregularity	-0.5	-0.5	-0.5	-0.5	-0.5	-0.5	-0.5	<u>-0.5</u>	<u>-0.5</u>	-0.5	-0.5	-0.5	-0.5	-0.5	0.5
Pre - Code	0	-1	-1	-0.8	-0.6	-0.8	-0.2	-1.2	-1	-2	-0.8	-1	-0.8	-0.2	
Post- Benchmark	2.4	2.4	1.4	1.4	N/A	1.6	N/A	<u>1.4</u>	<u>2.4</u>	N/A	2.4	N/A	2.8	2.6	N/A
Soil Type C	0	-0.4	-0.4	-0.4	-0.4	-0.4	-0.4	-0.4	-0.4	-0.4	-0.4	-0.4	-0.4	-0.4	-0.4
Soil Type D	0	-0.8	-0.6	-0.6	-0.6	-0.6	-0.4	-0.6	-0.6	-0.4	-0.6	-0.6	-0.6	-0.6	-0.6
Soil Type E	0	-0.8	-1.2	-1.2	-1	-1.2	-0.8	<u>-1.2</u>	<u>-0.8</u>	-0.8	-0.4	-1.2	-0.4	-0.6	0.8

FINAL SCORE, S 2.8 4.7

COMMENTS

- > There are two system of structure, i.e: MRF and SW
- > Irregularity in horizontal (plan) direction
- > Final score >= 2, No detail evaluation needed

Detail Evaluation Required

YES ☐ NO ☒

HIGH Seismicity

Sketch :

Address : Kampus Bina Widya
Universitas Riau

Other Identifiers KV

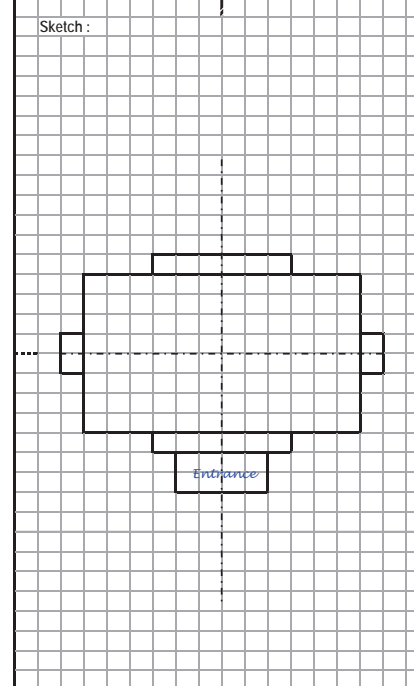

No. Stories 4 Year +/- 1995

Screener tbn Date 2016

Total Floor Area (sq. ft.)

Building Name Rektorat UR

Use Office room

OCCUPANCY		SOIL	TYPE		FALLING HAZARDS								
Assembly	Govt	<u>Office</u>	Number of Persons	A	B	C	D	<u>E</u>	F	<input type="checkbox"/> Unreinf.	<input checked="" type="checkbox"/> Parapets	<input type="checkbox"/> Cladding	<input checked="" type="checkbox"/> Other
Commercial	Historic	Residential	0 - 10	Hard	Avg.	Dense	Stiff	Soft	Poor	<input type="checkbox"/> Chimneys			
Emer. Services	Industrial	School	101 - 1000	Rock	Rock	Soil	Soil	Soil	Soil				

BUILDING TYPE	W1	W2	S1	S2	S3	S4	S5	C1	C2	C3	PC1	PC2	RM1	RM2	URM
Basic Score	4.4	3.8	2.8	3	3.2	2.8	2	<u>2.5</u>	<u>2.8</u>	1.6	2.6	2.4	2.8	2.8	1.8
Mid Rise (4 to 7 stories)	N/A	N/A	0.2	0.4	N/A	0.4	0.4	<u>0.4</u>	0.2	N/A	0.2	0.4	0.4	0	
High Rise (>7 stories)	N/A	N/A	0.6	0.8	N/A	0.8	0.8	0.6	0.8	0.3	N/A	0.4	N/A	0.6	N/A
Vertical Irregularity	-2.5	-0.2	-1	-1.5	N/A	-1	-1	-1.5	-1	-1	N/A	-1	-1	-1	-1
Plan Irregularity	-0.5	-0.5	-0.5	-0.5	-0.5	-0.5	-0.5	-0.5	-0.5	-0.5	-0.5	-0.5	-0.5	-0.5	0.5
Pre - Code	0	-1	-1	-0.8	-0.6	-0.8	-0.2	-1.2	-1	-2	-0.8	-1	-0.8	-0.2	
Post- Benchmark	2.4	2.4	1.4	1.4	N/A	1.6	N/A	<u>1.4</u>	<u>2.4</u>	N/A	2.4	N/A	2.8	2.6	N/A
Soil Type C	0	-0.4	-0.4	-0.4	-0.4	-0.4	-0.4	-0.4	-0.4	-0.4	-0.4	-0.4	-0.4	-0.4	-0.4
Soil Type D	0	-0.8	-0.6	-0.6	-0.6	-0.6	-0.4	-0.6	-0.6	-0.4	-0.6	-0.6	-0.6	-0.6	-0.6
Soil Type E	0	-0.8	-1.2	-1.2	-1	-1.2	-0.8	<u>-1.2</u>	<u>-0.8</u>	-0.8	-0.4	-1.2	-0.4	-0.6	0.8

FINAL SCORE, S 3.1

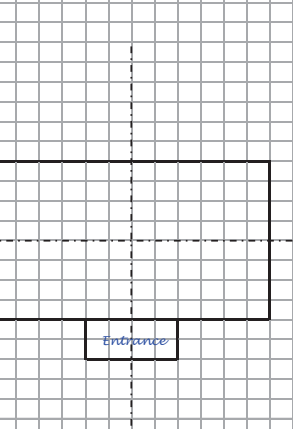

COMMENTS

- > Final score >= 2, No detail evaluation needed


Detail Evaluation Required

YES ☐ NO ☒

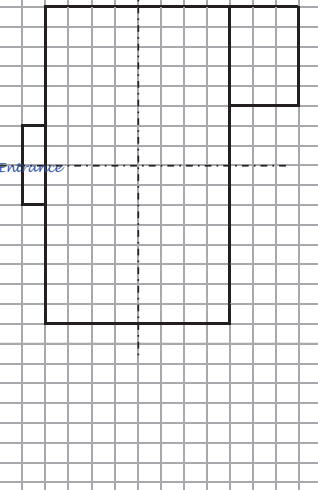

HIGH Seismicity

Sketch : 	Address : <u>Kampus Bina Widya Universitas Riau</u> <hr/> Other Identifiers <u>xx</u> No. Stories <u>2</u> Year <u>+/- 2010</u> Screener <u>tbn</u> Date <u>2016</u> Total Floor Area (sq. ft.) _____ Building Name <u>FEKON-1</u> Use <u>Educational & Office room</u>																																																										
																																																											
<table border="1" style="width: 100%; border-collapse: collapse;"> <thead> <tr> <th colspan="4" style="text-align: left;">OCCUPANCY SOIL</th> <th colspan="7" style="text-align: left;">TYPE</th> <th colspan="5" style="text-align: left;">FALLING HAZARDS</th> </tr> </thead> <tbody> <tr> <td>Assembly</td> <td>Govt</td> <td>Office</td> <td>Number of Persons</td> <td>A</td> <td>B</td> <td>C</td> <td>D</td> <td>E</td> <td>F</td> <td><input type="checkbox"/></td> <td><input type="checkbox"/></td> <td><input type="checkbox"/></td> <td><input checked="" type="checkbox"/></td> </tr> <tr> <td>Commercial</td> <td>Historic</td> <td>Residential</td> <td>0 - 10 11 - 100</td> <td>Hard Rock</td> <td>Avg. Rock</td> <td>Dense Soil</td> <td>Stiff Soil</td> <td>Soft Soil</td> <td>Poor Soil</td> <td>Unreinf. Chimneys</td> <td>Parapets</td> <td>Cladding</td> <td>Other</td> </tr> <tr> <td>Emer. Services</td> <td>Industrial</td> <td>School</td> <td>101 - 1000 1000+</td> <td></td> <td></td> <td></td> <td></td> <td></td> <td></td> <td></td> <td></td> <td><u>Rooftop</u></td> <td></td> </tr> </tbody> </table>		OCCUPANCY SOIL				TYPE							FALLING HAZARDS					Assembly	Govt	Office	Number of Persons	A	B	C	D	E	F	<input type="checkbox"/>	<input type="checkbox"/>	<input type="checkbox"/>	<input checked="" type="checkbox"/>	Commercial	Historic	Residential	0 - 10 11 - 100	Hard Rock	Avg. Rock	Dense Soil	Stiff Soil	Soft Soil	Poor Soil	Unreinf. Chimneys	Parapets	Cladding	Other	Emer. Services	Industrial	School	101 - 1000 1000+									<u>Rooftop</u>	
OCCUPANCY SOIL				TYPE							FALLING HAZARDS																																																
Assembly	Govt	Office	Number of Persons	A	B	C	D	E	F	<input type="checkbox"/>	<input type="checkbox"/>	<input type="checkbox"/>	<input checked="" type="checkbox"/>																																														
Commercial	Historic	Residential	0 - 10 11 - 100	Hard Rock	Avg. Rock	Dense Soil	Stiff Soil	Soft Soil	Poor Soil	Unreinf. Chimneys	Parapets	Cladding	Other																																														
Emer. Services	Industrial	School	101 - 1000 1000+									<u>Rooftop</u>																																															
BASIC SCORE, MODIFIERS, AND FINAL SCORE, S																																																											
BUILDING TYPE	W1	W2	S1 (MRF)	S2 (BR)	S3 (LM)	S4 (RC SW)	S5 (URM INF)	C1 (MRF)	C2 (SW)	C3 (URM INF)	PC1 (TU)	PC2	RM1 (FD)	RM2 (RD)	URM																																												
Basic Score	4.4	3.8	2.8	3	3.2	2.8	2	2.5	2.8	1.6	2.6	2.4	2.8	2.8	1.8																																												
Mid Rise (4 to 7 stories)	N/A	N/A	0.2	0.4	N/A	0.4	0.4	0.4	0.4	0.2	N/A	0.2	0.4	0.4	0																																												
High Rise (>7 stories)	N/A	N/A	0.6	0.8	N/A	0.8	0.8	0.6	0.8	0.3	N/A	0.4	N/A	0.6	N/A																																												
Vertical Irregularity	-2.5	-0.2	-1	-1.5	N/A	-1	-1	-1.5	-1	-1	N/A	-1	-1	-1	-1																																												
Plan Irregularity	-0.5	-0.5	-0.5	-0.5	-0.5	-0.5	-0.5	-0.5	-0.5	-0.5	-0.5	-0.5	-0.5	-0.5	0.5																																												
Pre - Code	0	-1	-1	-0.8	-0.6	-0.8	-0.2	-1.2	-1	-2	-0.8	-0.8	-1	-0.8	-0.2																																												
Post- Benchmark	2.4	2.4	1.4	1.4	N/A	1.6	N/A	1.4	2.4	N/A	2.4	N/A	2.8	2.6	N/A																																												
Soil Type C	0	-0.4	-0.4	-0.4	-0.4	-0.4	-0.4	-0.4	-0.4	-0.4	-0.4	-0.4	-0.4	-0.4	-0.4																																												
Soil Type D	0	-0.8	-0.6	-0.6	-0.6	-0.6	-0.4	-0.6	-0.6	-0.4	-0.6	-0.6	-0.6	-0.6	-0.6																																												
Soil Type E	0	-0.8	-1.2	-1.2	-1	-1.2	-0.8	-1.2	-0.8	-0.8	-0.4	-1.2	-0.4	-0.6	0.8																																												
COMMENTS <p>> Final score >= 2, No detail evaluation needed</p>													Detail Evaluation Required <div style="display: flex; justify-content: space-around;"> YES NO </div>																																														

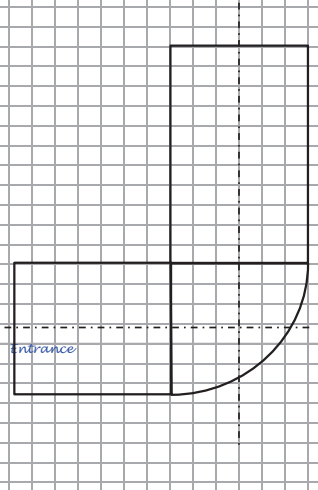

HIGH Seismicity

<p>Sketch :</p> <div style="border: 1px solid black; height: 150px; margin: 10px 0;"></div> <div style="border: 1px solid black; width: 100px; height: 30px; margin: 0 auto; text-align: center; line-height: 30px;">Entrance</div>	<p>Address : <u>Kampus Bina Widya</u> <u>Universitas Riau</u></p> <p>Other Identifiers <u>xx</u></p> <p>No. Stories <u>2</u> Year <u>+/- 2014</u></p> <p>Screener <u>tbn</u> Date <u>2016</u></p> <p>Total Floor Area (sq. ft.) _____</p> <p>Building Name <u>FEKON-2</u></p> <p>Use <u>Educational & Office room</u></p>																																																														
																																																															
<table border="1" style="width: 100%; border-collapse: collapse;"> <tr> <th colspan="4">OCCUPANCY SOIL</th> <th colspan="8">TYPE</th> <th colspan="8">FALLING HAZARDS</th> </tr> <tr> <td>Assembly</td> <td>Govt</td> <td>Office</td> <td>Number of Persons</td> <td>A</td> <td>B</td> <td>C</td> <td>D</td> <td>E</td> <td>F</td> <td><input type="checkbox"/></td> <td><input type="checkbox"/></td> <td><input type="checkbox"/></td> <td><input checked="" type="checkbox"/></td> </tr> <tr> <td>Commercial</td> <td>Historic</td> <td>Residential</td> <td>0 - 10</td> <td>Hard</td> <td>Avg.</td> <td>Dense</td> <td>Stiff</td> <td>Soft</td> <td>Poor</td> <td>Unrein.</td> <td>Parapets</td> <td>Cladding</td> <td>Other</td> </tr> <tr> <td>Emer. Services</td> <td>Industrial</td> <td>School</td> <td>101 - 1000</td> <td>Rock</td> <td>Rock</td> <td>Soil</td> <td>Soil</td> <td>Soil</td> <td>Soil</td> <td>Chimneys</td> <td colspan="3">Roof</td> </tr> </table>		OCCUPANCY SOIL				TYPE								FALLING HAZARDS								Assembly	Govt	Office	Number of Persons	A	B	C	D	E	F	<input type="checkbox"/>	<input type="checkbox"/>	<input type="checkbox"/>	<input checked="" type="checkbox"/>	Commercial	Historic	Residential	0 - 10	Hard	Avg.	Dense	Stiff	Soft	Poor	Unrein.	Parapets	Cladding	Other	Emer. Services	Industrial	School	101 - 1000	Rock	Rock	Soil	Soil	Soil	Soil	Chimneys	Roof		
OCCUPANCY SOIL				TYPE								FALLING HAZARDS																																																			
Assembly	Govt	Office	Number of Persons	A	B	C	D	E	F	<input type="checkbox"/>	<input type="checkbox"/>	<input type="checkbox"/>	<input checked="" type="checkbox"/>																																																		
Commercial	Historic	Residential	0 - 10	Hard	Avg.	Dense	Stiff	Soft	Poor	Unrein.	Parapets	Cladding	Other																																																		
Emer. Services	Industrial	School	101 - 1000	Rock	Rock	Soil	Soil	Soil	Soil	Chimneys	Roof																																																				
BASIC SCORE, MODIFIERS, AND FINAL SCORE, S																																																															
BUILDING TYPE	W1	W2	S1 (MRF)	S2 (BR)	S3 (LM)	S4 (RC SW)	S5 (URM INF)	C1 (MRF)	C2 (SW)	C3 (URM INF)	PC1 (TU)	PC2	RM1 (FD)	RM2 (RD)	URM																																																
Basic Score	4.4	3.8	2.8	3	3.2	2.8	2	2.5	2.8	1.6	2.6	2.4	2.8	2.8	1.8																																																
Mid Rise (4 to 7 stories)	N/A	N/A	0.2	0.4	N/A	0.4	0.4	0.4	0.4	0.2	N/A	0.2	0.4	0.4	0																																																
High Rise (>7 stories)	N/A	N/A	0.6	0.8	N/A	0.8	0.8	0.6	0.8	0.3	N/A	0.4	N/A	0.6	N/A																																																
Vertical Irregularity	-2.5	-0.2	-1	-1.5	N/A	-1	-1	-1.5	-1	-1	N/A	-1	-1	-1	-1																																																
Plan Irregularity	-0.5	-0.5	-0.5	-0.5	-0.5	-0.5	-0.5	-0.5	-0.5	-0.5	-0.5	-0.5	-0.5	-0.5	0.5																																																
Pre - Code	0	-1	-1	-0.8	-0.6	-0.8	-0.2	-1.2	-1	-2	-0.8	-0.8	-1	-0.8	-0.2																																																
Post- Benchmark	2.4	2.4	1.4	1.4	N/A	1.6	N/A	1.4	2.4	N/A	2.4	N/A	2.8	2.6	N/A																																																
Soil Type C	0	-0.4	-0.4	-0.4	-0.4	-0.4	-0.4	-0.4	-0.4	-0.4	-0.4	-0.4	-0.4	-0.4	-0.4																																																
Soil Type D	0	-0.8	-0.6	-0.6	-0.6	-0.6	-0.4	-0.6	-0.6	-0.4	-0.6	-0.6	-0.6	-0.6	-0.6																																																
Soil Type E	0	-0.8	-1.2	-1.2	-1	-1.2	-0.8	-1.2	-0.8	-0.8	-0.4	-1.2	-0.4	-0.6	0.8																																																
2.7																																																															
<p>Final Score, S</p>												<p>Detail Evaluation Required</p>																																																			
<p>COMMENTS</p>												<p>YES</p>																																																			
<p>> Final score >= 2, No detail evaluation needed</p>												<p>NO</p>																																																			

HIGH Seismicity

Sketch : 	Address : <u>Kampus Bina Widya</u> <u>Universitas Riau</u> Other Identifiers <u>xx</u> No. Stories <u>2</u> Year <u>+/- 2000</u> Screener <u>tbn</u> Date <u>2016</u> Total Floor Area (sq. ft.) _____ Building Name <u>FAPERIKA</u> Use <u>Educational & Office room</u>																																																								
																																																									
<table border="1" style="width: 100%; border-collapse: collapse;"> <tr> <th colspan="2">OCCUPANCY SOIL</th> <th colspan="8">TYPE</th> <th colspan="4">FALLING HAZARDS</th> </tr> <tr> <td>Assembly</td> <td>Govt</td> <td>Office</td> <td>Number of Persons</td> <td>A</td> <td>B</td> <td>C</td> <td>D</td> <td>E</td> <td>F</td> <td><input type="checkbox"/> Unreinf.</td> <td><input type="checkbox"/> Parapets</td> <td><input type="checkbox"/> Cladding</td> <td><input checked="" type="checkbox"/> Other</td> </tr> <tr> <td>Commercial</td> <td>Historic</td> <td>Residential</td> <td>0 - 10</td> <td>Hard</td> <td>Avg.</td> <td>Dense</td> <td>Stiff</td> <td>Soft</td> <td>Poor</td> <td><input type="checkbox"/> Chimneys</td> <td colspan="3"></td> </tr> <tr> <td>Emer. Services</td> <td>Industrial</td> <td>School</td> <td>101 - 1000</td> <td>Rock</td> <td>Rock</td> <td>Soil</td> <td>Soil</td> <td>Soil</td> <td>Soil</td> <td colspan="4">Roof</td> </tr> </table>		OCCUPANCY SOIL		TYPE								FALLING HAZARDS				Assembly	Govt	Office	Number of Persons	A	B	C	D	E	F	<input type="checkbox"/> Unreinf.	<input type="checkbox"/> Parapets	<input type="checkbox"/> Cladding	<input checked="" type="checkbox"/> Other	Commercial	Historic	Residential	0 - 10	Hard	Avg.	Dense	Stiff	Soft	Poor	<input type="checkbox"/> Chimneys				Emer. Services	Industrial	School	101 - 1000	Rock	Rock	Soil	Soil	Soil	Soil	Roof			
OCCUPANCY SOIL		TYPE								FALLING HAZARDS																																															
Assembly	Govt	Office	Number of Persons	A	B	C	D	E	F	<input type="checkbox"/> Unreinf.	<input type="checkbox"/> Parapets	<input type="checkbox"/> Cladding	<input checked="" type="checkbox"/> Other																																												
Commercial	Historic	Residential	0 - 10	Hard	Avg.	Dense	Stiff	Soft	Poor	<input type="checkbox"/> Chimneys																																															
Emer. Services	Industrial	School	101 - 1000	Rock	Rock	Soil	Soil	Soil	Soil	Roof																																															
BASIC SCORE, MODIFIERS, AND FINAL SCORE, S																																																									
BUILDING TYPE	W1	W2	S1	S2	S3	S4	S5	C1	C2	C3	PC1	PC2	RM1	RM2	URM																																										
			(MRF)	(BR)	(LM)	(RC SW)	(URM INF)	(MRF)	(SW)	(URM INF)	(TU)		(FD)	(RD)																																											
Basic Score	4.4	3.8	2.8	3	3.2	2.8	2	2.5	2.8	1.6	2.6	2.4	2.8	2.8	1.8																																										
Mid Rise (4 to 7 stories)	N/A	N/A	0.2	0.4	N/A	0.4	0.4	0.4	0.4	0.2	N/A	0.2	0.4	0.4	0																																										
High Rise (>7 stories)	N/A	N/A	0.6	0.8	N/A	0.8	0.8	0.6	0.8	0.3	N/A	0.4	N/A	0.6	N/A																																										
Vertical Irregularity	-2.5	-0.2	-1	-1.5	N/A	-1	-1	-1.5	-1	-1	N/A	-1	-1	-1	-1																																										
Plan Irregularity	-0.5	-0.5	-0.5	-0.5	-0.5	-0.5	-0.5	-0.5	-0.5	-0.5	-0.5	-0.5	-0.5	-0.5	0.5																																										
Pre - Code	0	-1	-1	-0.8	-0.6	-0.8	-0.2	-1.2	-1	-2	-0.8	-0.8	-1	-0.8	-0.2																																										
Post- Benchmark	2.4	2.4	1.4	1.4	N/A	1.6	N/A	1.4	2.4	N/A	2.4	N/A	2.8	2.6	N/A																																										
Soil Type C	0	-0.4	-0.4	-0.4	-0.4	-0.4	-0.4	-0.4	-0.4	-0.4	-0.4	-0.4	-0.4	-0.4	-0.4																																										
Soil Type D	0	-0.8	-0.6	-0.6	-0.6	-0.6	-0.4	-0.6	-0.6	-0.4	-0.6	-0.6	-0.6	-0.6	-0.6																																										
Soil Type E	0	-0.8	-1.2	-1.2	-1	-1.2	-0.8	-1.2	-0.8	-0.8	-0.4	-1.2	-0.4	-0.6	0.8																																										
FINAL SCORE, S														1.2																																											
COMMENTS > Irregularity in vertical direction at front building > Final score < 2, detail evaluation required												Detail Evaluation Required <div style="display: flex; justify-content: space-around;"> YES NO </div>																																													

HIGH Seismicity

Sketch : 	Address : <u>Kampus Bina Widya</u> <u>Universitas Riau</u> Other Identifiers <u>xx</u> No. Stories <u>2</u> Year <u>+/- 2014</u> Screener <u>tbn</u> Date <u>2016</u> Total Floor Area (sq. ft.) _____ Building Name <u>SPI building</u> Use <u>Office room</u>																																																								
																																																									
<table border="1" style="width: 100%; border-collapse: collapse;"> <tr> <th colspan="2">OCCUPANCY SOIL</th> <th colspan="8">TYPE</th> <th colspan="4">FALLING HAZARDS</th> </tr> <tr> <td>Assembly</td> <td>Govt</td> <td>Office</td> <td>Number of Persons</td> <td>A</td> <td>B</td> <td>C</td> <td>D</td> <td>E</td> <td>F</td> <td><input type="checkbox"/> Unreinf.</td> <td><input type="checkbox"/> Parapets</td> <td><input type="checkbox"/> Cladding</td> <td><input checked="" type="checkbox"/> Other</td> </tr> <tr> <td>Commercial</td> <td>Historic</td> <td>Residential</td> <td>0 - 10</td> <td>Hard</td> <td>Avg.</td> <td>Dense</td> <td>Stiff</td> <td>Soft</td> <td>Poor</td> <td><input type="checkbox"/> Chimneys</td> <td colspan="3"></td> </tr> <tr> <td>Emer. Services</td> <td>Industrial</td> <td>School</td> <td>101 - 1000</td> <td>Rock</td> <td>Rock</td> <td>Soil</td> <td>Soil</td> <td>Soil</td> <td>Soil</td> <td colspan="4">Roof</td> </tr> </table>		OCCUPANCY SOIL		TYPE								FALLING HAZARDS				Assembly	Govt	Office	Number of Persons	A	B	C	D	E	F	<input type="checkbox"/> Unreinf.	<input type="checkbox"/> Parapets	<input type="checkbox"/> Cladding	<input checked="" type="checkbox"/> Other	Commercial	Historic	Residential	0 - 10	Hard	Avg.	Dense	Stiff	Soft	Poor	<input type="checkbox"/> Chimneys				Emer. Services	Industrial	School	101 - 1000	Rock	Rock	Soil	Soil	Soil	Soil	Roof			
OCCUPANCY SOIL		TYPE								FALLING HAZARDS																																															
Assembly	Govt	Office	Number of Persons	A	B	C	D	E	F	<input type="checkbox"/> Unreinf.	<input type="checkbox"/> Parapets	<input type="checkbox"/> Cladding	<input checked="" type="checkbox"/> Other																																												
Commercial	Historic	Residential	0 - 10	Hard	Avg.	Dense	Stiff	Soft	Poor	<input type="checkbox"/> Chimneys																																															
Emer. Services	Industrial	School	101 - 1000	Rock	Rock	Soil	Soil	Soil	Soil	Roof																																															
BASIC SCORE, MODIFIERS, AND FINAL SCORE, S																																																									
BUILDING TYPE	W1	W2	S1	S2	S3	S4	S5	C1	C2	C3	PC1	PC2	RM1	RM2	URM																																										
			(MRF)	(BR)	(LM)	(RC SW)	(URM INF)	(MRF)	(SW)	(URM INF)	(TU)		(FD)	(RD)																																											
Basic Score	4.4	3.8	2.8	3	3.2	2.8	2	2.5	2.8	1.6	2.6	2.4	2.8	2.8	1.8																																										
Mid Rise (4 to 7 stories)	N/A	N/A	0.2	0.4	N/A	0.4	0.4	0.4	0.4	0.2	N/A	0.2	0.4	0.4	0																																										
High Rise (>7 stories)	N/A	N/A	0.6	0.8	N/A	0.8	0.8	0.6	0.8	0.3	N/A	0.4	N/A	0.6	N/A																																										
Vertical Irregularity	-2.5	-0.2	-1	-1.5	N/A	-1	-1	-1.5	-1	-1	N/A	-1	-1	-1	-1																																										
Plan Irregularity	-0.5	-0.5	-0.5	-0.5	-0.5	-0.5	-0.5	-0.5	-0.5	-0.5	-0.5	-0.5	-0.5	-0.5	0.5																																										
Pre - Code	0	-1	-1	-0.8	-0.6	-0.8	-0.2	-1.2	-1	-2	-0.8	-0.8	-1	-0.8	-0.2																																										
Post- Benchmark	2.4	2.4	1.4	1.4	N/A	1.6	N/A	1.4	2.4	N/A	2.4	N/A	2.8	2.6	N/A																																										
Soil Type C	0	-0.4	-0.4	-0.4	-0.4	-0.4	-0.4	-0.4	-0.4	-0.4	-0.4	-0.4	-0.4	-0.4	-0.4																																										
Soil Type D	0	-0.8	-0.6	-0.6	-0.6	-0.6	-0.4	-0.6	-0.6	-0.4	-0.6	-0.6	-0.6	-0.6	-0.6																																										
Soil Type E	0	-0.8	-1.2	-1.2	-1	-1.2	-0.8	-1.2	-0.8	-0.8	-0.4	-1.2	-0.4	-0.6	0.8																																										
FINAL SCORE, S														2.2																																											
COMMENTS > Irregularity in horizontal (plan) direction > Final score >= 2, No detail evaluation needed												Detail Evaluation Required <div style="display: flex; justify-content: space-around;"> YES NO </div>																																													

HIGH Seismicity

Sketch :

Address : Kampus Bina Widya
Universitas Riau

Other Identifiers KW

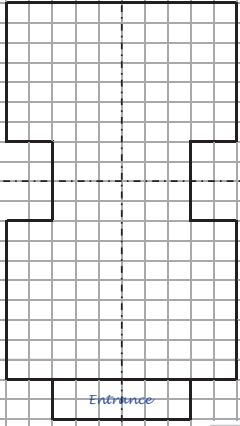

No. Stories 2 Year +/- 2010

Screener tbn Date 2016

Total Floor Area (sq. ft.) _____

Building Name Library UR

Use Office room

OCCUPANCY		SOIL	TYPE		FALLING HAZARDS								
Assembly	Govt	<u>Office</u>	Number of Persons	A	B	C	D	<u>E</u>	F	<input type="checkbox"/> Unreinf.	<input type="checkbox"/> Parapets	<input type="checkbox"/> Cladding	<input checked="" type="checkbox"/> Other
Commercial	Historic	Residential	0 - 10	Hard	Avg.	Dense	Stiff	Soft	Poor	<input type="checkbox"/> Chimneys	<input type="checkbox"/> Roof		
Emer. Services	Industrial	School	101 - 1000	Rock	Rock	Soil	Soil	Soil	Soil				

BASIC SCORE, MODIFIERS, AND FINAL SCORE, S

BUILDING TYPE	W1	W2	S1	S2	S3	S4	S5	<u>C1</u>	C2	C3	PC1	PC2	RM1	RM2	URM
			(MRF)	(BR)	(LM)	(RC SW)	(URM INF)	(MRF)	(SW)	(URM INF)	(TU)	(FD)	(RD)		
Basic Score	4.4	3.8	2.8	3	3.2	2.8	2	<u>2.5</u>	2.8	1.6	2.6	2.4	2.8	2.8	1.8
Mid Rise (4 to 7 stories)	N/A	N/A	0.2	0.4	N/A	0.4	0.4	0.4	0.2	N/A	0.2	0.4	0.4	0	
High Rise (>7 stories)	N/A	N/A	0.6	0.8	N/A	0.8	0.8	0.6	0.8	0.3	N/A	0.4	N/A	0.6	N/A
Vertical Irregularity	-2.5	-0.2	-1	-1.5	N/A	-1	-1	-1.5	-1	-1	N/A	-1	-1	-1	-1
Plan Irregularity	-0.5	-0.5	-0.5	-0.5	-0.5	-0.5	-0.5	<u>-0.5</u>	-0.5	-0.5	-0.5	-0.5	-0.5	-0.5	0.5
Pre - Code	0	-1	-1	-0.8	-0.6	-0.8	-0.2	-1.2	-1	-2	-0.8	-1	-0.8	-0.2	
Post- Benchmark	2.4	2.4	1.4	1.4	N/A	1.6	N/A	<u>1.4</u>	2.4	N/A	2.4	2.8	2.6	N/A	
Soil Type C	0	-0.4	-0.4	-0.4	-0.4	-0.4	-0.4	-0.4	-0.4	-0.4	-0.4	-0.4	-0.4	-0.4	-0.4
Soil Type D	0	-0.8	-0.6	-0.6	-0.6	-0.6	-0.4	-0.6	-0.6	-0.4	-0.6	-0.6	-0.6	-0.6	-0.6
Soil Type E	0	-0.8	-1.2	-1.2	-1	-1.2	-0.8	<u>-1.2</u>	-0.8	-0.8	-0.4	-1.2	-0.4	-0.6	0.8

FINAL SCORE, S 2.2

COMMENTS

> Irregularity in horizontal (plan) direction

> Final score >= 2, No detail evaluation needed

Detail Evaluation Required

YES ☐ NO ☒

HIGH Seismicity

Sketch :

Address : Kampus Bina Widya
Universitas Riau

Other Identifiers KW

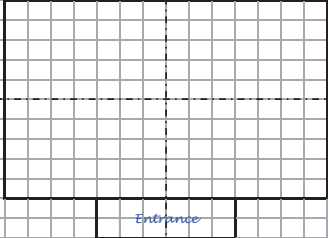

No. Stories 2 Year +/- 2000

Screener tbn Date 2016

Total Floor Area (sq. ft.) _____

Building Name LEMLIT building

Use Office room

OCCUPANCY		SOIL	TYPE		FALLING HAZARDS								
Assembly	Govt	<u>Office</u>	Number of Persons	A	B	C	D	<u>E</u>	F	<input type="checkbox"/> Unreinf.	<input type="checkbox"/> Parapets	<input type="checkbox"/> Cladding	<input checked="" type="checkbox"/> Other
Commercial	Historic	Residential	0 - 10	Hard	Avg.	Dense	Stiff	Soft	Poor	<input type="checkbox"/> Chimneys	<input type="checkbox"/> Roof		
Emer. Services	Industrial	School	101 - 1000	Rock	Rock	Soil	Soil	Soil	Soil				

BASIC SCORE, MODIFIERS, AND FINAL SCORE, S

BUILDING TYPE	W1	W2	S1	S2	S3	S4	S5	<u>C1</u>	C2	C3	PC1	PC2	RM1	RM2	URM
			(MRF)	(BR)	(LM)	(RC SW)	(URM INF)	(MRF)	(SW)	(URM INF)	(TU)	(FD)	(RD)		
Basic Score	4.4	3.8	2.8	3	3.2	2.8	2	<u>2.5</u>	2.8	1.6	2.6	2.4	2.8	2.8	1.8
Mid Rise (4 to 7 stories)	N/A	N/A	0.2	0.4	N/A	0.4	0.4	0.4	0.2	N/A	0.2	0.4	0.4	0	
High Rise (>7 stories)	N/A	N/A	0.6	0.8	N/A	0.8	0.8	0.6	0.8	0.3	N/A	0.4	N/A	0.6	N/A
Vertical Irregularity	-2.5	-0.2	-1	-1.5	N/A	-1	-1	-1.5	-1	-1	N/A	-1	-1	-1	-1
Plan Irregularity	-0.5	-0.5	-0.5	-0.5	-0.5	-0.5	-0.5	-0.5	-0.5	-0.5	-0.5	-0.5	-0.5	-0.5	0.5
Pre - Code	0	-1	-1	-0.8	-0.6	-0.8	-0.2	-1.2	-1	-2	-0.8	-1	-0.8	-0.2	
Post- Benchmark	2.4	2.4	1.4	1.4	N/A	1.6	N/A	<u>1.4</u>	2.4	N/A	2.4	2.8	2.6	N/A	
Soil Type C	0	-0.4	-0.4	-0.4	-0.4	-0.4	-0.4	-0.4	-0.4	-0.4	-0.4	-0.4	-0.4	-0.4	-0.4
Soil Type D	0	-0.8	-0.6	-0.6	-0.6	-0.6	-0.4	-0.6	-0.6	-0.4	-0.6	-0.6	-0.6	-0.6	-0.6
Soil Type E	0	-0.8	-1.2	-1.2	-1	-1.2	-0.8	<u>-1.2</u>	-0.8	-0.8	-0.4	-1.2	-0.4	-0.6	0.8

FINAL SCORE, S 2.7

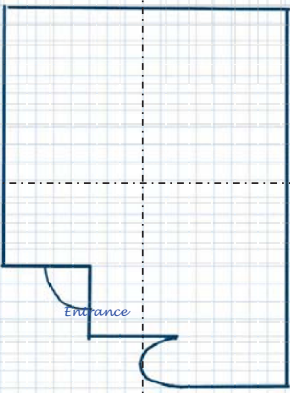

COMMENTS

> Final score >= 2, No detail evaluation needed

Detail Evaluation Required

YES ☐ NO ☒

HIGH Seismicity

Sketch : 	Address : <u>Kampus Bina Widya</u> <u>Universitas Riau</u> Other Identifiers <u>xx</u> No. Stories <u>10</u> Year <u>+/- 2015</u> Screener <u>tbn</u> Date <u>2016</u> Total Floor Area (sq. ft.) _____ Building Name <u>Awal Brosy</u> Use <u>Hospital and Office room</u>														
															
<table border="1" style="width: 100%; border-collapse: collapse;"> <tr> <th style="width: 20%;">OCCUPANCY</th> <th style="width: 20%;">SOIL</th> <th style="width: 20%;">TYPE</th> <th style="width: 40%;">FALLING HAZARDS</th> </tr> <tr> <td> Assembly Commercial <u>Emer. Services</u> </td> <td> Govt Historic Industrial <u>Office</u> Residential School </td> <td> A B C D <u>E</u> F </td> <td> <input type="checkbox"/> Unreinf. Chimneys <input checked="" type="checkbox"/> Parapets <input type="checkbox"/> Cladding <input checked="" type="checkbox"/> Other <u>Roof</u> </td> </tr> </table>		OCCUPANCY	SOIL	TYPE	FALLING HAZARDS	Assembly Commercial <u>Emer. Services</u>	Govt Historic Industrial <u>Office</u> Residential School	A B C D <u>E</u> F	<input type="checkbox"/> Unreinf. Chimneys <input checked="" type="checkbox"/> Parapets <input type="checkbox"/> Cladding <input checked="" type="checkbox"/> Other <u>Roof</u>						
OCCUPANCY	SOIL	TYPE	FALLING HAZARDS												
Assembly Commercial <u>Emer. Services</u>	Govt Historic Industrial <u>Office</u> Residential School	A B C D <u>E</u> F	<input type="checkbox"/> Unreinf. Chimneys <input checked="" type="checkbox"/> Parapets <input type="checkbox"/> Cladding <input checked="" type="checkbox"/> Other <u>Roof</u>												
BASIC SCORE, MODIFIERS, AND FINAL SCORE, S															
BUILDING TYPE	W1	W2	S1 (MRP)	S2 (BR)	S3 (LM)	S4 (RC SW)	S5 (URM INF)	C1 (MRP)	C2 (SW)	C3 (URM INF)	PC1 (TU)	PC2	RM1 (FD)	RM2 (RD)	URM
Basic Score	4.4	3.8	2.8	3	3.2	2.8	2	<u>2.5</u>	2.8	1.6	2.6	2.4	2.8	2.8	1.8
Mid Rise (4 to 7 stories)	N/A	N/A	0.2	0.4	N/A	0.4	0.4	0.4	0.2	N/A	0.2	0.4	0.4	0	
High Rise (>7 stories)	N/A	N/A	0.6	0.8	N/A	0.8	0.8	<u>0.6</u>	0.8	0.3	N/A	0.4	N/A	0.6	N/A
Vertical Irregularity	-2.5	-0.2	-1	-1.5	N/A	-1	-1	-1.5	-1	-1	N/A	-1	-1	-1	-1
Plan Irregularity	-0.5	-0.5	-0.5	-0.5	-0.5	-0.5	-0.5	<u>-0.5</u>	-0.5	-0.5	-0.5	-0.5	-0.5	-0.5	0.5
Pre - Code	0	-1	-1	-0.8	-0.6	-0.8	-0.2	-1.2	-1	-2	-0.8	-0.8	-1	-0.8	-0.2
Post- Benchmark	2.4	2.4	1.4	1.4	N/A	1.6	N/A	<u>1.4</u>	2.4	N/A	2.4	N/A	2.8	2.6	N/A
Soil Type C	0	-0.4	-0.4	-0.4	-0.4	-0.4	-0.4	-0.4	-0.4	-0.4	-0.4	-0.4	-0.4	-0.4	-0.4
Soil Type D	0	-0.8	-0.6	-0.6	-0.6	-0.6	-0.4	-0.6	-0.6	-0.4	-0.6	-0.6	-0.6	-0.6	-0.6
Soil Type E	0	-0.8	-1.2	-1.2	-1	-1.2	-0.8	<u>-1.2</u>	-0.8	-0.8	-0.4	-1.2	-0.4	-0.6	0.8
FINAL SCORE, S 2.8															
COMMENTS ➤ Irregularity in horizontal (plan) direction ➤ Final score >= 2, No detail evaluation needed												Detail Evaluation Required YES NO			